

DOPAMINE RECEPTOR STIMULATION REGULATES EXPRESSION OF
DEVELOPMENTAL GENES AND DISRUPTS NETRIN-1-MEDIATED AXON
GUIDANCE

By

STEPHANIE E. SILLIVAN

Dissertation

Submitted to the Faculty of the
Graduate School of Vanderbilt University
In partial fulfillment of the requirements

for the degree of

DOCTOR OF PHILOSOPHY

In

Neuroscience

December, 2011

Nashville, Tennessee

Approved:

Professor Sanika Chirwa

Professor Christine Konradi

Professor Ariel Deutch

Professor David Miller

Professor Karoly Mirnics

In loving memory of Christopher Michael Bronson

ACKNOWLEDGEMENTS

First and foremost, I would like to thank my mentor and friend, Dr. Christine Konradi. I feel very fortunate to have had the opportunity to work with Christine over the past five and a half years. I credit her with not only my professional development, but also aspects of my personal development as well. Her strong work ethic and passion for the field of neuroscience has set an example for my own studies and has fueled my inspiration to continue pursuing my career goals. Christine's endless creativity, combined with her hospitable and kind nature, has made my time at Vanderbilt happy, productive, and fun. I will truly miss seeing her everyday.

I would like to acknowledge my thesis committee chair, Dr. Karoly Mirnics, for his guidance and assistance over the years, but specifically for working with me extensively on an independent study project. I am grateful for his dedication to the graduate program and appreciate the high expectations he set for me, as they have strengthened my research. I would also like to thank my other thesis committee members, Drs Sanika Chirwa, Ariel Deutch, and David Miller, for dedicating their time and offering ideas and guidance for my thesis project.

Thank you to all members of the Konradi Lab, both past and present, for providing companionship and support over the years. Alipi Naydenov initiated me to the lab and I am very grateful that I got to work with him, even for a short amount of time. I would especially like to acknowledge Graham Goenne, Ryan Hanlin, Dr. Nicole Herring, and Andrew Luksik for their assistance in performing behavioral experiments and drug injection paradigms. I would also like to thank Dr. Randy Barrett of the Rat Neurobehavioral Core for her help in designing my behavioral experiments.

This work would not have been possible without the financial assistance and support of several funding sources, including the National Institutes of Health Training Grant awarded to the Vanderbilt Neuroscience Program (T32 MH064913). Additional support was received from a National Institutes of Health grant awarded to my advisor, Dr. Christine Konradi (DA19152). Data collection was performed in part through the use of the VUMC Cell Imaging Shared Resource, supported by NIH grants CA68485, DK20593, DK58404, HD15052, DK59637, and Ey008126.

I would like to acknowledge the Vanderbilt Brain Institute, the Center for Molecular Neuroscience, and the Kennedy Center for providing resources to aid in my research. Thank you to the Biomedical Research Education and Training Office (BRET), the Vanderbilt Neuroscience Graduate Program, and the Interdisciplinary Graduate Program (IGP) for preparing and organizing the curriculum in my didactic coursework. I would especially like to thank the director of the Brain Institute, Mark Wallace, the director of graduate studies in the Neuroscience Program, Doug McMahon, and the administrative staff- Rosalind Johnson, Mary Michael-Woolman, and Shirin Pulous- for investing so much of their time and resources into my education. I really admire their commitment to the program and the support they provide to students.

In addition, I would like to thank the collaborators who contributed to this research. Dr. Alex Bonnin shared with me his expertise in the field of developmental neuroscience and instructed me on how to perform explant outgrowth assays. Dr. Deyu Li and Bryson Brewer of the Mechanical Engineering Department designed the microfluidic chambers used to study axonal outgrowth.

Finally, I would like to thank my loving family for their support and encouragement over the last 5 years. My parents, Tim and Elaine Bronson, are the most giving people I have ever met and their high moral standards have always encouraged me to pursue a profession that helps to benefit the lives of others. The experiences we shared with my late brother, Chris Bronson, are what motivated me to go to graduate school to study mental illnesses. Their patience and perseverance in trying to help my brother has always resonated with me and inspires me to continue working on scientific problems, despite all the setbacks that come with them.

Thank you to my English bulldog, Dublin, for always making me smile! No matter how sad or frustrated I get, Dublin keeps me laughing every day. Last, thank you to my husband, Chris Sullivan, for providing me with love and encouragement, but also for never letting me feel sorry for myself. You have given me the confidence I needed to become successful and that is priceless.

TABLE OF CONTENTS

	Page
DEDICATION	ii
ACKNOWLEDGEMENTS	iii
LIST OF TABLES	x
LIST OF FIGURES	xi
LIST OF ABBREVIATIONS.....	xiii
Chapter:	
I. INTRODUCTION	1
<i>Overview of the dopamine system</i>	1
Dopaminergic projections	2
Dopamine receptors	3
Signaling mechanisms of dopamine receptors.....	4
Dysregulation of DA in psychiatric disorders	8
Frontal cortex projections	10
<i>Axon guidance</i>	11
Classification of axon guidance molecules.....	12
Mechanisms of axon guidance.....	13
Netrin-1 mediated axon guidance	15
Regulation of axon guidance molecules by DA signaling	18
<i>Rationale</i>	19
<i>Hypothesis</i>	20
<i>Specific Aims of Thesis</i>	20
II. EXPRESSION AND FUNCTIONALITY OF DOPAMINE RECEPTORS IN THE EMBRYONIC RAT BRAIN: IMPLICATIONS FOR MODULATION OF DEVELOPMENTAL PROCESSES.....	21
<i>Abstract</i>	21
<i>Introduction</i>	22
<i>Materials and Methods</i>	24
Animals.....	24
Primary neuronal cultures.....	25
Generation of nested RNA probes	25
Northern blot method	26

<i>In situ</i> hybridization	26
QPCR	27
Western blotting.....	28
Statistics	30
<i>Results</i>	31
Detection of DR mRNA transcripts in the developing rat brain.....	31
Quantification of DR mRNA transcripts by QPCR analysis	31
Activation of DRs in embryonic cultures regulates the phosphorylation status of second messenger molecules.....	39
<i>Discussion</i>	44

III. DOPAMINE RECEPTOR STIMULATION DISRUPTS NETRIN-1 AXON GUIDANCE IN CORTICAL NEURONS..... 48

<i>Abstract</i>	48
<i>Introduction</i>	48
<i>Materials and Methods</i>	50
Animals.....	50
RNA probe synthesis and <i>in situ</i> hybridization	51
Primary neuronal cultures.....	51
QPCR.....	51
Western blotting.....	52
Immunohistochemistry	52
Explant assays.....	53
Analysis of explant cultures.....	54
Microfluidic devices	54
<i>Results</i>	56
Expression of netrin-1 receptors in the developing rat cortex	56
Colocalization of DRs and netrin-1 receptors in cortical neurons.....	57
Netrin-1 attracts neurites from explants of the mFC	59
DR stimulation disrupts netrin-1 mediated axon guidance.....	59
DR stimulation reduces axon attraction to netrin-1	60
DR stimulation increases Ntn-1 receptor expression.....	64
<i>Discussion</i>	68

IV. POSTNATAL COCAINE ADMINISTRATION REGULATES AXON GUIDANCE MOLECULES IN THE PFC AND STRIATUM71

<i>Abstract</i>	71
<i>Introduction</i>	71
<i>Materials and Methods</i>	72
Animals.....	72
Drug administration	73
QPCR.....	73

<i>Results</i>	75
Cocaine administration regulates expression of axon guidance genes in the PFC and STR.....	75
<i>Discussion</i>	78
V BINGE COCAINE ADMINISTRATION IN ADOLESCENT RATS AFFECTS AMYGDALAR GENE EXPRESSION PATTERNS AND ALTERS ANXIETY-RELATED BEHAVIOR IN ADULTHOOD	80
<i>Abstract</i>	80
<i>Introduction</i>	81
<i>Materials and Methods</i>	82
Animals	82
Drug administration protocol.....	83
Elevated plus maze	84
Contextual fear conditioning.....	84
Open field.....	85
Hole board food search and exploration tasks	85
Morris Water Maze	86
Microarrays	87
QPCR	88
Western blotting.....	89
<i>Results</i>	92
Adolescent cocaine exposure decreases anxiety and conditioned fear behaviors in adult rats	92
Adolescent cocaine exposure increases novelty seeking and exploratory behaviors in adult rats	94
Adolescent cocaine exposure does not impair spatial learning and memory in adult rats	94
Binge cocaine exposure regulates amygdalar gene expression in adolescent rats	96
Wnt signaling is dysregulated following adolescent cocaine exposure	98
<i>Discussion</i>	103
VI. SUMMARY AND FUTURE DIRECTIONS.....	108
<i>DRD1 and DRD2 have unique expression patterns in the developing brain</i>	108
<i>DR signaling cascades are functional in the absence of DR innervation</i>	110
<i>Ntn-1 receptors are expressed in the developing mFC</i>	112
<i>DR stimulation disrupts Ntn-1 mediated attraction of mFC axons</i>	113
<i>DR stimulation regulates the abundance of Ntn-1 receptor transcripts</i>	114

<i>Postnatal cocaine administration regulates expression of axon guidance-related genes</i>	118
<i>Adolescent binge cocaine administration regulates expression of developmental and synaptic genes</i>	119
<i>Adolescent binge cocaine administration decreases fear and anxiety in adult rats</i>	120
FULL AUTHOR LIST	122
REFERENCES	122

LIST OF TABLES

Table	Page
1.1: Classification of axon guidance families	13
2.1: List of primer sequences used for synthesis of in situ probes and QPCR	29
2.2: Ratio of DRD1 over DRD2 mRNA expression in the developing rat brain.....	36
2.3: Ratio of DR mRNA in the mFC over STR.....	36
3.1: Primer pairs used for RNA probe synthesis and QPCR	56
3.2: The ratio of DCC to UNC5C mRNA expression in mFC neurons and tissue.....	61
4.1: List of primer sequences used in QPCR experiments.....	75
4.2: mRNA analysis of axon guidance-related proteins	77
4.3: Summary of gene changes in the PFC and STR after postnatal cocaine exposure	77
5.1: Primer sequences for QPCR reactions.....	91
5.2: Adolescent cocaine exposure leads to downregulation of plasma membrane and synaptic genes in the amygdala.....	99
5.3: Adolescent cocaine exposure alters the expression of axon guidance genes in the amygdala.....	99
5.4: Adolescent cocaine exposure alters the expression of Wnt signaling pathway genes in the amygdala	100

LIST OF FIGURES

Figure	Page
1.1: Ontogeny of dopaminergic innervation.....	3
1.2: Dopamine receptor signaling pathways.....	5
1.3: Ntn-1 signaling pathways	16
2.1: Generation of DR probes to measure mRNA transcripts in rat brain.....	32
2.2: <i>In situ</i> hybridization of DRD1 development in rat mFC and STR.....	33
2.3: <i>In situ</i> hybridization of DRD2 development in rat mFC and STR.....	34
2.4: DR mRNA expression measured by <i>in situ</i> hybridization and QPCR	37
2.5: DR mRNA expression in mFC and STR neuronal cultures increases over time ...	39
2.6: DRD1-mediated activation of signal transduction pathways in embryonic neuronal cultures from the rat mFC and STR.....	42
2.7: DRD2-mediated activation of signal transduction pathways in embryonic neuronal cultures from the rat mFC and STR.....	43
2.8: PPHT mediated activation of GSK3 β is specific for DRD2	44
3.1: Expression of Ntn-1 receptors DCC and UNC5C in the developing mFC	58
3.2: Colocalization of DRs and Ntn-1 receptors in mFC neurons	61
3.3: Stimulation of DRs disrupts Ntn-1-mediated attraction in mFC explants.....	62
3.4: DR agonists inhibit the attractive properties of Ntn-1 in mFC explants	63
3.5: DR agonists impair Ntn-1-mediated outgrowth.....	65
3.6: DR agonists regulate mRNA levels of Ntn-1 receptors.....	66
3.7: Model depicting DR modulation of Ntn-1 mediated axon guidance mechanisms.....	67
4.1: Overview of drug paradigm for postnatal cocaine administration	74

4.2:	Postnatal cocaine exposure regulates expression of axon guidance genes in the PFC and STR	76
5.1:	Overview of experimental time courses	83
5.2:	Adolescent binge cocaine exposure disrupts fear learning and anxiety behaviors in adult rats	93
5.3:	Exploration and novelty seeking is increased in adult rodents after binge cocaine administration in adolescence.....	95
5.4:	Spatial learning and memory were not altered in adult rats after adolescent cocaine exposure	97
5.5:	Adolescent cocaine exposure affects the expression of synaptic and developmental genes in the amygdala	101
5.6:	Cocaine administration during adolescence regulates GSK3B phosphorylation patterns in the amygdala	102
5.7:	Schematic representation of cocaine-induced amygdalar gene changes in the Wnt pathway	107

LIST OF ABBREVIATIONS

5-HT	serotonin
AC	adenylyl cyclase
AGM	axon guidance molecule
AKAP	a kinase anchor protein
Akt	protein kinase B/ v-akt murine thymoma viral oncogene homolog 1
ANOVA	analysis of variance
APD	antipsychotic drug
ATP	adenosine triphosphate
BCIP	5-Bromo-4-chloro-3-indolyl phosphate
Bp	base pairs
BSA	bovine serum, albumin
Ca ²⁺	calcium
cAMP	cyclic adenosine monophosphate
Cdc42	Cell division control protein 42
cDNA	complementary deoxyribonucleic acid
cm	centimeter
CNC	cyclic nucleotide gated channel
CPu	caudate putamen
CREB	cAMP response element binding
CS	conditioned stimulus
Ctx	cortex
DRD1,-2,-3,-4,-5	dopamine receptors 1, 2, 3, 4, and 5

DA	dopamine
DAG	diacylglycerol
DARPP-32	dopamine- and cAMP-regulated neuronal phosphoprotein
DAT	dopamine transporter
dB	decibel
DCC	deleted in colorectal cancer
DIV	days in vitro
DMSO	dimethyl sulfoxide
DR	dopamine receptor
E	embryonic day
EDTA	ethylenediaminetetraacetic acid
ERK1/2	extracellular signal-regulated kinase 1/2
FC	frontal cortex
g	grams
GDP	guanosine diphosphate
GPCR	g-protein coupled receptor
GSK3B	glycogen synthase kinase 3-beta
GTP	guanosine triphosphate
h	hours
HCl	hydrochloric acid
HEK293	Human Embryonic Kidney 293 cells
HP	hippocampus
HRP	horseradish peroxidase

I-1	Inhibitor 1
i.p.	intraperitoneally
IP3	Inositol triphosphate
IVT	in vitro transcription
Kg	kilogram
kHz	kilohertz
LV	lateral ventricle
M	molar
mA	milliamp
MAPK	mitogen-activated protein kinase
MFB	medial forebrain bundle
mg	milligram
ml	milliliter
mM	millimolar
MOPS	3-(N-morpholino)propanesulfonic acid
NAcc	nucleus accumbens
NaCl	sodium chloride
NBT	nitroblue tetrazolium salt
NC	neocortex
NMDA	N-Methyl-D-aspartate
Ntn-1	netrin-1
OB	olfactory bulb
PBS	phosphate buffered saline

PFA	paraformaldehyde
PFC	prefrontal cortex
PI3K	phosphatidylinositol 3- and 4-kinase
PIP2	phosphatidylinositol 4,5-bisphosphate
PKA	protein kinase A
PKC	protein kinase C
PLC	phospholipase C
PLD	phospholipase D
PN	postnatal day
PP1	protein phosphatase 1
PP2A	protein phosphatase 2A
PPHT	(±)-2-(N-Phenethyl-N-propyl)amino-5-hydroxytetralin hydrochloride
PVDF	polyvinylidene fluoride
QPCR	quantitative polymerase chain reaction
Rac1	Ras-related C3 botulinum toxin substrate 1
RH	rhinencephalon
Rho	Ras homolog gene family
RNA	ribonucleic acid
s	seconds
s.c.	subcutaneously
SEM	standard error of the mean
SNc	substantia nigra pars compacta

SP	septum
SSC	saline sodium citrate
ST	striatum
STR	striatum
SZ	schizophrenia
TBS-T	tris-buffered saline with Tween-20
TH	tyrosine hydroxylase
t.i.d.	ter in die, three times per day
UNC5	Uncoordinated-5
US	unconditioned stimulus
VTA	ventral tegmental area
VZ	ventricular zone
Wnt	Wingless-type MMTV integration site family
μg	microgram
μl	microliter
μM	micromolar

CHAPTER I

INTRODUCTION

Overview of the dopamine system

Dopamine (DA) is a modulatory neurotransmitter that functions in the human body to regulate numerous aspects of behavior, mood, and motor function (Girault and Greengard, 2004). From sleep cycles, appetite, and emotion- to sex, addiction, and psychopathy- the dopamine system contributes to components of humanity that are both necessary and evil (Lu and Zee, 2010, Blum et al., Buckholtz et al.). In the mammalian brain, dopaminergic projections innervate brain regions adversely affected in psychiatric illnesses, including Parkinson's disease, schizophrenia, attention deficit hyperactivity disorder, addiction, and mood disorders (Sillitoe and Vogel, 2008). However, the contribution of the DA system to the establishment of neuronal circuitry and the significance of DA signaling during development of the central nervous system remain unclear. Understanding how dopaminergic pathways impact a developing brain may shed light on the organization of connectivity in diseases with a neurodevelopmental component. Moreover, if DA is required for normal brain development, then early exposure to agents that interfere with the DA system could disrupt the trajectory of developmental events, precipitating behavioral abnormalities and even psychiatric illnesses.

Dopaminergic projections

DA neurons originate mainly from two midbrain regions, the substantia nigra pars compacta (SNc) and the ventral tegmental area (VTA) (Figure 1.1) (Van den Heuvel and Pasterkamp, 2008). SNc neurons project via the medial forebrain bundle (MFB) to the dorsal caudate nuclei of the striatum (STR), forming the nigrostriatal pathway (Prasad and Pasterkamp, 2009). The STR participates in extrapyramidal motor circuits involving the thalamus and motor cortex (Herrero et al., 2002). VTA neurons send dopaminergic projections to the prefrontal cortex (PFC), forming the mesocortical pathway, and to the nucleus accumbens (NAcc), amygdala, and hippocampus to form the mesolimbic pathway (Van den Heuvel and Pasterkamp, 2008). The mesolimbic system mediates pleasure seeking, reward, and addictive behavior (Kauer and Malenka, 2007). The PFC controls executive function, decision-making, working memory tasks, and critical thinking skills (Arnsten and Li, 2005).

In the rat brain, the first MFB axons first reach the STR at embryonic day (E)14, then go on to enter the cortex (Van den Heuvel and Pasterkamp, 2008). Tyrosine hydroxylase (TH)+ fibers immediately begin innervation of the STR and are diffuse by E18 (Van den Heuvel and Pasterkamp, 2008). Conversely, dopaminergic axons do not innervate the cortex right away. TH+ fibers enter the subplate and intermediate zone but wait to enter the cortical plate (Verney et al., 1982). A two day “waiting period” coincides with the progressive thickening of the cortex and expansion of white matter (Kriegstein et al., 2006). The innervation and establishment of functional DA synapses in the FC begins at E20 and is not complete until after birth (Van den Heuvel and Pasterkamp, 2008).

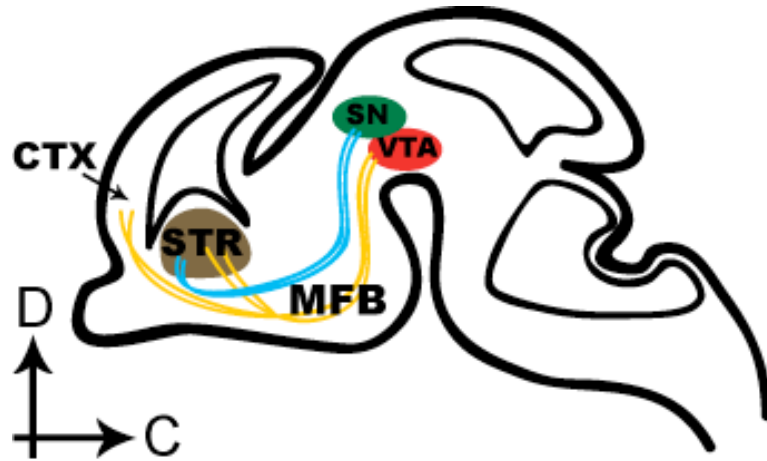


FIGURE 1.1: Ontogeny of dopaminergic innervation. A sagittal view of an embryonic rodent brain. DA axons extend from the midbrain to innervate striatal and cortical areas. The SN projects to the caudate putamen (blue lines), while the VTA projects to the ventral nucleus accumbens in the STR and the cortex (yellow lines). Abbreviations: C, caudal; CTX, cortex; D, dorsal; MFB, medial forebrain bundle; SN, substantia nigra; STR, striatum; VTA, ventral tegmental area.

Dopamine receptors

The five main dopamine receptors (DR)- DRD1, DRD2, DRD3, DRD4, and DRD5- are g-protein coupled receptors (GPCR) that are classically characterized by their ability to activate or inhibit production of cyclic AMP (cAMP)(Neve et al., 2004). DRD1 and DRD5 are considered “D1 like”, because both increase cAMP synthesis, and are structurally comparable, with each containing a single exon that is conserved in both human and rodent brains (Zhou et al., 1990, Girault and Greengard, 2004). DRD2, DRD3, and DRD4 are “D2 like” and couple to $G_{\alpha i}$, inhibiting adenylyl cyclase (AC) and thus decreasing cyclic nucleotide levels (Enjalbert and Bockaert, 1983, Girault and Greengard, 2004). Members of the D2 family of receptors are encoded by multiple exons in both rodents and human, and various splice variants have been reported for these genes (Bunzow et al., 1988, Zhang et al., 2007). For example, DRD2 exists in a common “long form” postsynaptically and a “short form” presynaptically (Lindgren et al., 2003). The

presynaptic DRD2 receptors are autoreceptors that lack a portion of exons 5-6 and are expressed only in dopaminergic neurons (Goldstein et al., 1990). While expression of DRs is mostly concentrated in regions receiving dense DA innervation, DRs are expressed throughout the brain. The highest levels of DRD1 and DRD2 are in the basal ganglia, and lower levels of DRs are found in the PFC, amygdala, nucleus accumbens, and hippocampus (Araki et al., 2007).

Signaling mechanisms of dopamine receptors

As stated previously, the D1 class of dopamine receptors couples primarily to the stimulatory G-protein $G_{as/olf}$, named for its ability to stimulate the production of cAMP (Neve et al., 2004). After binding GTP, $G_{as/olf}$ activates AC, a 12-transmembrane domain protein that converts ATP to cAMP (Figure 1.2) (Patel et al., 2001). G_{as} in the GTP-bound form has a tenfold greater affinity for activating AC compared to the GDP-bound form (Sunahara et al., 1997). The complex of AC and $G_{as/olf}$ functions as an active enzyme with AC comprising the catalytic unit and $G_{as/olf}$ the regulatory unit (Kandel, 2000). AC production of cAMP is terminated when $G_{as/olf}$ dissociates from the complex.

cAMP is a diffusible molecule with two primary actions. First, cAMP can bind to cyclic nucleotide-gated ion channels (CNC) to modulate ion permeability. CNCs are non-selective cation channels that promote Ca^{2+} entry into the cell (Kaupp and Seifert, 2002). Fluctuations in Ca^{2+} concentration can play a role in depolarization of the cell but are also very important for developmental and metabolic processes (Rutecki, 1992). The second role of cAMP is to activate the cyclic AMP dependent kinase protein kinase A

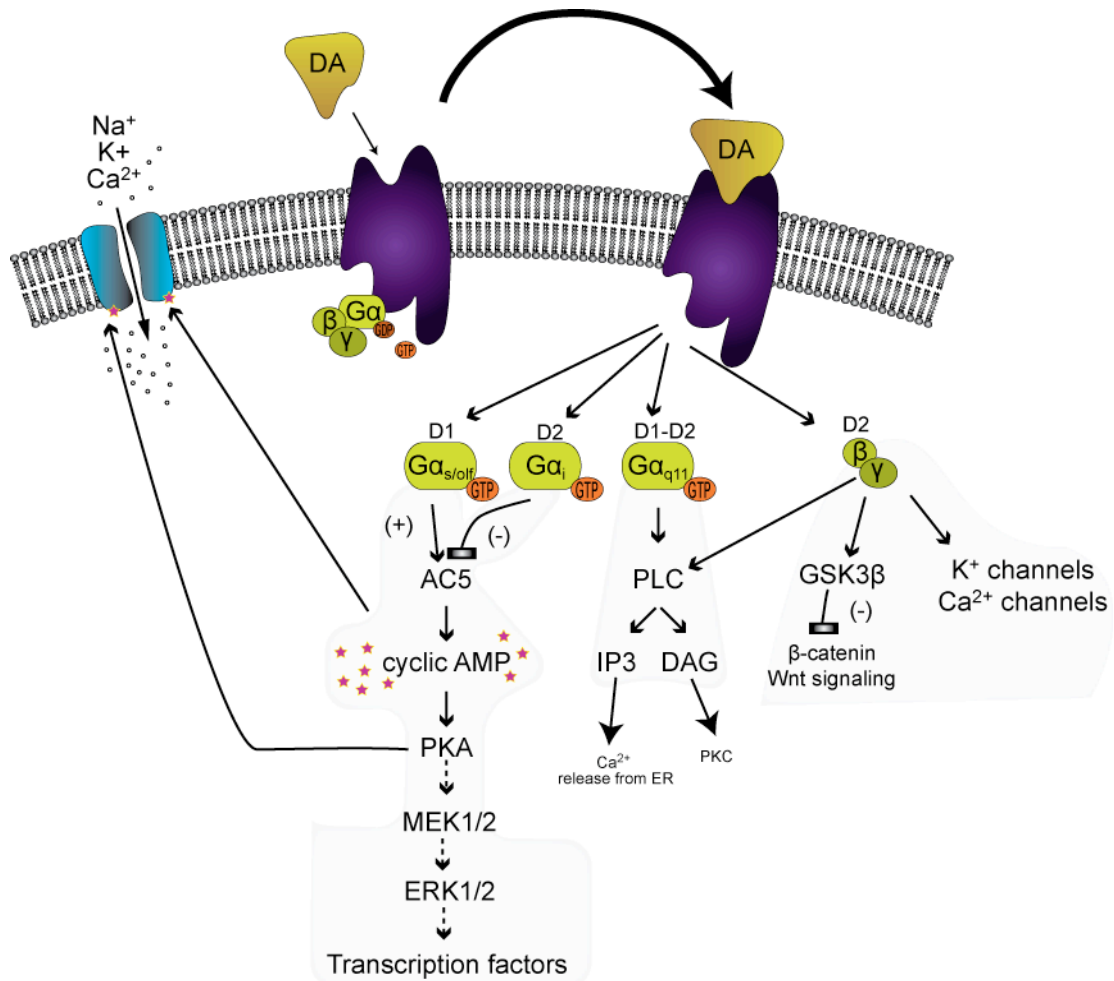


FIGURE 1.2: Dopamine receptor signaling pathways.

DA interacts with subtypes of DRs that activate GPCRs. Activation of a DR results in conformational changes, allowing the G_{βγ} subunits dissociate from the G_α subunit. Depending on the properties of G_α, specific second messenger pathways are activated. D1 like receptors activate G_{α_s}, which leads to accumulation of cAMP and activation of PKA and ERK1/2-mediated signaling cascades. PKA phosphorylates membrane-bound ion channels that promote entry of calcium into the cell and membrane depolarization. D2 like receptors inhibit this pathway by activating the G_{α_i} protein. The dissociated G_{βγ} subunit of the D2 receptor can activate signal transduction pathways in its own right, including the PLC pathway and GSK3B-mediated signaling. PLC activation triggers release of calcium from stores in the endoplasmic reticulum. Heterodimers of D1 and D2 receptors also activate the PLC pathway by activating the G_{α_q} protein. Adapted from (Bronson and Konradi, 2010).

(PKA) (Montminy, 1997). PKA transfers a phosphate from ATP onto the amino acids serine or threonine within particular amino acid consensus sequences in substrate proteins (Kandel, 2000). These consensus sequences confer increased substrate specificity (Ubersax and Ferrell, 2007).

PKA can modulate neuronal excitability as well. Sodium and L-type Ca^{2+} channels have PKA phosphorylation sites that open the channels while potassium channels remain closed after PKA phosphorylation (Cantrell et al., 1997, Surmeier et al., 2007). The influx of cations will promote a state of depolarization in the cell and can facilitate activity of NMDA ionotropic receptors (Dudman et al., 2003). NMDA receptors cannot be active unless the cell is initially depolarized to remove a Mg^{2+} ion that sits in the pore of the NMDA channel (Cavara et al., 2010). The activation of DRD1 receptors and the cAMP pathway therefore functions to synergistically allow for NMDA receptor neurotransmission (Cepeda and Levine, 1998).

PKA has many substrates but a group of proteins called A Kinase Anchoring-Proteins (AKAPs) enhance PKA specificity (Dell'Acqua et al., 2006). These proteins target PKA to a specific substrate depending on the needs of the cell and a given stimulus (Wong and Scott, 2004). PKA affects such a diverse group of substrates and AKAPs aid in this process by anchoring PKA directly to a substrate (Wong and Scott, 2004). The transcription factor cyclic AMP response element binding protein (CREB) is activated by PKA as well as kinases involved in the mitogen-activated protein kinase (MAPK) pathway (Montminy, 1997). PKA also promotes amplification of its own kinase activity by phosphorylating inhibitor 1 (I-1 or DARPP-32) (Figure 1.2B) (Svenningsson et al., 2004). I-1 associates with protein phosphatase-1 (PP1) when I-1 is phosphorylated and prevents PP1 from removing phosphate molecules from PKA substrates, therefore amplifying PKA signals (Svenningsson et al., 2004). When phosphorylated, DARPP-32 no longer associates with I-1 but instead directly inhibits PKA activity (Svenningsson et al., 2004).

D2-like receptors couple to a second G-protein, G_{ai} (Beaulieu and Gainetdinov, 2011). G_{ai} is an inhibitory G-protein, named for its ability to inhibit the AC and attenuate cAMP production (Brasser and Spear, 2004). G_{ai} coupled receptors directly oppose $G_{as/olf}$ activation of cyclic AMP and promote hyperpolarization by inhibiting sodium and calcium ion flow while opening potassium channels (Surmeier et al., 2007). DRD2 is also present on presynaptic cells, where it inhibits neurotransmitter release (Fisone et al., 2007). DRD2 autoreceptors are expressed at midbrain dopaminergic synapses and are activated after dopamine is released from SN or VTA cells (Lindgren et al., 2003). Activation of the autoreceptor hyperpolarizes the presynaptic terminals to inhibit subsequent neurotransmitter release (Lindgren et al., 2003).

Recent studies have shown that D2-GPCRs exert some of their effects in vivo through cAMP-independent mechanisms (Beaulieu et al., 2007). The $G\beta\gamma$ effectors of DRD2 can act as receptor-regulated scaffolds and mediate a variety of receptor signaling and regulatory processes (Lefkowitz and Shenoy, 2005). This new mode of dopamine receptor signaling involves β -arrestin, protein kinase B (Akt) and protein phosphatase 2A (PP2A), proteins that have been classically implicated in GPCR desensitization (Beaulieu and Gainetdinov, 2011). The formation of this complex results in the dephosphorylation/inactivation of Akt by PP2A and the subsequent stimulation of GSK-3 β -mediated signaling (Beaulieu et al., 2005). GSK3 β is a regulator of many cellular functions, including cell architecture, motility, and survival (Jope and Johnson, 2004). In the Wnt signaling pathway, GSK3 β forms a protein complex with PP2A, axin, and casein kinase that regulates the availability of free beta catenin, and in turn, transcription of Wnt-related genes (Jope and Johnson, 2004).

In addition, some neurons express both DRD1 and DRD2 receptors (George and O'Dowd, 2007). The presence of multiple GPCRs in a given cell can regulate many aspects of neuronal signaling. DRD1 and DRD2 can form hetero-oligomers which couple to $G_{\alpha q/11}$ (Rashid et al., 2007). $G_{\alpha q/11}$ activates PLC, which converts phosphatidylinositol-4,5-bisphosphate into diacylglycerol (DAG) and IP3 (Figure 1.2C) (Selbie and Hill, 1998). DAG is a glycerol derivative, which is found at low levels in biological membranes during resting potentials (Merida et al., 2008). Upon stimulation, the PLC isozymes cleave phosphatidylinositol-4,5-bisphosphate (PIP2) into DAG and IP3 (Suh et al., 2008). Phospholipase D (PLD) can also metabolize phosphatidylcholine to form DAG (Brose et al., 2004). The most prominent target of DAG is the protein kinase C (PKC) family of Ser/Thr kinases (Yang and Kazanietz, 2003). Ultimately, integration of signaling properties from both types of G-proteins will play a role in determining how the cell signals in response to dopamine release.

Dysregulation of DA in psychiatric disorders

Schizophrenia (SZ) is a devastating and debilitating mental disorder that affects approximately 1% of the world population (Picchioni and Murray, 2007). Originally described by Kraepelin as “dementia praecox”, the term “schizophrenia”, meaning “split mind”, was coined by the Swiss physician Bleuler (Andreasen and Carpenter, 1993). The disease is characterized by positive symptoms (hallucinations, psychosis, delusions), negative symptoms (withdrawal, avolition, anhedonia), and cognitive deficits that first appear during late adolescence or early adulthood (Picchioni and Murray, 2007). It is widely accepted that a combination of prenatal insults, gene expression, and environmental factors lead to the manifestation of this illness (Lewis and Levitt, 2002,

Karlsgodt et al., 2008). However, several pieces of evidence demonstrate DA system dysfunction in SZ, including: i) DRD2 antagonists ameliorate psychotic symptoms (Seeman, 2006); ii) function of the PFC, a region with DRs that receives DA innervation, is impaired (Seamans and Yang, 2004); iii) postmortem analysis of SZ brains reveals a decrease in (TH)+ and (DAT)+ axons innervating the PFC (Akil et al., 1999); and iv) administration of drugs that elevate the amount of synaptic DA, such as amphetamine and cocaine, induce psychosis in healthy individuals (Seeman et al., 2006).

An imbalance of DA innervation routes is believed to contribute to the symptomology of SZ whereby an overactive mesolimbic system elicits positive symptoms but an underactive mesocortical system leads to negative and cognitive symptoms by hindering cortical processing (Howes and Kapur, 2009). From a neuroanatomical perspective, many lines of evidence suggest that schizophrenia is also a neurodevelopmental disorder of connectivity (McGlashan and Hoffman, 2000). Genetic studies have shown association of the disease with the expression of polymorphisms of many developmental genes including those related to axon guidance, cell adhesion, and patterning of circuitry. These include DISC1, ERBB4, Netrin-G1/G-2, NRG1, PLXN2A, ROBO1, SEMA3A, and SEMA3D (Eastwood et al., 2003, Li et al., 2006a, Mah et al., 2006, Blackwood et al., 2007, Eastwood and Harrison, 2008, Fujii et al., 2011, Vehof et al., 2011). Interestingly, patients with a microdeletion on chromosome 22q11, also called DiGeorge syndrome or velo-cardio-facial syndrome, have a 20-30 fold higher risk of developing schizophrenia than the general population (Gothelf et al., 2009). The genes in the 22q11 region that are deleted encode transcription factors that pattern the formation of the cerebral cortex and genes that modulate DA metabolism, including COMT, FGF8,

PITX2, PRODH, and TBX1 (Prasad et al., 2008, Gothelf et al., 2009). Early life insults, especially those involving the DA system, may profoundly contribute to the pathophysiology of schizophrenia and alter nervous system development in such a way that it cannot be corrected later in life. Understanding how the DA system affects development of the cortex, as well as how DA circuits mature in patients with psychiatric disorders, is crucial to developing treatments for these conditions.

Frontal cortex projections

Cortical neurons make synaptic contact with both local and distant targets. Neurons in cortical layers II and III project via the corpus callosum to contralateral cortical neurons. Layer IV neurons project to the thalamus while layers V and VI project to other subcortical structures including the amygdala, hippocampus, and STR. Therefore, the miswiring of cortical circuitry has the potential to impair the function of multiple brain regions and may result in a wide range of behavioral deficits.

In addition to cognition, the PFC processes information from external stimuli that encode cues for drug-seeking behaviors, anxiety, and fear learning (Davidson, 2002). The PFC projects to the amygdala, a group of nuclei that mediate behaviors of fear, anxiety, and emotional processing (Davidson, 2002, Fuchs et al., 2007). Deficits in associative learning and memory are observed in individuals with schizophrenia, who also display flattened affect, or lack of emotion (Benes, 2010). Structurally, the PFC can be segregated into prelimbic and infralimbic regions that modulate different components of fear processing: prelimbic FC afferent connections to the amygdala are required for the

consolidation and expression of learned fear behaviors, whereas infralimbic FC-amygdala connections modulate extinction behaviors (Corcoran and Quirk, 2007).

Exposure to the psychostimulant drug cocaine increases dopaminergic tone and produces long lasting changes in the brain (Nestler, 2005). Adolescent binge cocaine exposure in rats regulated gene expression in the PFC and resulted in altered attentional processing in adulthood (Black et al., 2006). Cocaine administration can be used induce excess DA signaling in the developing brain. DR activation from cocaine exposure may regulate other PFC-mediated behaviors, such as fear learning and anxiety, by regulating genes that establish PFC-amygdala circuits.

Axon guidance

DR stimulation activates second messenger molecules that have been shown to modulate axon guidance, suggesting that DR-mediated signaling may contribute to the establishment of neuronal circuits (Xiang et al., 2002, Nishiyama et al., 2003, Bouchard et al., 2004, Rajadhyaksha and Kosofsky, 2005). During development of the cerebral cortex, neural progenitor cells proliferate in the ventricular zone (VZ), a region bordering the lateral ventricle of the forebrain (Caviness et al., 2008). Neurons born in the VZ migrate along radial glia columns to the 6 layers of the cortex in an inside-out fashion, such that deep layer 6 forms first and more superficial layers form last (Caviness et al., 2008). Once they have reached their laminar position, neurons extend axonal processes and their growth cones begin the course of axon pathfinding (Caviness et al., 2008). Axon guidance factors influence the directional steering of axonal growth cones throughout the entire nervous system (Charron and Tessier-Lavigne, 2005). Axonal

pathfinding allows neurons to locate their target synaptic location and is essential for establishment of neurotransmission. In the cerebral cortex, this time period coincides with the innervation of DRs from efferent dopaminergic axons (Van den Heuvel and Pasterkamp, 2008).

Classification of axon guidance molecules

Molecules present in the neuronal environment guide axons to their targets where synapse formation will occur (Chen and Cheng, 2009). The classical axon guidance molecules (AGMs) are categorized into four main groups: netrins, slits, ephrins, and semaphorins (see table 1.1) (Plachez and Richards, 2005). Netrin, Sanskrit for “one who guides”, is a secreted molecule that interacts with its receptors, deleted in colorectal cancer (DCC), uncoordinated 5 (UNC5), and Down’s syndrome cell adhesion molecule (DSCAM) on the cell surface to mediate attraction or repulsion (Moore et al., 2007). Other forms of netrin, including netrin G1 and G2, have recently been characterized as membrane bound axon guidance molecules that interact with netrin-g ligands (Rajasekharan and Kennedy, 2009). Slits are secreted molecules that only mediate repulsive events through the roundabout (ROBO) family of receptors (Bashaw and Klein, 2010). The semaphorins are a large group of axon guidance molecules with many different subgroups that mediate repulsion or attraction by interacting with neuropilin (NRP) and plexin receptors (Tamagnone and Comoglio, 2000). Ephrins are membrane bound ligands that interact with eph receptors to signal contact-mediated repulsive events (Bashaw and Klein, 2010). While many distinct patterns of expression exist for these axon guidance molecules throughout the nervous system, the combined expression of

guidance cues, receptors, and environmental signals in a given cell dictates the direction of outgrowth for an axon (Gallo and Letourneau, 1999, Yu and Bargmann, 2001).

TABLE 1.1: Classification of axon guidance families.

Family	Secreted/Membrane bound	Receptors	Attractive or repulsive
Ephrin	Membrane-bound	Ephs	Repulsive
Netrin	Both	DCC, UNC-5, DSCAM	Both
Slit	Secreted	Robos	Repulsive
Semaphorin	Both	Plexins and Neuropilins	Both

Mechanisms of axon guidance

Mechanisms for axon guidance differ depending on the signal transduction cascade of a given receptor but essentially all guidance events begin with the reorganization of the actin cytoskeleton in the growth cone region (Gallo and Letourneau, 2004). The activation of a receptor signals GTPase molecules to trigger biochemical cascades involved in a number of cellular processes related to axon outgrowth and cytoskeletal remodeling (Dickson, 2001). In the GDP-bound form, GTPases are activated by guanine exchange factors (GEFs) that exchange GDP for GTP (Hall and Lalli, 2010). Conversely, GTPase activity is increased by GTPase-activating proteins (GAPs), that lead to attenuation of GTPase activity (Hall and Lalli, 2010). Repulsive events are triggered by the activation of the GTPase Rho, which causes the formation of stress fibers, growth cone collapse, retraction of lamellipodia and filopodia, and depolymerization of actin (O'Donnell et al., 2009). Repulsion requires the growth cone to change the direction of axon outgrowth, away from the source of the repulsive axon guidance molecule, and towards an environment that is permissible for reestablishment of

the growth cone (Plachez and Richards, 2005). Attraction is mediated by the inhibition of Rho and the activation of the GTPases Cdc42 and Rac, which promote the formation of lamellipodia and filopodia on the growth cone, resulting in actin polymerization and extension of the growth cone towards the source of the guidance factor (O'Donnell et al., 2009). Rac is also required for some repulsive events but its activation is receptor-specific (O'Donnell et al., 2009). Each family of AGMs has a unique signal transduction cascade involving the activation or inhibition of effector molecules that transduce signals from GTPases into cytoskeletal rearrangement, resulting in the directional steering of the axon (Hall and Lalli, 2010).

Axon guidance events are extremely sensitive to changes in the neuronal environment and can be modified rapidly. Micropipette manipulations of axon guidance molecules can induce growth cone collapse within just 10 minutes and enhance attraction in 15 minutes (Lin and Holt, 2007). These robust effects require asymmetrical organization of actin polymerization for directional steering, and the translation of new proteins within close proximity of the advancing growth cone (Leung et al., 2006, Lin and Holt, 2007). A number of second messenger molecules involved in GPCR signaling cascades have been shown to modulate the response to a guidance cue. Increases in cyclic nucleotides enhance attraction while decreases trigger repulsion (Piper et al., 2007). Likewise, activation of PKA, PI3K, and PLC γ cause attraction while their inhibition causes repulsion (Akiyama and Kamiguchi, Ming et al., 1999, Bouchard et al., 2004). These effects are most likely accomplished through the regulation of L-type calcium channels and intracellular calcium channels (Xiang et al., 2002, Nishiyama et al., 2003). Local calcium transients in the growth cone can greatly influence axon guidance

events, whereby too much or too little calcium will cause repulsion but an optimum amount mediates attraction (Gomez and Zheng, 2006).

Netrin-1 mediated axon guidance

Netrin-1 (ntn-1) is a secreted cue that guides axons over short and long distances (Rajasekharan and Kennedy, 2009). Under basal conditions, a small amount of the ntn-1 receptor DCC is present on the plasma membrane surface and vesicular stores of DCC are maintained near the growth cone (Bouchard et al., 2004). The interaction of ntn-1 with a DCC receptor on the surface of a growth cone leads to the formation of DCC homodimers and the activation of a DCC-anchored signaling complex that contains focal adhesion kinase (Fak) and non-catalytic region of tyrosine kinase adaptor protein 1 (Nck1) (Figure 1.3A) (Shekarabi et al., 2005). Ntn-1 binding induces Fak autophosphorylation and recruits the Src family kinases Src and Fyn to phosphorylate the cytoplasmic tail of DCC (Round and Stein, 2007). These events lead to the activation of the GTPases Cdc42 and Rac1 and the inhibition of Rho (O'Donnell et al., 2009). The effector molecule Pak1 links Cdc42 and Rac1 with the scaffold protein Nck1, while Trio and Dock1 function as GEFs for Rac1 (Lai Wing Sun et al., 2011). DCC signaling also regulates Arp2/3 activity and activates the actin-binding proteins neuronal Wiskott-Aldrich syndrome protein (N-WASP) and Enabled/vasodilator-stimulated phosphoproteins (ENA/VASP), which not only mediate actin assembly but also function as modulators of synapse formation as the growth cone advances to its target (Lai Wing Sun et al., 2011). The combined result of these effects is directed attraction of an advancing growth cone toward the ntn-1 gradient.

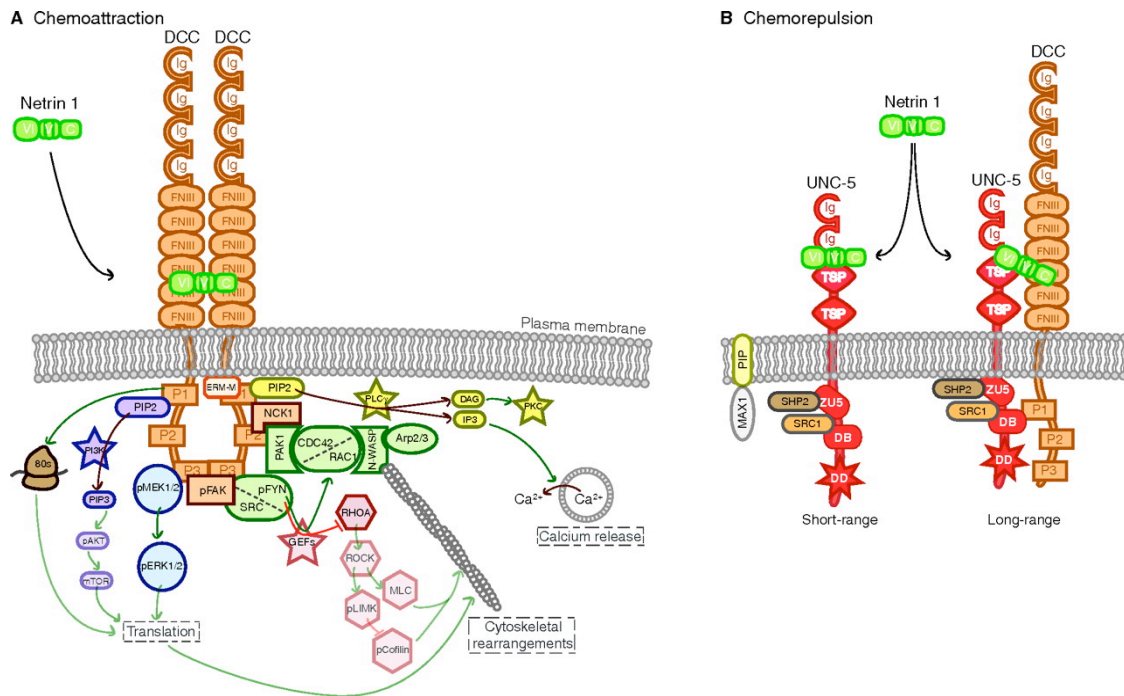


FIGURE 1.3: Ntn-1 signaling pathways.

(A) Chemoattraction mediated by the DCC receptor. (B) Chemorepulsion mediated by DCC and UNC5 receptors. **Adapted from Lai Wing Sun et al. *Development* (2011).**

Abbreviation: 80s, eukaryotic ribosomes; Arp2/3, complex of the actin-related proteins ARP2 (ACTR2) and ARP3 (ACTR3); CDC42, cell division cycle 42; DAG, diacylglycerol; ERM-M, ezrin/radixin/moesin and merlin protein family; GEFs, guanine exchange factors; IP3, inositol 1,4,5-triphosphate; MAX1, motor axon guidance PH/MyTH4/FERM domain cytoplasmic protein; MLC, myosin light chain; mTOR, mammalian target of rapamycin; N-WASP, neuronal Wiskott-Aldrich syndrome protein; NCK1, non-catalytic region of tyrosine kinase adaptor protein 1; pAKT, phosphorylated RAC-alpha serine/threonine protein kinase; pCofilin, phosphorylated cofilin; pERK1/2, phosphorylated extracellular signal-regulated kinase 1/2; pFAK, phosphorylated focal adhesion kinase; pFYN, phosphorylated Src family kinase FYN; pLIMK, phosphorylated LIM domain kinase 1; pMEK1/2, phosphorylated mitogen-activated protein kinase kinase 1/2; PAK1, p21-activating kinase 1; PI3K, phosphatidylinositol-3 kinase; PIP, phosphatidylinositol phosphate; PIP2, phosphatidylinositol (4,5) bisphosphate; PIP3, phosphatidylinositol (3,4,5) triphosphate; PKC, protein kinase C; PLCγ, phospholipase Cγ; RAC1, ras-related C3 botulinum toxin substrate 1; RHOA, Ras homologue gene family member A; ROCK, RhoA kinase; SHP2, Src homology region 2 domain-containing phosphatase 2; SRC, tyrosine kinase sarcoma.

Work in a *Drosophila* model indicates that the UNC5 receptor alone can mediate short-range repulsive events but DCC is required for long-range repulsion from ntn-1 (Figure 1.3B) (Keleman and Dickson, 2001). In mammals, repulsion from ntn-1 cues is mediated by heterodimers of DCC and UNC5 receptors (Hong et al., 1999). Ntn-1 binding leads to the phosphorylation of multiple residues on the intracellular part of UNC5 and the recruitment of the tyrosine phosphatase Shp2 (Tong et al., 2001, Li et al., 2006b). While these effects are mediated by Src and Fak (Li et al., 2006b), little is known about the effector molecules that function downstream of UNC5 activation or how the DCC receptor participates in repulsive signaling cascades. Shp2 can regulate activity of a number of effectors and second messengers known to induce cytoskeletal remodeling, including PLC γ , PI3K, and RhoA, but additional studies are needed to link UNC5 involvement to these pathways (Tong et al., 2001, Round and Stein, 2007).

As mentioned above, ntn-1-mediated axon guidance properties are sensitive to neuronal changes induced by second messenger cascades, many of which are regulated by DR signaling. For example, the two classes of DRs modulate neurotransmission and cell excitability by regulating the activity of ion channels and intracellular calcium levels (Surmeier et al., 2007). Neuronal depolarization and PKA activation can rapidly enhance netrin-mediated insertion of DCC into the plasma membrane (Bouchard et al., 2004, Bouchard et al., 2008, Nishiyama et al., 2008). PKA activation alone does not have the ability to mediate axon outgrowth or switch a cue from repulsion to attraction, but it can modify a growth cone's sensitivity to ntn-1 gradients (Moore and Kennedy, 2006). The ratio of the cyclic nucleotides cAMP and cGMP, as well as intracellular calcium levels, can determine if a cell is attracted or repelled from ntn-1 (Ming et al., 1997, Hong et al.,

2000, Nishiyama et al., 2003). Calcium-mediated activation of calcium/calmodulin dependent protein kinase II (CamKII) and calcineurin phosphatase I (PPI), which have been studied extensively for their role in dopaminergic and glutamatergic neurotransmission, induce attraction or repulsion, respectively, to ntn-1 cues (Wen et al., 2004).

Currently, it is not known if DR stimulation alone can modify ntn-1 mediated axon guidance. The aforementioned studies suggest that activation of a GPCR cascade involving $G_{\alpha s}$ will promote attraction to ntn-1 through the regulation of PKA, cAMP, and L-type calcium channels. Conversely, activation of $G_{\alpha i}$ may trigger repulsion from ntn-1 by inhibiting activity of these signaling molecules. This theory is supported by data that indicate that the Unc5 homolog Unc5H2 can associate with the $G_{\alpha i}$ protein in the presence of cAMP (Komatsuzaki et al., 2002). Under conditions of ntn-1 mediated attraction, Unc5 might bind $G_{\alpha i}$ to ensure attraction and not repulsion (Komatsuzaki et al., 2002). Decreases in cAMP would release Unc5 from $G_{\alpha i}$, allowing $G_{\alpha i}$ to inhibit adenylyl cyclase production and decrease cyclic nucleotide levels (Komatsuzaki et al., 2002).

Dopamine has the ability to activate both $G_{\alpha s}$ and $G_{\alpha i}$, as well as a third g-protein, $G_{\alpha q}$, which could also regulate axon guidance through activation of the second messenger molecules PLC, IP3, and PI3K (Ming et al., 1999, Xiang et al., 2002). Additionally, another monoamine, serotonin (5-HT), has been shown to function as a modulator of ntn-1-mediated guidance in the mouse brain (Bonnin et al., 2007). 5-HT receptors, like DRs, are GPCRs and stimulation of 5-HT_{1B} and 5-HT_{1D} receptors, which both couple to $G_{\alpha i}$, converts attractive ntn-1 cues to repulsive cues (Bonnin et al., 2007). *In vivo* data with in

utero electroporation of 5-HT_{1B/1D} siRNA in E14 mouse thalamocortical axons revealed drastic changes in the trajectory of these axons, suggesting that monoamine receptor stimulation is required for ntn-1-mediated guidance events (Bonnin et al., 2007). The interaction of g-proteins with netrin receptors represents a novel field of study that may explain the relationship between neurotransmitter systems and developmental cues in establishing neuronal circuitry.

Regulation of axon guidance molecules by DA signaling

Given the role that AGMs play in the establishment of neuronal circuitry, it is imperative that their signaling mechanisms are tightly regulated. Recent studies have shown that AGMs are regulated by DR agonists and psychostimulants that increase dopaminergic tone (Halladay et al., 2000, Bahi and Dreyer, 2005, Jassen et al., 2006, Yetnikoff et al., 2007). In a neuroepithelial cell line, the DRD1 agonist SKF81927 and the partial DRD1/DRD2 agonist dihydrexidine regulated expression of receptors for ntn-1, ephrin, and semaphorin (Jassen et al., 2006). Pre- and peri-natal cocaine exposure increased expression of EphB1 the cortex and STR (Halladay et al., 2000).

Interestingly, drugs of abuse regulate axon guidance molecules and their receptors in adolescent and adult animals, well after initial axon guidance events have taken place. Amphetamine administration in adolescent rats increased protein expression of both ntn-1 receptors in the PFC (Yetnikoff et al., 2007). An extensive study in adult rats showed regulation of semaphorin and ephrin family molecules in multiple brain regions after acute and chronic cocaine exposure, as well as in response to cocaine sensitization and withdrawal (Bahi and Dreyer, 2005). Large, treatment-specific patterns of regulation

were observed, with some genes regulated by a cocaine challenge after withdrawal, and others regulated throughout all treatment paradigms (Bahi and Dreyer, 2005). These data suggest that the regulation of axon guidance molecules in response to cocaine may be associated with other processes that contribute to the addiction process- such as the onset of addiction and cravings, drug reinstatement cues, or withdrawal.

Expression of AGMs in adult animals suggests that AGMs have another role after axon guidance processes cease, such as the maintenance of synapses and dendritic architecture. This could be a mechanism of plasticity following the drug treatment, emphasizing the importance to study the effects of DR stimulation in development as well as postnatal periods. The interaction of DA signaling properties with axon guidance systems may represent not only a relationship that is crucial for circuit formation, but also one that contributes to the behavioral and cognitive impairment in psychiatric illnesses.

Rationale

The DA system modulates frontal cortex (FC) activities such as working memory and attentional processing. Dysfunction of the FC has been observed in psychiatric illnesses with a neurodevelopmental basis and thus processes that govern the formation of FC circuitry need to be thoroughly understood. In the developing rodent brain, DRs are expressed in the FC during periods of axonal pathfinding. Ntn-1 is a secreted axon guidance cue that guides cortical neurons that express its receptors, DCC and UNC5C. DCC homodimers mediate attraction, while DCC-UNC5C heterodimers cause repulsion. DR stimulation activates G-proteins that regulate molecules known to influence ntn-1

mediated axon guidance, including cyclic nucleotides, protein kinase A (PKA), phospholipase C (PLC), and calcium. Abnormalities in DR activity during ntn-1 mediated axon guidance may alter FC neuronal circuitry and lead to dysfunction of the FC later in life.

Hypothesis

We hypothesized that DR stimulation during early cortical development regulates the response of cortical neurons to the ntn-1 cue and can alter PFC-mediated behaviors later in life.

Specific Aims of Thesis

- I. Determine expression levels of the ntn-1 system and DRs in the developing rodent FC.
- II. Determine how DR stimulation affects the expression levels of ntn-1 receptors.
- III. Determine how DR stimulation affects FC axon guidance in the presence of ntn-1.
- IV. Determine the effect of adolescent cocaine administration on PFC-associated behaviors of fear and anxiety.

CHAPTER II

EXPRESSION AND FUNCTION OF DOPAMINE RECEPTORS IN THE DEVELOPING MEDIAL FRONTAL CORTEX AND STRIATUM OF THE RAT

Abstract:

The timeline of dopamine (DA) system maturation and the signaling properties of dopamine receptors (DRs) during rat brain development are not fully characterized. We used in situ hybridization and quantitative PCR to map DR mRNA transcripts in the medial frontal cortex (mFC) and striatum (STR) of the rat from E15 to E21. The developmental trajectory of DR mRNAs revealed distinct patterns of DA receptors 1 and 2 (DRD1, DRD2) in these brain regions. Whereas the mFC had a steeper increase in DRD1 mRNA, the STR had a steeper increase in DRD2 mRNA. Both DR mRNAs were expressed at a higher level in the STR compared to the mFC. To identify the functional properties of DRs during embryonic development, the phosphorylation states of CREB, ERK1/2, and GSK3 β were examined after DR stimulation in primary neuronal cultures obtained from E15 and E18 embryos and cultured for three days to ensure a stable baseline level. DR-mediated signaling cascades were functional in E15 cultures in both brain regions. Because DA fibers do not reach the mFC by E15, and DA was not present in cultures, these data indicate that DRs can become functional in the absence of DA innervation. Since activation of DR signal transduction pathways can affect network organization of the developing brain, maternal exposure to drugs that affect DR activity may be liable to interfere with fetal brain development.

Introduction

The monoamine dopamine (DA) modulates neurotransmission and neuronal excitability via activation of second messenger cascades coupled to DA receptors (DRs). DRs are g-protein coupled receptors (GPCRs), characterized by the g-protein that they couple to: DRD1 “like” couple to G_{α_s} and DRD2 “like” couple to G_{α_l} (Girault and Greengard, 2004, Neve et al., 2004, Seamans and Yang, 2004, Bronson and Konradi, 2010). Abnormal function of the DA system has been associated with neuro-psychiatric disorders such as Parkinson’s disease, attention deficit hyperactivity disorder (ADHD), and schizophrenia (Barzilai and Melamed, 2003, Goto and Grace, 2007, Genro et al., 2010). The DA system is furthermore involved in reward pathways and addiction to drugs such as cocaine and amphetamine (Kauer and Malenka, 2007).

While DA pathways have been studied in great detail in the adult brain, the role and functional state of the DA system during development is not well established in rats. In the rodent brain, DRs have been detected in mid to late embryonic development in the medial frontal cortex (mFC), a heavily interconnected brain area involved in attention, cognition, and working memory (Schambra et al., 1994). At around the same time, DA receptors appear in the striatum (STR), a brain area implicated in motor behavior, motivation, and reward (Sales et al., 1989, Jung and Bennett, 1996, Arnsten and Li, 2005, Araki et al., 2007, Van den Heuvel and Pasterkamp, 2008). During early brain development, events such as cell proliferation, differentiation, neuronal migration, and axon guidance are creating neuronal patterns and connections that determine brain function throughout life. Neuronal progenitor cells from the ventricular zone proliferate and begin to populate cortical layers V and VI around embryonic day (E) E15 in the rat

brain (Kriegstein et al., 2006). Simultaneously, interneurons from the ganglionic eminences migrate tangentially into the cortex (Marin and Rubenstein, 2001). Midbrain ventral tegmental area (VTA) and substantia nigra (SN) neurons project via the medial forebrain bundle (MFB), arriving in the ventral and lateral regions of the rat STR at E14, and in the remaining areas of the STR by E18. MFB projections from the VTA continue past the STR and reach the subplate and intermediate zone of the mFC at E18 (Verney et al., 1982, Berger et al., 1983, Kalsbeek et al., 1988). DA positive fibers remain in this region for two days before entering the cortical plate at E20 (Van den Heuvel and Pasterkamp, 2008).

Because the rodent brain undergoes rapid changes during embryogenesis, a detailed characterization of the spatial and temporal expression patterns of DRD1 and DRD2 in the prenatal rat brain is essential. It is currently not known at what age DRs become functional and whether their signaling cascades in the embryonic brain reflect the known properties of DRs in adult animals.

In adult neurons, DRD1 activates adenylate cyclase, increases levels of cyclic nucleotides, activates protein kinase A (PKA) and mediates the phosphorylation of substrate molecules such as cyclic AMP response element binding protein (CREB) (Dudman et al., 2003), and extracellular signal-related kinase 1/2 (ERK1/2) (Valjent et al., 2000). DRD2 stimulation inhibits adenylate cyclase (Enjalbert and Bockaert, 1983) and activates beta arrestins and protein phosphatase 2A (PP2A) which inhibit protein kinase B (Akt), leading to the dephosphorylation and activation of glycogen synthase kinase 3 beta (GSK3 β), a kinase involved in Wnt signaling (Cross et al., 1995, Beaulieu et al., 2009).

DRs activated in the embryonic brain modify neuronal migration, cell cycle activity, and cell morphology (Sales et al., 1989, De Vries et al., 1992, Todd, 1992, Schmidt et al., 1996, Stanwood et al., 2001, Song et al., 2002, Zhang and Lidow, 2002, Ohtani et al., 2003, Popolo et al., 2004, Zhang et al., 2005, Crandall et al., 2007). Recent studies indicate that monoamines and their signaling pathways can modulate axon guidance events in the embryonic brain by altering levels of cyclic nucleotides in the growth cone (Ming et al., 1997, Ming et al., 1999, Halladay et al., 2000, Nishiyama et al., 2003, Bouchard et al., 2004, Bonnin et al., 2007). Moreover, stimulation of the DA system in the adult brain, via external factors such as drugs of abuse, has also been shown to regulate axon guidance molecules in various brain regions (Bahi and Dreyer, 2005, Jassen et al., 2006, Yetnikoff et al., 2007, Sullivan et al., 2011).

Knowledge of the expression and functional state of DRD1 and DRD2 during early embryonic development is vital for our understanding of how the DA system contributes to cortical and subcortical organization and thus might be involved in the developmental aspects of neuro-psychiatric disorders such as schizophrenia. In the present study, we address this question in the mFC and STR of the developing rat brain.

Material and Methods:

Animals

All animals were housed and maintained in accordance with the policies of Vanderbilt University, which is accredited by the Association for the Assessment of Accreditation of Laboratory Animal Care. Timed-pregnant female Sprague-Dawley rats (Charles River, Wilmington, MA) were anesthetized with pentobarbital (65mg/kg,

Sigma, St. Louis, MO) and embryos were removed and washed in sterile phosphate buffered saline (PBS).

Primary neuronal cultures

mFC or STR tissue from E15 and E18 embryos were dissected under a stereo microscope (see figure 2.1), dissociated in media, and plated onto 6 well plates at a density of approximately 500,000 cells per well, as previously described (Rajadhyaksha et al., 1999). For stimulation of DRs, cells were grown for 72 hours in vitro and treated for 15 minutes with 50 μ M of the DR agonists (+)-SKF 82958 hydrobromide, or (\pm)-PPHT hydrochloride (N-0434) (Sigma). Experiments were carried out at least in duplicates and in at least two independent dissections.

Generation of nested RNA Probes

RNA extraction and cDNA synthesis were performed as previously described (Sullivan and Konradi, 2011). PCR products were used for vitro transcription with modifications of a published protocol (Kuppenbender et al., 2000). Two sets of nested primers were designed for each target sequence within DRD1 and DRD2 with the help of Primerblast (<http://www.ncbi.nlm.nih.gov/tools/primer-blast>), whereby the internal primer pair included sequences that encoded either Sp6 or T7 RNA polymerase recognition sites (table 2.1A). One μ g of the nested PCR product was used to synthesize digoxigenin-labeled RNA probes using Sp6 (sense) or T7 (antisense) polymerase with the Dig RNA Labeling Kit (Roche Applied Science, Porterville, CA).

Northern blot method

Three μg of whole rat brain RNA was loaded per well of a denaturing formaldehyde gel (1X 4-Morpholinepropanesulfonic acid (MOPS) with 10% formaldehyde). Following size-separation, RNA was electrophoretically transferred to a charged nylon membrane in 1X tris-acetate-ethylenediaminetetraacetic acid (EDTA) (TAE) buffer. The membrane was UV-crosslinked and dried overnight before hybridization. Prehybridization was carried out in NorthernMax Hybridization Buffer (Ambion, Austin, TX) followed by hybridization of probe at 0.25 ng/ μl . The membrane was washed twice at room temperature in 2X saline-sodium-citrate (SSC) buffer and twice at 65°C in 0.2XSSC for 30 minutes. The membrane was incubated in blocking solution (100mM Tris-HCl, 150mM NaCl with 3% blocking reagent; Roche) followed by alkaline phosphatase-conjugated anti-digoxigenin antibody at a 1: 50,000 dilution (Roche). After washing in 0.1M maleic acid buffer (pH 7.5), the membrane was equilibrated with diluted (1:250) alkaline-phosphatase luminescent substrate 2-chloro-5-(4-methoxyspiro(1,2-dioxetane-3,2'-(5'-chloro)tricyclo[3.3.1.1^{3,7}]decan)-4-yl)-phenylphosphate (CDP-Star) (Roche) and imaged using a Kodak I440 CS Imaging system (Kodak, Rochester, NY).

In situ hybridization

Embryonic brains were fixed overnight in 4% paraformaldehyde (PFA), freeze-protected in a series of graded sucrose solutions (10-30%), and cut to a thickness of 20 μm on a cryostat. Hybridization was carried out as described (Bonnin et al., 2007) with modifications. A cocktail of three digoxigenin-labeled probes, covering three separate

mRNA stretches for each gene of interest was hybridized at a concentration of 0.25-ng/ μ l per probe to the sections for 18 hours at 60°C. Adjacent sections were incubated in parallel with antisense and sense probes to control for nonspecific binding, and each slide contained brain slices from an entire developmental set (E15, E17, E19, E21). Following hybridization, sections were blocked with 3% blocking reagent (Roche) and incubated overnight in alkaline phosphatase-conjugated anti-digoxigenin antibody at 1:2,000 dilution (Roche). The phosphatase reaction was carried out in a solution containing 0.2mM 5-bromo-4-chloro-3-indolyl phosphate (BCIP) and 0.2mM nitroblue tetrazolium (NBT). Sections were dehydrated and mounted with Permount (Fisher). Images were captured using Stereo Investigator software (MBF BioScience, Williston, VT). Densitometric analyses were done with Kodak Imaging software using 2 animals per time point. Measurements were taken from the cortical plate of the mFC and the STR (see figures 2.2, 2.3). To control for nonspecific hybridization and endogenous phosphatase activity, the intensity of the antisense signal was normalized to the sense signal from each adjacent section.

QPCR

For mRNA analysis of DRs in tissue, samples were collected from E15, E17, E19, and E21 embryos and frozen at -80°C until RNA extraction. RNA extraction, cDNA synthesis, and QPCR were performed as previously described (Sullivan and Konradi, 2011). Prior to cDNA synthesis, RNA was treated with DNase I, amplification grade (Invitrogen), for 15 minutes at room temperature to prevent DNA contamination. DNase activity was stopped with 25mM EDTA and incubation at 65°C. Primer sequences are

listed in table 2.1B. All samples were examined in duplicate and values were normalized to the internal controls β -actin and 18S ribosomal RNA (18S rRNA), two genes that are among the more evenly expressed during development (McCurley and Callard, 2008). To ensure that the normalization control genes were not introducing false results, all data were analyzed without normalization, with each individual normalization control gene and with both normalization control genes combined. Although β -actin had a tendency to be regulated in the same direction as the dopamine receptor mRNAs, comparable statistical differences were seen in each analysis. Each QPCR plate had a standard curve of which efficiency and coefficient of determination values were examined to verify the quality of the experiment. Expression levels were calculated using the formula $(1/2^{\Delta Ct})$ and all data were collected at the same fluorescence threshold. Five samples were analyzed for each time point with each sample generated from multiple animals. Each individual QPCR sample was composed of tissue from 4 animals for E15, 3 animals for E17, and 2 animals for E19 and E21.

Western Blotting

Primary neuronal cultures were harvested in 1X Laemmli buffer and sonicated. Samples were heated to 80°C for 10 minutes and separated on 10-20% Tris-Glycine gradient gels (Invitrogen). Proteins were transferred to polyvinylidene fluoride (PVDF) membranes (Perkin Elmer, Waltham, MA) and membranes blocked with animal-free blocking solution (Vector Laboratories, Burlingame, CA). Primary antibodies were diluted in blocking solution and incubated with membranes overnight at 4°C. The following antibodies were used: anti-phospho CREB (Serine 133) 1:4000, anti-phospho

TABLE 2.1: List of primer sequences used for synthesis of in situ probes (A), and QPCR (B).

A) Primers used to synthesize RNA probes		
Name	Genbank #	sequence
DRD1 outer primer 1	NM_012546.2	F: 5'-ACCTCCCTGGAGGACACCGA-3' R: 5'-AGAGCCACAGAAGGGCACCA-3'
DRD1 outer primer 2	NM_012546.2	F: 5'-TGAGGGGCAAGTCCCCGGAA-3' R: 5'-AGCCCAGTACCTGTCCACGCT-3'
DRD1 outer primer 3	NM_012546.2	F: 5'-GCCACGAGTCCCTTGGGCTT-3' R: 5'-ATCCCACTCCTGCTGTAAGGCT-3'
DRD2 outer primer 1	NM_012547.1	F: 5'-AGGCAGACAGGCCCCACTACA-3' R: 5'-TCCGAAGAGCAGTGGCCAGGA-3'
DRD2 outer primer 2	NM_012547.1	F: 5'-TCCATCCCACCACGGCCTACA-3' R: 5'-TGTGCAGGCAAGGGGCAGAC-3'
DRD2 outer primer 3	NM_012547.1	F: 5'-TGCCAACCCTGCCTTTGTGTC-3' R: 5'-GCTGGTGGTGACTGGGAGGGAT-3'
DRD1 nested primer 1	NM_012546.2	F: 5'-AAGCATTTAGGTGACACTATACTTTTACATCCCCGTAGCCA-3' R: 5'-AAGCTCTAATACGACTCACTATAGGGAACACCCCATGATCACAGA-3'
DRD1 nested primer 2	NM_012546.2	F: 5'-AAGCATTTAGGTGACACTATACTGCCACCCGAGAGGGATT-3' R: 5'-AAGCTCTAATACGACTCACTATAGGGTGGACGCCGTAGAGCACATGA-3'
DRD1 nested primer 3	NM_012546.2	F: 5'-AAGCATTTAGGTGACACTATAACAGGAGATCCCTCTGCTGCTT-3' R: 5'-AAGCTCTAATACGACTCACTATAGGGTCTCGGACAGTTTTAGCACCTG-3'
DRD2 nested primer 1	NM_012547.1	F: 5'-AAGCATTTAGGTGACACTATACTGGTGTGCATGGCTGTATC-3' R: 5'-AAGCTCTAATACGACTCACTATAGGGCTTGGAGCTGTAGCGTGTGT-3'
DRD2 nested primer 2	NM_012547.1	F: 5'-AAGCATTTAGGTGACACTATAAGGCAAAACCCGGACCTCCCT-3' R: 5'-AAGCTCTAATACGACTCACTATAGGGAGGCCCTTGCGGAACTCGATG-3'
DRD2 nested primer 3	NM_012547.1	F: 5'-AAGCATTTAGGTGACACTATACTGCCCTTATCGTCACTCTGC-3' R: 5'-AAGCTCTAATACGACTCACTATAGGGTGGGGGACTGGTCTTGACAG-3'
B) Primers used for QPCR		
Name	Genbank #	sequence
DRD1	NM_012546.2	F: 5'-GCGTGATCAGCGTGGACAGG-3' R: 5'-AGGGCCATGTGGGCTTTGCC-3'
DRD2	NM_012547.1	F: 5'-GGTGGCCACACTGGTAATGCC-3' R: 5'-CAGTAACTCGGCGCTTGGAGCT-3'
18s RNA	V01270.1	F: 5'-TGGCTCAGCGTGTGCCTACC-3' R: 5'-TAGTAGCGACGGCGGTGTG-3'
Beta actin	NC_005111	F: 5'-CTATGAGCTGCCTGACGGT-3' R: 5'-TGGCATAGAGGTCTTTACGGA-3'

ERK1/2 (P44/42 MAPK-Threonine 202/Tyrosine 204) 1:2000, and anti-phospho GSK3 β (Serine 9) 1:2000 (Cell Signaling, Danvers, MA). Membranes were washed 6 times in 50mM tris-buffered-saline with 0.05% tween-20 (TBS-T) and incubated for 30 min at room temperature with horseradish peroxidase (HRP)-conjugated secondary antibodies (Vector Laboratories) prepared in blocking solution. Blots were immersed in chemiluminescent reagents (Pierce, Rockford, IL) and exposed using a Kodak Imaging Station. MemCode Reversible Protein Stain (Thermo Scientific, Rockford, IL) was used prior to immunodetection to measure total protein per well. Proteins of interest were

normalized to total protein (Aldridge et al., 2008) or beta actin (1:20,000; Sigma), detailed in the figure legends.

Statistics

Analyses of variance (ANOVAs) were applied to developmental timecourses of each receptor, and multivariate ANOVAs were applied to compare differences in the developmental trajectories between DRD1 and DRD2 mRNA expression levels (repeated measures), as well as between mFC and STR. Post-hoc tests included paired t-tests to compare the expression of DRD1 to DRD2 within each sample at each time point and unpaired t-test for comparisons between the mFC and STR. For western blots and in situ hybridization, unpaired t-tests were used for 2-group comparisons and ANOVAs in cases of 3 or more groups. The JMP computer program (Cary, NC) was used for all analyses. Multiple comparison corrections were carried out for Western blots using the correction method developed by Benjamini and Hochberg (Benjamini and Hochberg, 1995), correcting for the three different phosphorylation antibodies within each time point and brain area. However, since Western data are only semi-quantitative and were obtained from independent dissections with independent control samples, multiple-comparison corrections might not be appropriate and may introduce false-negative findings. This is supported by the observation that some of the significant data that did not survive multiple-comparison corrections should be significant according to the literature (see ‘Results’ for details). We therefore present simple t-tests and note whenever data did not survive multiple comparison corrections.

Results

Detection of DR mRNA transcripts in the developing rat brain

The individual probes for DRD1 and DRD2 detected a single band of mRNA transcript of the expected size (figure 2.1A). mRNA expression of DRD1 and DRD2 was assessed spatially and temporally by *in situ* hybridization in coronal brain slices of embryonic rats from E15 to E21, at two different levels for mFC and STR (figure 2.1B).

In both brain areas, little expression of DR mRNAs was detected at early time points but expression increased for both receptors over time (figure 2.2, 2.3). In a preliminary analysis, we used t-tests to compare the expression levels of DRD1 and DRD2 mRNA at each developmental time point after subtracting the sense intensity measure from the antisense intensity to correct for background levels (figure 2.4A, 2.4B). Whereas no significant differences were seen at early time points, levels of DRs were significantly different at E19 in the mFC and at E21 in the STR. This analysis suggested that the trajectories of DRs were divergent, with more DRD1 mRNA in the mFC, compared to DRD2, but more DRD2 than DRD1 in the STR.

Quantification of DR mRNA transcripts by QPCR analysis

The *in situ* method provided an anatomical overview over the brain areas of interest, but it was only semi-quantitative and for repeated measures relied on densitometry estimates across different slides with some variation in background intensities. For quantification purposes we employed QPCR analysis in samples from an independent cohort of embryonic rats, a method well suited for a comprehensive

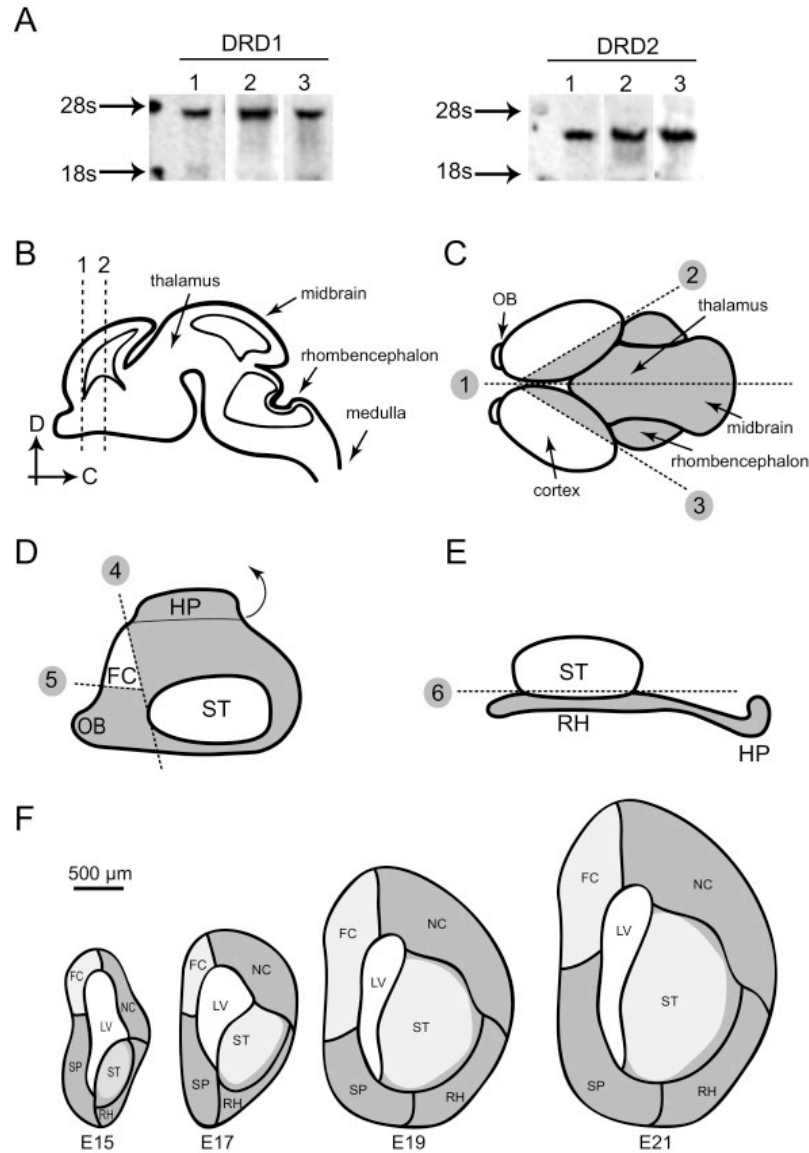


FIGURE 2.1: Generation of DR probes to measure mRNA transcripts in rat brain.

Three non-overlapping RNA probes were generated for both DRD1 and DRD2 and combined for *in situ* hybridization studies. Each probe (labeled ‘1’, ‘2’, ‘3’) was examined individually in Northern blots using RNA from whole rat brain (A). Arrows indicate the 28S and 18S rRNA bands. Expected size of DRD1 mRNA is approximately 4 kB and DRD2 is approximately 2.7kB (Beaulieu et al., 2007, Iwakura et al., 2008). The approximate size of the 28S band in rats is 4.8 kB and 18S is 1.9 kB. (B) Schematic of an embryonic rodent brain. For *in situ* analyses, probes were hybridized to coronal sections taken from the mFC (1) or STR (2). D=dorsal, C=caudal. (C-E) Dissection strategy for primary neuronal cultures, QPCR and Western blots. (C) Dorsal view with the first three cuts (1-3) that removed septum and midbrain. (D) Hemispheres were rotated to a sagittal view from the lateral ventricle onto the inside of the cortex. The part of the hippocampus that was not removed by cuts 2 or 3 was lifted up and FC was cut out as shown (cuts 4 and 5). (E) Coronal view to show how striatum was removed from RH and NC (cut 6). (F) Coronal brain slices from E15 to E21. The lighter colored regions indicate the approximate area of mFC and STR dissected. mFC was dissected rostral to this area, and STR caudal to this area. Abbreviations: FC: frontal cortex; HP, hippocampus; LV, lateral ventricle; NC, neocortex; OB, olfactory bulb; RH, rhinencephalon; SP, septum; ST, striatum. Scale bar 500μM.

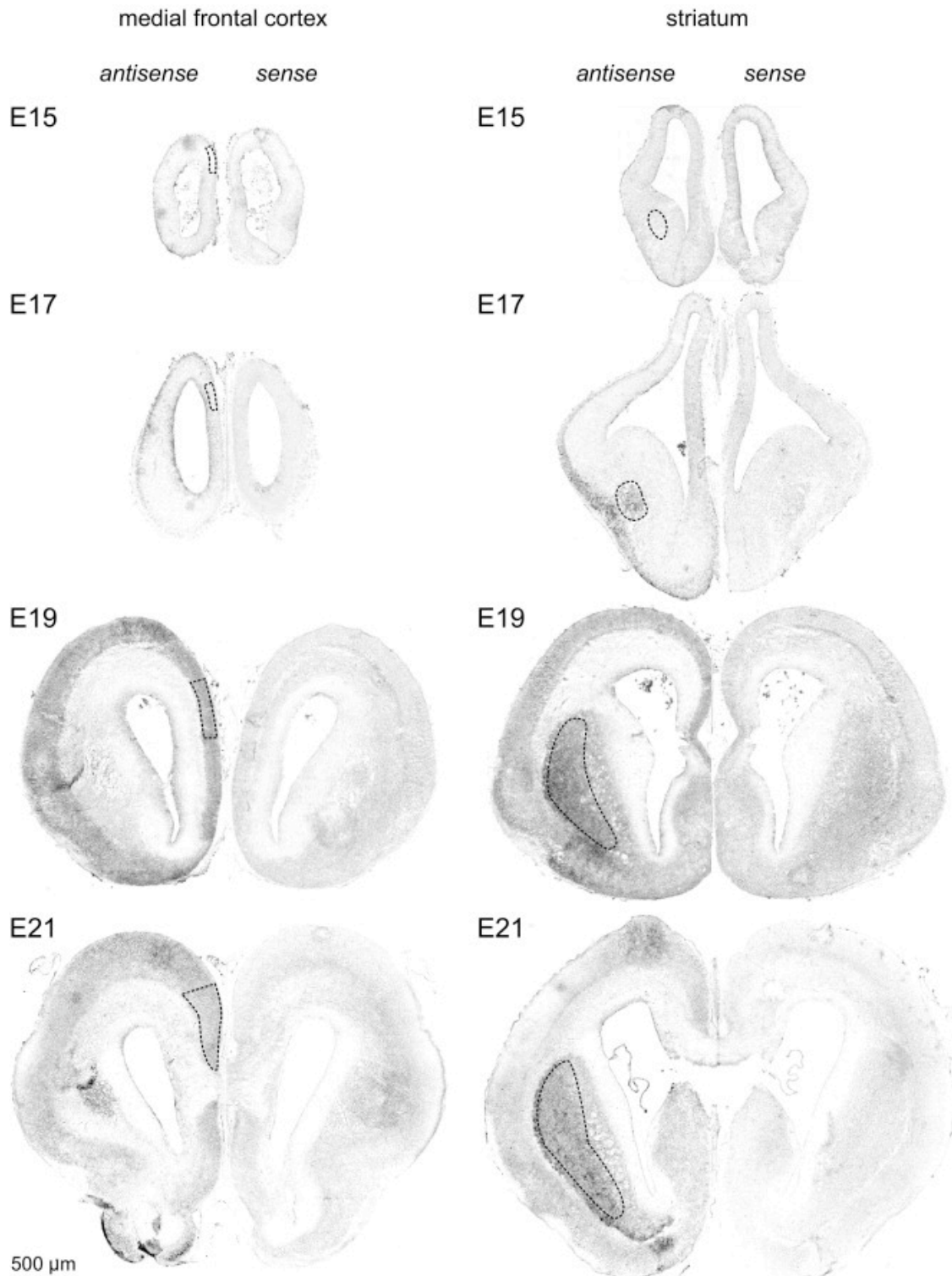


FIGURE 2.2: *In situ* hybridization of DRD1 development in rat mFC and STR.

Representative photomicrographs of *in situ* hybridization of coronal sections of embryonic rat brains at E15, E17, E19, and 21. A combination of three DRD1 probes was used to visualize the expression of receptors in mFC (left panel) and STR (right panel). For each time point, a representative antisense slide is shown next to a sense slide to show background levels of hybridization. Boxes indicate the regions used to measure *in situ* densitometry. Scale bar is 500 μ M.

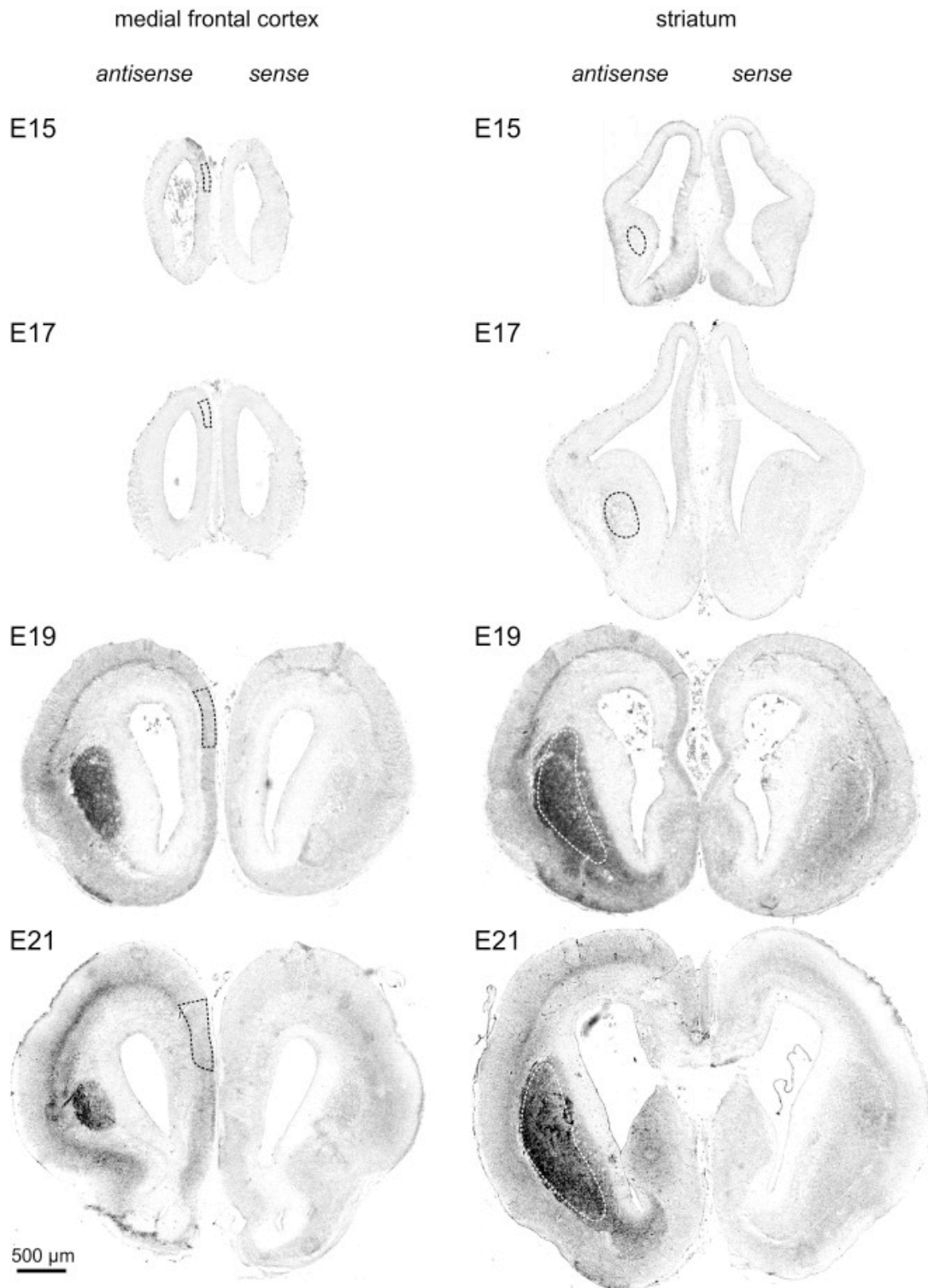


FIGURE 2.3: *In situ* hybridization of DRD2 development in rat mFC and STR.

Representative photomicrographs of *in situ* hybridization of DRD2 receptors in coronal sections of embryonic rat brains from E15 to E21. A combination of three DRD2 probes was used to detect receptors in mFC (left panel) and STR (right panel). For each time point, a representative antisense slide is shown next to a sense slide to show background levels of hybridization. Boxes indicate the regions used to measure *in situ* densitometry. Scale bar is 500 μ M.

statistical analysis. Similar patterns to the *in situ* hybridization were found, with the exception that measurable amounts of mRNA could be detected at E15 (figure 2.4C, 2.4D). From E15 to E21 both receptors were significantly increasing in the mFC (DRD1: $F_{3,16}=47.0$, $p\leq 0.0001$; DRD2: $F_{3,16}=191.7$, $p\leq 0.0001$, (figure 2.4C). Levels of DRD1 increased more than levels of DRD2, and this difference was supported in a multivariate ANOVA which showed significant differences between DRD1 and DRD2 ($F_{3,16}=8.1$, $p\leq 0.0017$; repeated measure [DRD1, DRD2] x embryonic day). In concordance, the ratio of DRD1/DRD2 in the mFC was different at different developmental stages ($F_{3,16}=24.5$, $p\leq 0.0001$), (table 2.2A). Except for E15, DRD1 levels were significantly higher than DRD2 levels in the mFC at all time points (table 2.2A), supporting the preliminary findings in the *in situ* hybridization analysis.

In the STR, both receptors showed a steady increase from E15 to E21 as well (DRD1: $F_{3,16}=15.0$, $p\leq 0.0001$; DRD2: $F_{3,16}=19.8$, $p\leq 0.0001$), with significant differences between DRD1 and DRD2 ($F_{3,16}=17.1$, $p\leq 0.0001$; repeated measure [DRD1, DRD2] x embryonic day). The ratio of DRD1/DRD2 in the STR was different at different developmental stages ($F_{3,16}=10.2$, $p\leq 0.0005$), (table 2.2B). Levels of DRD2 were significantly higher than levels of DRD1 at all time points (figure 2.4D). The overall expression of both receptor mRNAs was higher in the STR than the mFC ($F_{3,16}=10.7$, $p\leq 0.0004$ for DRD1; $F_{3,16}=16.3$, $p\leq 0.0001$ for DRD2; repeated measure [mFC, STR] x embryonic day), (table 2.3; figures 2.2, 2.3, and 2.4).

To examine functional maturation of the receptors, the signaling properties of each receptor were evaluated with specific DR agonists in primary neuronal cultures.

TABLE 2.2: Ratio of DRD1 over DRD2 mRNA expression in the developing rat brain.

The ratio of the two receptors +/- S.E.M. is shown at each developmental time point in the mFC (A) and the STR (B). QPCR values for each receptor were normalized to the control genes beta actin and 18S rRNA, and averaged from five samples per developmental time point. Paired t-tests were used to analyze the difference between DRD1 and DRD2 levels.

A. mFC	Developmental timepoint	DRD1/DRD2	t-test
	E15	0.90 ± 0.04	0.0470
	E17	1.97 ± 0.15	0.0046
	E19	2.35 ± 0.16	0.0002
	E21	1.37 ± 0.12	0.0398
B. STR			
	E15	0.45 ± 0.07	0.0325
	E17	0.82 ± 0.05	0.0488
	E19	0.82 ± 0.05	0.0149
	E21	0.67 ± 0.05	0.0066

TABLE 2.3: Ratio of DR mRNA in the mFC over STR.

The ratio of each receptor in the STR compared to the mFC +/- S.E.M. is shown at each developmental time point for DRD1 (A) and DRD2 (B). QPCR values for each receptor were normalized to the control genes beta actin and 18S rRNA, and averaged from five samples per developmental time point. Unpaired t-tests were used to analyze the difference between receptor expression levels in the two brain regions.

A. DRD1	Developmental timepoint	STR/mFC	t-test
	E15	0.58 ± 0.10	0.0649
	E17	3.24 ± 0.66	0.0007
	E19	6.87 ± 1.34	0.0011
	E21	3.57 ± 0.74	0.0078
B. DRD2			
	E15	1.29 ± 0.28	0.4564
	E17	7.83 ± 0.56	0.0002
	E19	18.57 ± 2.19	0.0001
	E21	7.05 ± 1.62	0.0017

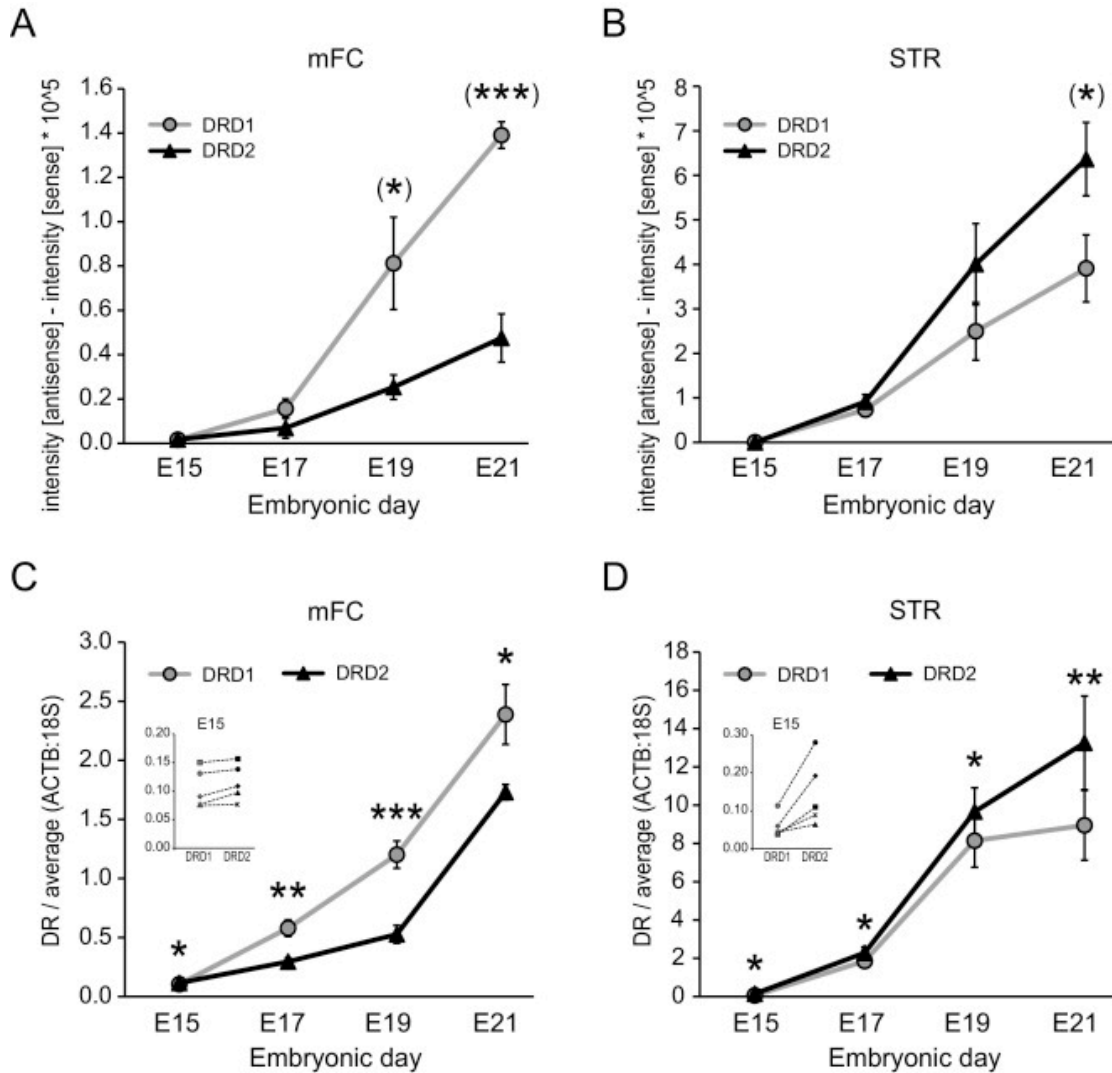


FIGURE 2.4: DR mRNA expression measured by *in situ* hybridization and QPCR. Densitometric analyses of *in situ* hybridization results for DRD1 and DRD2 reveals significant increases in mFC (A) and STR (B) in a preliminary statistical analysis. Shown are the levels of intensity of antisense probes, normalized to the background signal generated by sense probes from an adjacent section. N=12-17 area measurements in 2 slices per time point. QPCR was used to measure mRNA transcript levels of DRD1 and DRD2 in samples from mFC (C) and STR (D). Values were normalized to the control genes beta actin (ACTB) and 18S rRNA. Inserts: Magnification of expression levels at E15. n=5 samples/time point. *p<0.05, **p<0.01, *** p<0.001 in the comparison of DRD1 to DRD2 at individual time points; mean \pm SEM. Brackets around asterisks denote that these data are semiquantitative. Paired t-tests were used in (C) and (D).

Neurons from both brain regions were isolated at two time points, E15 and E18, and grown for 72 hours to ensure a stable baseline following the disruption during dissociation. Dissociation causes the release of metabolites that lead to the activation of signal transduction pathways which could mimic DR-mediated signaling pathways. After 72 hours in culture neurons have re-grown their processes and established synaptic connections. The embryonic time points were chosen to examine the ability of DRs to activate second messenger pathways before and after DA fibers have reached the mFC and STR. DA fibers are not reaching to the mFC at E15, but will have arrived at the subplate and intermediate zone of the mFC at E18 (Verney et al., 1982, Berger et al., 1983, Kalsbeek et al., 1988). In the STR, DA fibers are starting to innervate at E15 with a high density observed at E18 (Verney et al., 1982, Berger et al., 1983, Kalsbeek et al., 1988).

Initially, we examined the expression of DR mRNAs during each day in culture. In mFC neurons plated at E15, we observed a significant induction of DRD1 mRNA over time in culture ($F_{5,11}=149.7$, $p \leq 0.0001$), while the change in DRD2 mRNA was much smaller, though still significant over time ($F_{5,11}=8.4$, $p \leq 0.0017$), (figure 2.5A). A multivariate ANOVA showed significant differences between DRD1 and DRD2 during time in vitro ($F_{5,11}=70.3$, $p \leq 0.0001$; repeated measure [DRD1, DRD2] x day in vitro). In STR cultures plated at E15, both DRD1 ($F_{5,12}=45.2$, $p \leq 0.0001$) and DRD2 ($F_{5,12}=60.3$, $p \leq 0.0001$) mRNAs were induced rapidly (figure 2.5B), and multivariate ANOVA showed significant differences between DRD1 and DRD2 during time in vitro ($F_{5,12}=10.4$, $p \leq 0.0005$; repeated measure [DRD1, DRD2] x day in vitro). mFC

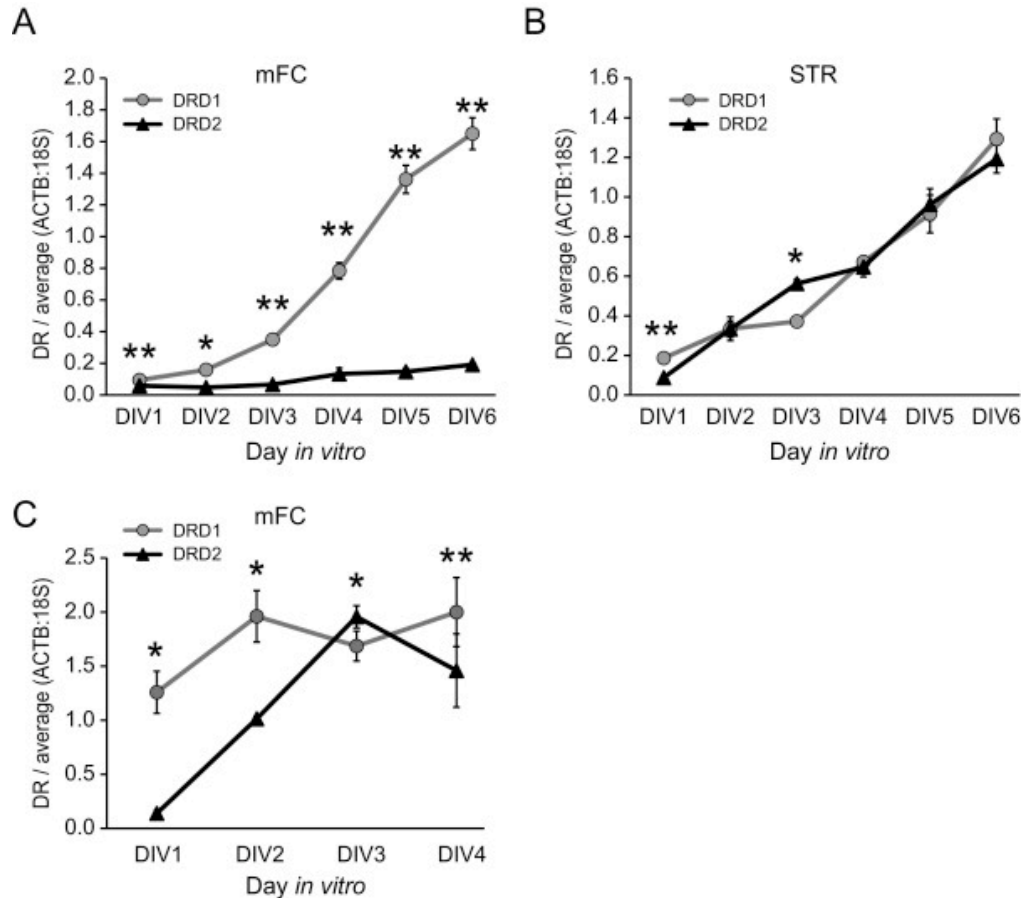


FIGURE 2.5: DR mRNA expression in mFC and STR neuronal cultures increases over time.

The developmental trajectory of mRNA transcript levels of DRD1 and DRD2 was examined in primary culture from mFC (A) and STR (B) plated at E15, and primary culture from mFC at E18 (C). DIV = day in vitro starting 24 hours after plating as DIV 1. Values were normalized to the control genes beta actin (ACTB) and 18S rRNA. Data mean \pm SEM; paired t-tests: * $p < 0.05$, ** $p < 0.01$; $n = 3$ per time point. Expression levels for both DRs were significantly altered over time in all experiments (see ‘Results’).

neurons plated at E18 had a much larger induction of DRD2 mRNA than on E15 ($F_{3,8} = 18.8$, $p \leq 0.0006$) (figure 2.5C).

Activation of DRs in embryonic cultures regulates the phosphorylation status of second messenger molecules

Cultures were treated for 15-minutes with either the DRD1 agonist SKF82958 or the DRD2 agonist PPHT, and the phosphorylation status of the second messenger

proteins CREB, ERK1/2, and GSK3 β was assessed with western blots (figure 2.6 and 2.7). In E15 cultures, activation of DRD1 was observed in both brain regions (figure 2.6). SKF82958 increased ERK1/2 phosphorylation in the mFC at this early time point (t(20)=2.6, p<=0.016), whereas in the STR CREB phosphorylation (t(18)=2.6, p<=0.02), ERK1/2 phosphorylation (t(15)=3.6, p<=0.0027) and GSK3 β phosphorylation (t(18)=3.8, p<=0.0015) were increased. In E18 cultures, SKF82958 increased CREB phosphorylation in the mFC (t(31)=2.2, p<=0.033), and STR (t(22)=2.9, p<=0.0089), as well as ERK1/2 phosphorylation in the mFC (t(30)=2.8, p<=0.0082), and STR (t(24)=2.2, p<=0.038). Interestingly, the striatal data did not survive multiple-comparison corrections (Benjamini and Hochberg, 1995), though it is well-known that both CREB and ERK1/2 do get phosphorylated in STR cultures from E18 in response to DRD1 stimulation (Konradi et al., 1996a, Rajadhyaksha et al., 1998, Brami-Cherrier et al., 2002, Dudman et al., 2003). GSK3 β phosphorylation status was unaffected in either brain region in E18 cultures.

DRD2 activation by the agonist PPHT decreased GSK3 β phosphorylation in E15 cultures in both the mFC (t(16)=2.4, p<=0.027) and STR (t(7)=3.6, p<=0.0085; mFC data do not survive multiple-comparison corrections), as well as in E18 cultures (mFC: t(10)=6.2, p<=0.0001; STR: t(7)=2.4, p<=0.0494; STR data do not survive multiple-comparison corrections), (figure 2.7). PPHT also decreased CREB phosphorylation in the mFC at E18 (t(19)=4.0, p<=0.0007), and ERK1/2 phosphorylation in the STR at both time points (E15: t(7)=3.0, p<=0.020; E18: t(6)=3.3, p<=0.017; STR data at E18 do not survive multiple-comparison corrections).

The specificity of DR activation was assessed by co-treatment of E18 mFC neurons with the DRD1 antagonist SCH23390, and the DRD2 agonist PPHT. Antagonism of the DRD1 receptor in conjunction with DRD2 stimulation did not change PPHT-mediated dephosphorylation of GSK3 β ($F(3,8)=7.5$, $p=0.0104$), (figure 2.8). Post hoc t-tests showed a significant difference between DMSO-control and PPHT ($t(4)=4.6$, $p<0.0103$) as well as DMSO-control and PPHT pretreated with SCH23390 ($t(4)=3.6$, $p<.0234$) but not between DMSO-control and SCH23390 ($t(4)=1.7$, $p<0.1556$).

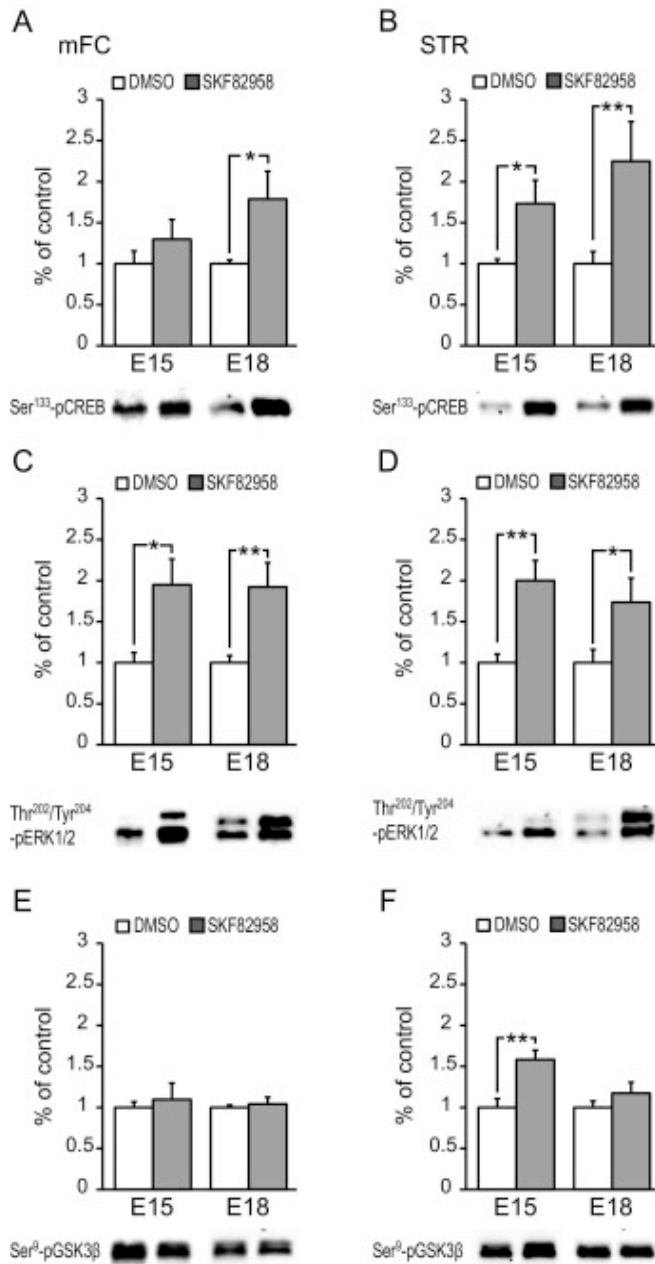


FIGURE 2.6: DRD1-mediated activation of signal transduction pathways in embryonic neuronal cultures from the rat mFC and STR.

Phosphorylation of CREB (A, B), ERK1/2 (C, D), and GSK3 β (E, F) was measured in embryonic neurons from mFC (A, C, E) or STR (B, D, F) at E15 and E18 in response to 15-minute treatments with the DRD1 agonist SKF82958. All neurons were cultured for 3 days. Bands were normalized to total protein on the membrane. Representative blots are shown beneath each histogram. Data mean \pm SEM; t-tests: * = $p < 0.05$, ** = $p \leq 0.01$. N=10-14 per group.

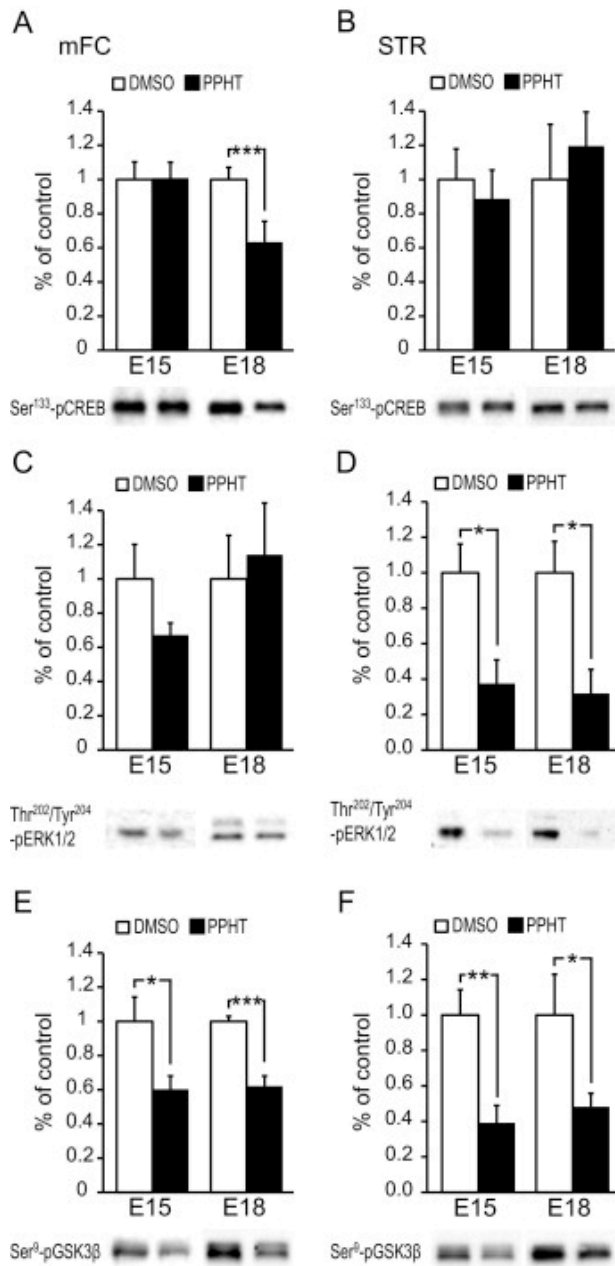


FIGURE 2.7: DRD2-mediated activation of signal transduction pathways in embryonic neuronal cultures from the rat mFC and STR.

Phosphorylation of CREB (A, B), ERK1/2 (C, D), and GSK3 β (E, F) was measured in embryonic neurons from mFC (A, C, E) or STR (B, D, F) at E15 and E18 in response to 15-minute treatments with the DRD2 agonist PPHT. All neurons were cultured for 3 days. Bands were normalized to total protein on the membrane. Representative blots are shown beneath each histogram. Data mean \pm SEM; t-tests: * = $p < 0.05$, ** = $p \leq 0.01$, *** = $p \leq 0.001$. N=4-12 per group.

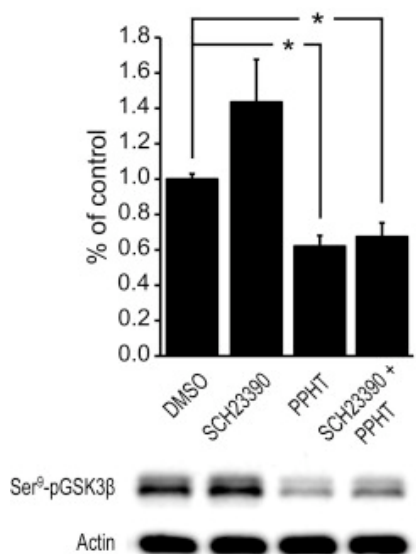


FIGURE 2.8: PPHT mediated activation of GSK3 β is specific for DRD2.

Co-treatment of E18 mFC neuronal cultures for 15 minutes with the potent DRD2 agonist PPHT and the DRD1 antagonist SCH23390. Antagonism of DRD1 in conjunction with PPHT did not affect PPHT-mediated activation of GSK3 β . Bands were normalized to β -actin. Representative blots are shown beneath histogram. Data mean \pm SEM; t-tests: * = $p < 0.05$. N=3 per group.

Discussion:

The expression pattern and signaling properties of DRs in the rat brain change considerably during embryonic development, with unique developmental trajectories of mFC and STR. Whereas the mFC had higher levels of DRD1 than DRD2 mRNA, the opposite pattern was seen in the STR. At E15, expression levels of DRs were low in both brain regions, but increased steadily over the course of embryonic development, reaching higher levels in the STR than in the mFC. The DR expression data agree with trends reported in a previous study in the murine brain but are not fully comparable as the murine study had somewhat different time points (Araki et al., 2007). We furthermore

extend the previous study by showing that DRD1 and DRD2 are functional by E15, and by providing a detailed description of DR expression at time points between E15 and birth.

DR expression rose sharply during mid gestation in both the mFC and STR. DRs in the mFC exhibited the greatest rate of change from E19 to E21, concurrent with the arrival of DA fibers at the subplate and intermediate zone of the mFC at E18 (Verney et al., 1982, Berger et al., 1983, Kalsbeek et al., 1988) and the innervation of the mFC at E20 (Van den Heuvel and Pasterkamp, 2008). The slope of DR mRNA expression in the STR was greatest from E17 to E19, as DA fibers innervate the STR. This pattern of expression suggests that DR mRNA transcripts are timed with the arrival of midbrain DA efferents.

To examine if DR mRNA expression in cortical and striatal neurons depends on DA axon innervation, we measured levels of DR mRNAs in cultured neurons isolated at either E15, before DA fibers innervate these areas or at E18, during innervation, and grown for 3 days in vitro. Similar to tissue, mRNA levels of both DRs increased steadily in the mFC and the STR, though the induction of DRD2 mRNA in the mFC was small when cultures were started at E15 and larger in E18 cultures. Since expression and functional activation of both DRs was detected at E15, DA axon innervation does not seem to be required for DR expression.

Causes for the moderate induction of DRD2 mRNA at E15 could include the need for external growth or guidance factors, absence of glial support in the cultures, missing environmental cues or an underrepresentation of DRD2 expressing neurons in the mFC at E15. At E15 the cortex consists of a thin layer of pre-plate cells, and only a subset of the

DRD2-positive neurons may have matured (Kriegstein et al., 2006). Birth of the remaining DRD2 population may occur between E15 and E19, thus accounting for the larger induction of DRD2 mRNA in E18 cultured neurons.

DRD1 agonists activate PKA and facilitate the phosphorylation of CREB and ERK1/2 (Valjent et al., 2000, Dudman et al., 2003). DRD1 and DRD2 have opposing effects on the Akt second messenger pathway and on GSK3 β phosphorylation: DRD1 agonists cause phosphorylation of GSK3 β , while DRD2 agonists cause dephosphorylation of GSK3 β (Iwakura et al., 2008, Beaulieu et al., 2009, Beaulieu and Gainetdinov, 2011, Souza et al., 2011). The phosphorylation patterns of CREB, ERK1/2 and GSK3 β were used to examine if DRs were functionally coupled to signal transduction pathways in embryonic neurons. In E15 cultures of the mFC, DRD1 was coupled to ERK1/2 phosphorylation. Coupling of DRD1 pathways was even stronger in mFC neurons cultured at E18, causing both CREB and ERK1/2 phosphorylation. In the STR, coupling of DRD1 to CREB and ERK1/2 signal transduction pathways was evident in neurons cultured at either E15 or E18. These findings are in agreement with studies that have shown cocaine-mediated phosphorylation of ERK1/2 exclusively in DRD1-expressing neurons, and inhibition of amphetamine-mediated CREB, ERK1/2, and Akt phosphorylation after pretreatment with the DRD1 antagonist SCH23390 (Bertran-Gonzalez et al., 2008, Shi and McGinty, 2011).

DRD2 activation with PPHT led to dephosphorylation of GSK3 β in both brain regions as early as in E15 cultures. PPHT mediated signaling was mediated by DRD2 and was not affected by a DRD1 antagonist. Inhibition of CREB phosphorylation by PPHT was observed in the mFC in E18 cultures, and of ERK1/2 phosphorylation in the

STR in E15 and E18 cultures. This inhibition might have resulted from the inhibitory action of DRD2 on PKA pathways (Enjalbert and Bockert, 1983) or an interaction of AKT with signal transduction pathways regulating CREB and ERK1/2 phosphorylation. The data indicate that DR mRNA expression as well as activation of DR signal transduction pathways can be induced in the absence of DA innervation, suggesting an internal timing mechanism of DR expressing neurons in mFC and STR.

Many of the previous studies that have examined DR-mediated modulation of Akt- GSK3 β activity were carried out in STR tissue or cultured neurons (Beaulieu et al., 2007, Iwakura et al., 2008). We present evidence that DRD2 activation increases GSK3 β activity in the mFC as well as the STR.

CHAPTER III

DOPAMINE RECEPTOR STIMULATION DISRUPTS NETRIN-1 AXON GUIDANCE IN CORTICAL NEURONS

Abstract

Schizophrenia is a neurodevelopmental disorder with increased activity of the dopamine system, decreased activity of the glutamate system and reduced function of the medial frontal cortex (mFC). Dopamine receptors (DR) are active in the mFC during the formation of neural circuits in embryogenesis. Netrin-1 is a bifunctional secreted axon guidance molecule with stage-dependent attractant or repellant properties in the developing cortex. We hypothesized that increased DR activity in the mFC during embryogenesis influences the response to netrin-1, thus linking dopamine hyperactivity to abnormal axonal pathway formation of glutamatergic cells and reduced function of the mFC. In primary neuronal cultures and neuronal tissue outgrowth assays of the rat mFC we found that DR agonists prevented the attraction of mFC axons toward a source of netrin-1, by modulating the expression of netrin-1 receptors. The results suggest that abnormal DR activity during embryogenesis can impact neuronal circuit formation in the mFC and could provide a mechanism for the developmental origin of schizophrenia.

Introduction:

Schizophrenia (SZ) is characterized by decreased glutamate activity in the frontal cortex (FC) caused by neuronal miswiring during early brain development (Marek et al., Volk and Lewis). Dopamine (DA) D2 receptor (DRD2) antagonists improve the positive

clinical symptoms of SZ, suggesting a connection between a hyperactive DA system and a hypoactive glutamate system in SZ (Seeman, 2009). In support of this notion, agents that increase the activity of the dopaminergic system as well as agents that decrease the activity of the glutamate system can evoke psychotic symptoms in previously healthy individuals (Flaum and Schultz, 1996, Coyle, 2006).

DA receptors (DRs) are expressed early in the developing rodent medial FC (mFC), (Sales et al., 1989, Schambra et al., 1994, Araki et al., 2007, Sullivan and Konradi, 2011) and influence developmental processes such as cell proliferation, migration, and neurite outgrowth (Zhang and Lidow, 2002, Ohtani et al., 2003, Popolo et al., 2004, Crandall et al., 2007, McCarthy et al., 2007, Collo et al., 2008, Donohoe et al., 2008). DRs regulate the synthesis and activity of growth factors and their receptors during brain development (Alberch et al., 1991, Mena et al., 1998, Dawson et al., 2001, Guo et al., 2002, Iwakura et al., 2008). Unphysiological activation of DRs during brain development, such as through cocaine exposure, alters dendrite morphology and structural proteins that regulate the actin cytoskeleton (Harvey et al., 2001, Stanwood et al., 2001).

Netrin-1 (Ntn-1) is a bifunctional secreted axon guidance factor with stage-dependent attractant or repellent properties (Serafini et al., 1996, Hong et al., 1999). Homodimers of the receptor deleted in colorectal cancer (DCC) attract growth cones toward Ntn-1, while heterodimers of DCC and the uncoordinated-5c receptor (UNC5C) guide growth cones away from Ntn-1 (Lai Wing Sun et al., 2011). Although components of DR-mediated signaling cascades, including protein kinase A, calcium, and cyclic nucleotides, have been shown to modulate the response to axon guidance molecules such

as Ntn-1 (Bouchard et al., 2004, Wen et al., 2004, Gomez and Zheng, 2006, Piper et al., 2007), a direct involvement of DRs in axon guidance events has not been studied.

Ntn-1 receptors are expressed in regions that receive DA innervation and, in adult rodents, are regulated by amphetamine administration (Gad et al., 1997, Shu et al., 2000, Finger et al., 2002, Yetnikoff et al., 2007). We hypothesized that abnormal DR activity in the fetal brain influences the development of glutamatergic axonal pathways in the FC, which could have long-term effects on the establishment of their connection patterns. An investigation of this theory could clarify if a hyperactive DA system during development could contribute to the miswiring of glutamate neurons observed in SZ. It would incorporate the most salient observations in SZ, DA hyperactivity, glutamate hypoactivity, abnormal functional integration of brain processes and a neurodevelopmental component (Lewis and Levitt, 2002, Snitz et al., 2005, Marek et al.)

Here, we examined the effects of DA hyperactivity on ntn-1-mediated axon guidance in the rat mFC by selective stimulation of DRD1 and DRD2. We show that stimulation of either DR subtype diminishes a growth cone's attraction to ntn-1. The results demonstrate that DR hyperactivity in early brain development could contribute to the etiology of SZ.

Material and Methods:

Animals

All animals were housed and maintained in accordance with the policies of Vanderbilt University, which is accredited by the Association for the Assessment of Accreditation of Laboratory Animal Care. Timed-pregnant female Sprague-Dawley rats

(Charles River, Wilmington, MA) were anesthetized with pentobarbital (65mg/kg, Sigma, St. Louis, MO) and embryos were removed and washed in sterile phosphate buffered saline (PBS).

RNA probe synthesis and *in situ* hybridization

Digoxigenin-labeled probe synthesis and hybridization were performed as previously described (Sullivan and Konradi, 2011). The list of primer pairs used for the probe synthesis is shown in table 3.1. Images were captured using Stereo Investigator software (MBF BioScience, Williston, VT).

Primary neuronal cultures

mFC cells from E15 embryos were cultured as previously described (Sullivan and Konradi, 2011). For quantitation of the trajectory of netrin-1 receptors in culture, cells were grown for 1-5 days without drug treatments. For stimulation of DRs, cells were grown for 72 hours in vitro and treated for 1-4 hours with the DRD1 agonist (+)-SKF 82958 hydrobromide, the DRD2 agonists (+)-quinpirole HCl and (±)-PPHT hydrochloride (N-0434), or the partial DRD1/DRD2 agonist R(-)-apomorphine hydrochloride (Sigma).

QPCR

RNA extraction, cDNA synthesis, and QPCR were performed with cultured neurons and tissue from the mFC as previously described (Sullivan et al., 2011). Tissue was collected from E15, E17, E19, and E21 embryos and frozen at -80°C until RNA extraction. Values were normalized to the internal controls beta actin, 18s RNA, and

general transcription factor IIB. Primer pair sequences are listed in table 3.1. For individual developmental trajectories of DCC, and UNC5C, analysis of variance (ANOVA) was used to determine statistical significance and repeated measures multivariate ANOVAs were used to compare both receptors over time. For DR stimulation time courses, ANOVAs were used and post-hoc analyses were performed by comparing each treatment to an untreated control using Dunnett's test to correct for multiple comparisons. GraphPad InStat software (GraphPad, La Jolla, CA) was used for statistical analyses.

Western Blotting

Primary neuronal cultures from E15 mFC cells were grown for 1-5 DIV, harvested in 1X Laemmli buffer and sonicated. Western blotting was performed as previously described (Sullivan and Konradi, 2011) with the following antibodies: anti-DCC (BD Pharmingen, San Diego, CA) 1:4000, anti-UNC5C (R&D Systems, Minneapolis, MN) 1:4000, and anti-actin (Sigma) 1:120,000. Proteins of interest were normalized to total protein.

Immunohistochemistry

E15 mFC neurons were grown for 3 DIV on coated slide chambers and washed briefly with 1X PBS. Cells were fixed with 4% paraformaldehyde (PFA) for 30 minutes at room temperature, permeabilized with .1% Triton for 10 minutes, and then incubated in 4% horse serum blocking solution for 2 hours. Primary antibodies were diluted in blocking solution and incubated with cells overnight at 4°C on a rocking platform. The

following primary antibodies were used: anti-DCC (1:1000); anti-UNC5C (1:1000), anti-dopamine receptor (DRD1) (Sigma) (1:500); and anti-dopamine receptor 2 (DRD2) (Millipore, Billerica, MA) (1:500). The specificity of DR antibodies has been reported elsewhere (Lee et al., 2004). Excess primary antibody was removed with four 10-minute PBS washes at room temperature. Cy-conjugated secondary antibodies (Jackson ImmunoResearch Laboratories, West Grove, PA) were diluted in blocking solution and incubated with cells for 2 hours at room temperature. Slides were washed four more times in PBS then dried briefly in a dark container. Pro-gold anti-fade mounting media (Invitrogen) was applied to prevent fluorescent signal from fading. Cells were imaged using a 63X oil immersion lens on a Leica LSM510M inverted confocal microscope at the Vanderbilt Cell Imaging Resource Core.

Explant Assays

HEK293T cells that constitutively express Ntn-1 and GFP or the vector backbone only, supplied by Jane Wu (Liu et al., 2004), were grown for several days to create “hanging drops” of concentrated cells. HEK293T cell drops were placed in 75 μ l of Matrigel (BD Biosciences) in a culture dish fitted with a microscope slide (MatTek, Ashland, MA), allowing secreted Ntn-1 to create a gradient in the collagen matrix (Bonnin, 2010). E15 mFC explants were obtained as described above and placed around the HEK293T cells. Neurobasal medium supplemented with B-27 and N-2 was added 30 minutes after the collagen solidified, and 20 μ M SKF82958 or quinpirole was added 2 hours after plating explants. Explants were grown for 48 hours then fixed with 4% PFA overnight at 4°C. To visualize neurites, cultures were blocked for 2 hours in 2% BSA/

.1% triton, then incubated with mouse anti-TUJ1-Alexa488 (beta tubulin) antibody (Covance, Princeton, New Jersey) diluted 1:1000 for 24 hours at 4°C. Cultures were washed 4 times in PBS and imaged using a fluorescent microscope.

Analysis of explant cultures:

Image J software (NIH, Bethesda, MD) (Abramoff, 2004) with Neuron J plugin (Meijering, 2010) was used to analyze explant images. All images were blind-scored by 3 independent investigators to determine the direction of growth in response to HEK293T cells and Pearson chi-square (χ^2) correlation was used to determine statistical significance. For axon bundle density, the number of axons per quadrant (proximal, distal, symmetrical) was calculated at a distance of 100 μ m from the edge of the explant. The ratio of [proximal-distal axons/total axons] was used as a measure of axon guidance while the ratio of [proximal + distal axons/total axons] was used as a measure of outgrowth. An ANOVA was performed with all treatment conditions combined and the Tukey-Kramer HSD Multiple Comparisons Test was used for post-hoc analysis.

Microfluidic devices

Devices were fabricated and prepared as previously described, with modification (Majumdar et al., 2011). Each device consisted of two chambers separated by a 100 μ m polydimethylsiloxane (PDMS) wall with microgrooves at the bottom. After equilibration with cell culture media, ~100,000 E15 mFC neurons were added to one chamber. 24 hours later, 10ng/ml recombinant Ntn-1 protein (R & D Systems) was added to the other chamber, with DR agonists if needed. The neuronal chamber contained a slightly higher

volume of media to ensure that Ntn-1 protein only diffuses through the microgrooves to form a concentration gradient, similar to the approach developed by Taylor et al. (Taylor et al., 2005). After 48 hours in culture, neurons were fixed with 4% PFA/ 0.6M sucrose overnight at 4°C. For visualization of neuronal processes that extended across the microgrooves from one side of the device to the other, cells were stained as described above with anti-beta tubulin antibody and imaged using a fluorescent microscope. The length of axons that entered the microgrooves was measured using Image J Software and the Neuron J plugin. The average of the 15 longest neurites was calculated per slide and normalized to the percentage of growth in untreated slides. Kruskal-Wallis nonparametric ANOVAs were used to determine statistical significance by comparing all treatment groups and Dunn's Multiple Comparisons Test was used for post-hoc analysis.

TABLE 3.1: List of primer sequences used for probe synthesis (A) and QPCR (B). F/R indicates primer direction, forward or reverse.

A) Primers used to synthesize RNA probes		
Name	F/R	sequence
DCC outer primer 1	F	5'- TCCCAAGCCTGCCATCCCA-3'
	R	5'-GCATAGGCAGGGGGTCCCA-3'
DCC outer primer 2	F	5'-GGGTGAGATGGAAACACTGG-3'
	R	5'-TGAGAACTCGACTCCAGCCT-3'
DCC outer primer 3	F	5'-AGCAGCGAAGAAGCCCCAGCA-3'
	R	5'-AAAGGCGGAGCCCCGTGATGGCA-3'
UNC5C outer primer 1	F	5'-CGTGCGCATTGCGTATCTGC-3'
	R	5'-GGGCTGGGTTGGTGCAGGT-3'
UNC5C outer primer 2	F	5'-AGACTCTCAGACCCTGCTGA-3'
	R	5'-AGGGCATCCTGTGTGTCATC-3'
UNC5C outer primer 3	F	5'-TCCACAACCTGCGCCTCTCAA-3'
	R	5'-GGGGCATCCAGGCTGCTACA-3'
DCC nested primer 1	F	5'-AAGCATTTAGGTGACACTATAAGCATCCTCCCTTCTGCTCCCA-3'
	R	5'-AAGCTCTAATACGACTCACTATAGGGTCAGGCTGAGTGGCCACCTTGA-3'
DCC nested primer 2	F	5'-AAGCATTTAGGTGACACTATATTCACAGGATTGGAGAAGGG-3'
	R	5'-AAGCTCTAATACGACTCACTATAGGGATAAGGGCTGCCAACACCAT-3'
DCC nested primer 3	F	5'-AAGCATTTAGGTGACACTATAAGCCTGTGTGCGGCCAACTC-3'
	R	5'-AAGCTCTAATACGACTCACTATAGGGTGGCTGGATCCTCTGTTGGCT-3'
UNC5C nested primer 1	F	5'-AAGCATTTAGGTGACACTATAAGTGCCGGCCACCTGAAGGGAT-3'
	R	5'-AAGCTCTAATACGACTCACTATAGGGCACAGACCATTCTGCCCAGGTG-3'
UNC5C nested primer 2	F	5'-AAGCATTTAGGTGACACTATAACCTAACCCGAGGACTGGAA-3'
	R	5'-AAGCTCTAATACGACTCACTATAGGGTACTCCAGGGAAGAGCAGCA-3'
UNC5C nested primer 3	F	5'-AAGCATTTAGGTGACACTATAACCACATCTGGAGTGGCTCTCA-3'
	R	5'-AAGCTCTAATACGACTCACTATAGGGTGCCGGATAGGAAGAGGGATGC-3'
B) Primers used for QPCR		
Name	F/R	sequence
18s RNA	F	5'-TGGCTCAGCGTGTGCCTACC-3'
	R	5'-TAGTAGCGACGGGCGGTGTG-3'
Beta actin	F	5'-CTATGAGCTGCCTGACGGT-3'
	R	5'-TGGCATAGAGGTCTTTACGGA-3'
DCC	F	5' - CTATGCAAATGGTCCGGTTC - 3'
	R	5' - GAGCACTTGGCACATCTGAA - 3'
GTF2B	F	5' - TGCGATAGCTTCTGCTTGTG - 3'
	R	5' - TCAGATCCACGCTCGTCTC - 3'
UNC5C	F	5' - TGTTGTGGTTGTTGGAGAGG - 3'
	R	5' - AGGGCATCCTGTGTGTCATC - 3'

Results:

Expression of netrin-1 receptors in the developing rat cortex

mRNA expression of the Ntn-1 receptors, DCC and UNC5C, was examined in the mFC of developing rat embryos (figure 3.1). Strong expression of DCC was found throughout the cortical plate at E15 and a distinct medial to lateral gradient of DCC was

found at E18 (figure 3.1A, 3.1B). UNC5C expression was extremely low in the developing mFC with an increase between E15 and E18 (figure 3.1C, 3.1D). QPCR was used to quantify mRNA expression patterns of DCC and UNC5C in mFC tissue. From E15 to E21 mRNA levels of both receptors were significantly changing (DCC: $F[3,16]=8.96$, $p\leq 0.0010$; UNC5C: $F[3,16]=10.61$, $p\leq 0.0004$) (figure 3.1E). At early stages of gestation, levels of DCC were much higher than levels of UNC5C but the ratio of DCC to UNC5C decreased with age (table 3.2). A multivariate ANOVA showed significant differences between DCC and UNC5C over time ($F[3,16]=9.98$, $p\leq 0.0006$; repeated measure [DCC, UNC5C] x embryonic day).

To determine whether these expression patterns exist *in vitro*, we cultured mFC neurons from E15 embryos for 1-6 days and found similar expression patterns for DCC ($F[5,11]=13.81$, $p\leq 0.0002$) as well as UNC5C ($F[3,11]=101.80$, $p\leq 0.0001$) over time as well as in relation to each other ($F[5,11]=18.40$, $p\leq 0.0001$; repeated measure [DCC, UNC5C] x embryonic day) (figure 3.1E). Protein expression of Ntn-1 receptors in mFC neuronal cultures coincided with the reported mRNA expression, with a peak of DCC protein at E18, shortly after the peak of mRNA, while levels of UNC5C protein were more evenly expressed (figure 3.1F).

Colocalization of DRs and netrin-1 receptors in cortical neurons

Previously we reported the expression profile of DRD1 and DRD2 in the mFC throughout embryonic development (Sullivan et al., 2011). We verified colocalization of Ntn-1 receptors and DRs, with double immunocytochemistry in E15 mFC cells, cultured for 3 DIV (figure 3.2).

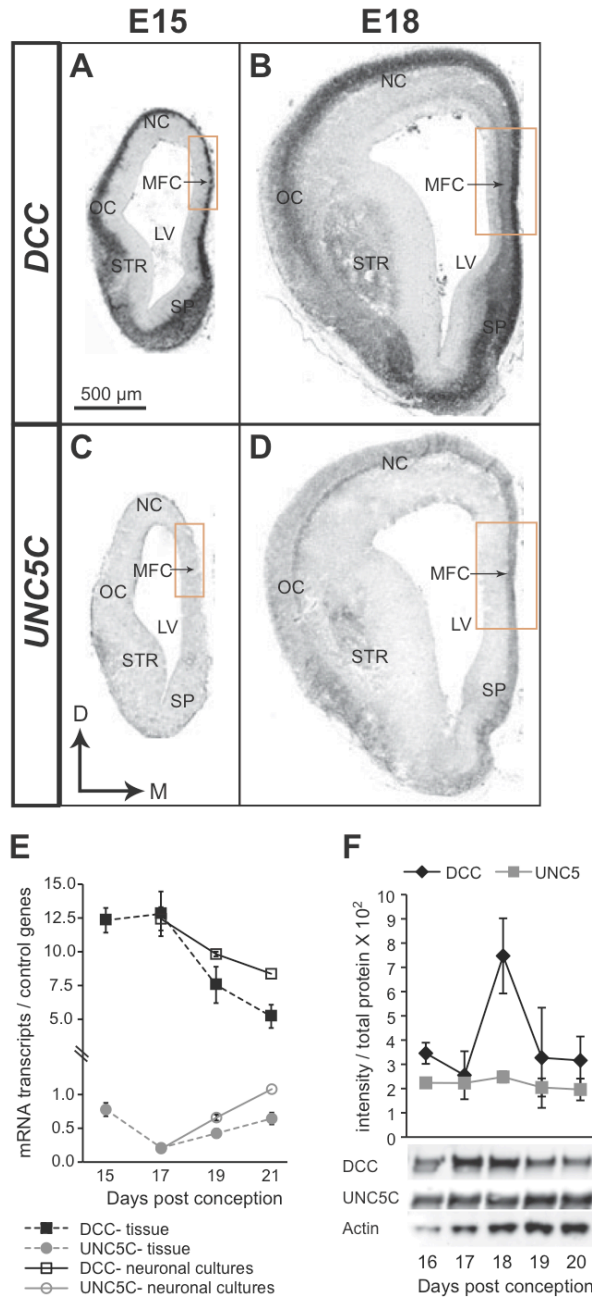


FIGURE 3.1: Expression of Ntn-1 DCC and UNC5C in the developing mFC.

In situ hybridization of DCC (A, B) and UNC5C (C, D) in the mFC at embryonic day 15 (A, C) and 18 (B, D). High levels of DCC are seen along the midline in the mFC and septum, while UNC5C is expressed at much lower levels. Scale bar = 500µm. 2-3 animals were examined per timepoint. E. Similar trajectories of DCC and UNC5C mRNA expression in the mFC in embryonic tissue and primary neuronal culture. Levels of mRNA transcripts were measured by QPCR. Neurons were isolated at E15 and cultured for 1-6 days. Mean +/- S.E.M. N=3-5 per timepoint. F. Protein expression of DCC and UNC5C in neurons cultured at E15. Mean +/- S.E.M. N=3 per timepoint.

Netrin-1 attracts neurites from explants of the mFC

To examine the functional significance of DR activity in Ntn-1 receptor expressing cells, we used an in vitro axon guidance assay (figure 3.3). HEK293T cells expressing Ntn-1 attracted mFC explants while HEK293T cells with the vector backbone only (parent) did not (figure 3.3A, 3.3B). Treatment with 20 μ M of the DRD1 agonist SKF82958 or the DRD2 agonist quinpirole disrupted Ntn-1 mediated attraction, resulting in more neurite outgrowth in the symmetrical and distal quadrants (figure 3.3C, 3.3D).

DR stimulation disrupts netrin-1 mediated axon guidance

Three independent investigators without knowledge of treatment examined the main direction of neurite outgrowth relative to the HEK cells. The number of explants with neurites growing towards, away or symmetrical, was calculated, as well as the axon bundle density in each quadrant (figure 3.4A). mFC explants displayed significantly different outgrowth patterns in the presence of Ntn-1-expressing HEK cells (figure 3.4B). A majority of mFC explants placed next to parent HEK293T cells showed symmetrical outgrowth, while explants grown with Ntn-1 expressing HEK cells showed preferential outgrowth in the direction of the cells (Ntn-1 alone versus parent alone: $\chi^2 = 15.74$, $p < .0004$, d.f.=2). Stimulation of DRs altered the response of mFC neurites to Ntn-1 (figure 3.4D; Ntn-1 alone versus Ntn-1 with SKF82958: $\chi^2 = 6.82$, $p < .0330$, d.f.=2; Ntn-1 alone versus Ntn-1 with quinpirole: $\chi^2 = 10.46$, $p < .0053$, d.f.=2), whereas DR agonists did not affect outgrowth in explants placed next to the parental cell line (figure 3.4C).

The number of axon bundles was counted in each quadrant- proximal, distal, and symmetrical- at a distance of 100 μ M from the edge of the explant. A one-way ANOVA

between treatments was conducted to compare the guidance ratio of [proximal-distal/total axons] in all conditions. Ntn-1 significantly affected the percentage of neurites in each quadrant, a situation that was blocked by DR agonists (figure 3E, [F[5,132]=3.83; p=.0029]), Post hoc comparisons with the Tukey Kramer HSD test showed that the mean ratio for explants cultured with Ntn-1 was significantly different from those cultured with the parental cell line, or from those treated with SKF82958 and quinpirole in the presence of Ntn-1 cells. SKF82958- or quinpirole-treated explants cultured with Ntn-1 were not significantly different from SKF82958- or quinpirole-treated explants cultured with parental cells. An outgrowth ratio, obtained by calculating [proximal+distal/total axons], indicated no significant differences in total axon outgrowth in the proximal and distal quadrants between the treatment groups (figure 3F).

DR stimulation reduces axon attraction to netrin-1

Outgrowth of individual mFC axons was examined using microfluidic chambers that allow for the culture of neurons next to a chemoattractive gradient. The devices consist of two chambers linked by microgrooves that permit individual axon growth into the other chamber. Cultures were grown in the absence or presence of recombinant Ntn-1 protein and/or DR agonists in the adjacent chamber (figure 3.5). Results were consistent with explant experiments, with significant differences observed among the treatment groups (KW=60.51, p<.0001 using Kruskal-Wallis test). Application of 10ng/ml recombinant Ntn-1 increased the length of axons entering the microwells over that of the untreated control, but co-treatment with 20 μ M SKF82958 or the more potent DRD2 agonist PPHT disrupted this effect (figure 3.5G). Axon length in cultures treated

TABLE 3.2: The ratio of DCC:UNC5C mRNA expression in mFC neurons (A) and tissue (B).

A) Neurons

Days PC	Ratio DCC/Unc5	Paired T-test
17	64	0.0035
19	15	0.0078
21	8	0.0137

B) Tissue

Days PC	Ratio DCC/Unc5	Paired T-test
15	16	0.0002
17	61	0.0015
19	18	0.0054
21	8	0.0051

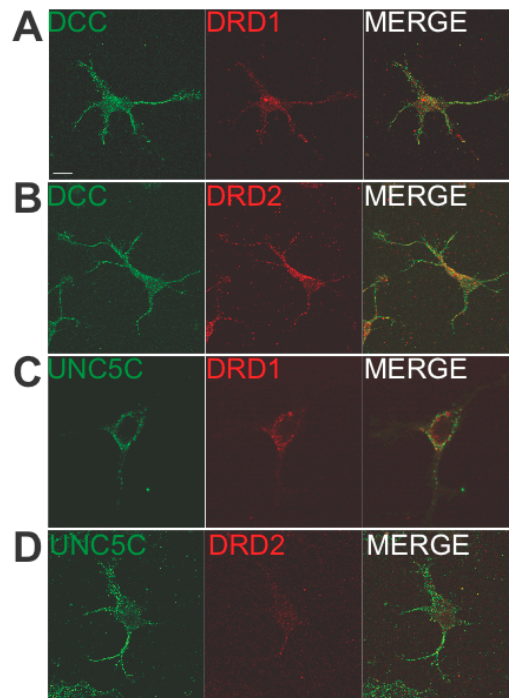


FIGURE 3.2: Colocalization of DRs and Ntn-1 receptors in mFC neurons. Immunocytochemistry of E15 mFC neurons, cultured for 3 DIV, shows that both DRD1 (A, C) and DRD2 (B, D) colocalize with Ntn-1 receptors DCC (A, B) and UNC5C (C, D). Scale bar = 10 μ m.

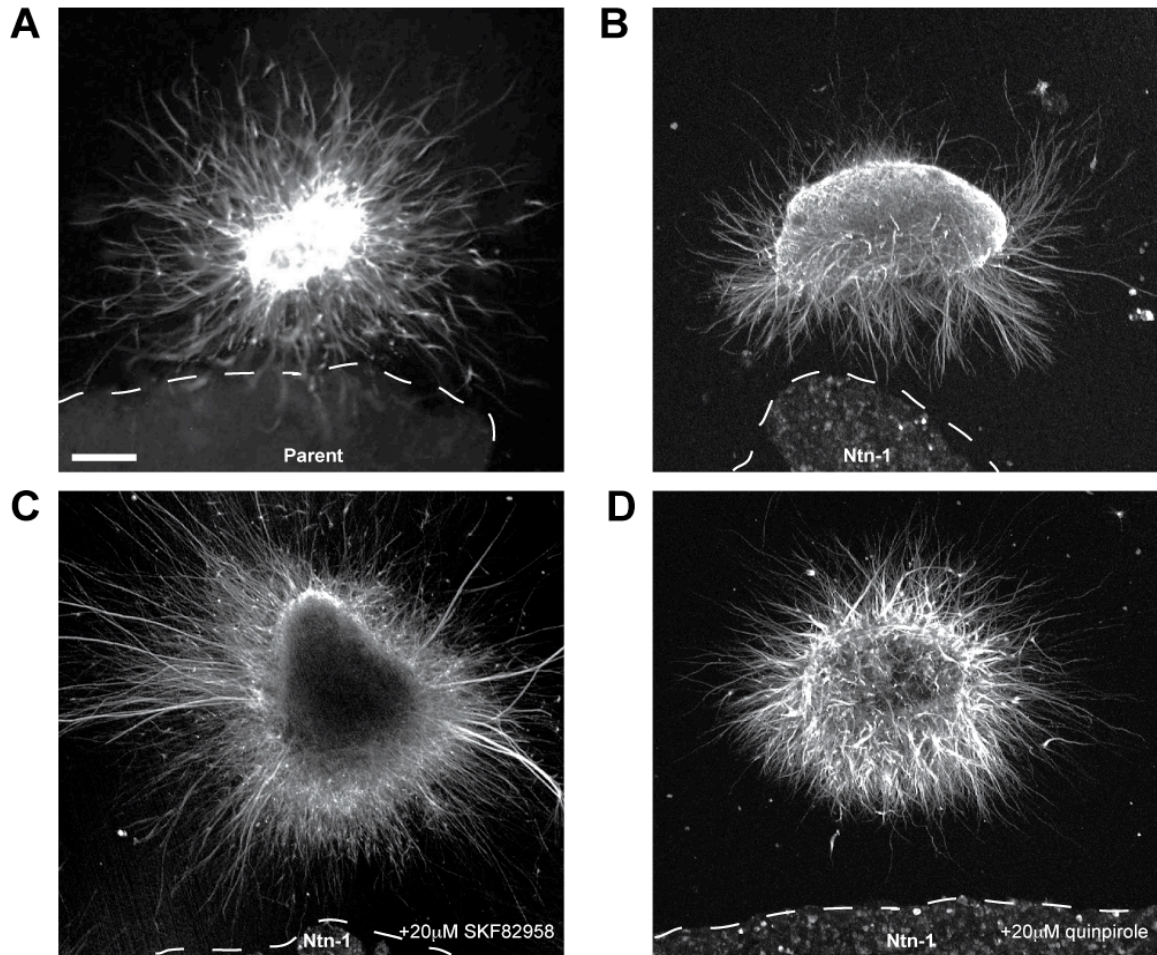


FIGURE 3.3: Stimulation of DRs disrupts Ntn-1-mediated attraction in mFC explants.

E15 mFC explants were cultured near Ntn-1-expressing HEK293T cells for 72 hours to examine the chemoattractant properties of Ntn-1 in the mFC. A. Explants cultured with the parental cell line, which does not express Ntn-1, display symmetrical outgrowth. B. Ntn-1 attracts neurites from mFC explants. More outgrowth occurs in regions proximal to the Ntn-1-expressing cells. Treatment with the DRD1 agonist SKF82958 (C) or the DRD2 agonist quinpirole (D) disrupts Ntn-1-mediated attraction in mFC explants. Scale bar = 100 μ m.

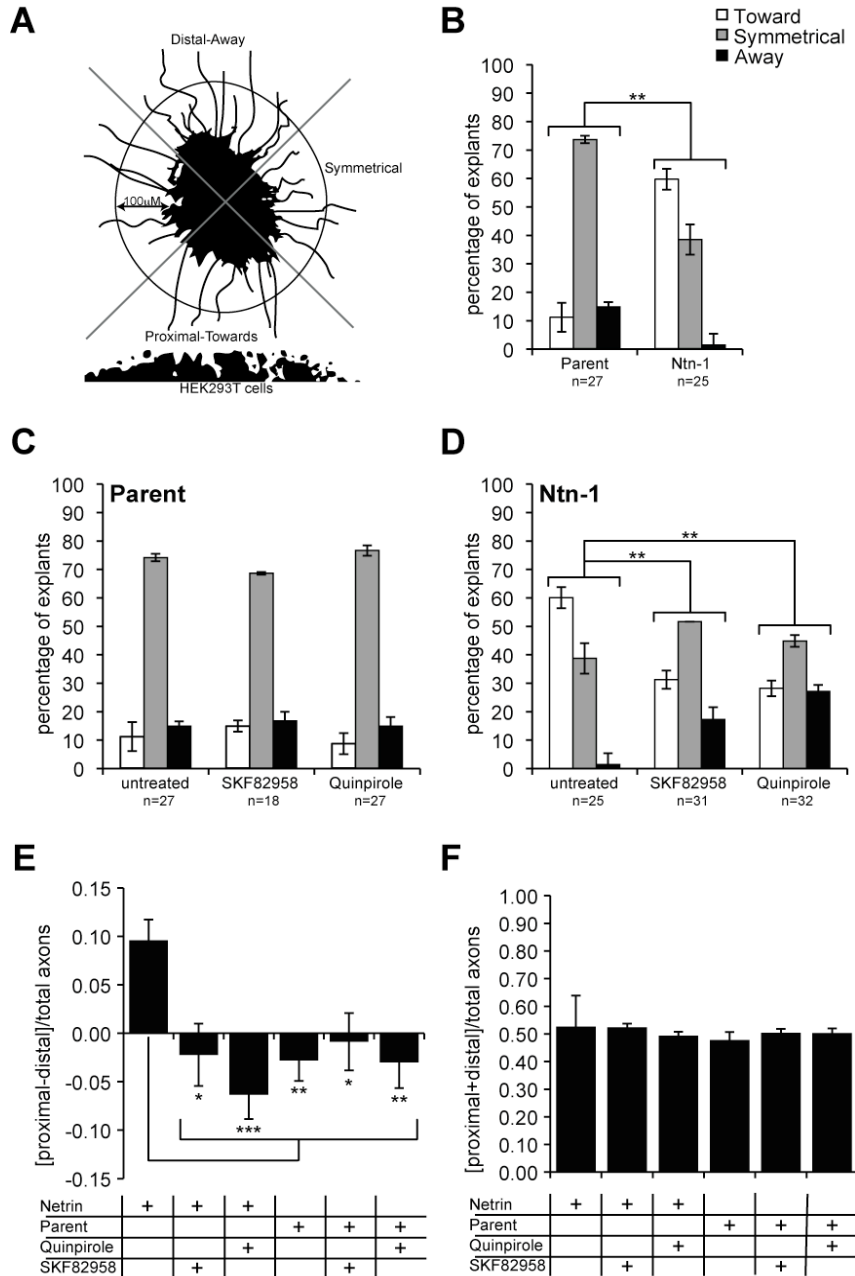


FIGURE 3.4: DR agonists inhibit the attractive properties of Ntn-1 in mFC explants.

A. Illustration of the strategies used to analyze explant images. *B*, *C*, *D*. The direction of neurite outgrowth with respect to the location of the HEK293T cells was quantified by blind scoring and is depicted as percentage of explants that grew towards (white column), symmetrically (grey column), or away (black column) from HEK293T cells. *B*. mFC explants are attracted to Ntn-1 expressing cells. *C*. mFC explants cultured with the parental cell line display predominantly symmetrical outgrowth. *D*. Treatment with 20µM of the DRD1 agonist SKF82958 or the DRD2 agonist quinpirole changes the direction of outgrowth of mFC neurites in response to Ntn-1. *E*, *F*. Quantification of the number of axon bundles 100µM from the explant in the proximal and distal regions, in relation to the HEK293T cells. *E*. A measure of guidance: the ratio of the difference in axon number in proximal versus distal regions divided by the total number of axons. *F*. Total outgrowth was comparable between all treatments. The ratio of the sum of proximal and distal axons over the total number of axons. Mean +/- S.E.M. **p*<.05; ** *p*<.01; ****p*<.001.

with DR agonists in the absence of Ntn-1 did not differ from untreated controls (figure 3.5H).

DR stimulation increases Ntn-1 receptor expression

Taken together, these results suggest that DR stimulation modifies Ntn-1 mediated guidance of mFC neurites. To further examine this finding, we stimulated DRs in E15 mFC cultured neurons and measured mRNA levels of the Ntn-1 receptors DCC and UNC5C (figure 3.6). DCC expression was not altered by treatment with DR agonists. Treatment with the DRD1 agonist SKF82958 increased the expression of UNC5C, the Ntn-1 receptor involved in repulsion, ($F[3,53]=4.05$, $p=0.0115$), and post hoc comparisons showed a significant increase after 4 hours ($t[15]=2.65$, $p<.05$) (figure 3.6A). The DRD2 agonist quinpirole increased UNC5C mRNA levels ($F[3,64]=3.00$, $p=0.0368$) after 1 hour ($t[18]=2.87$, $p<.05$) (figure 3.6B). The potent DRD2 agonist PPHT showed even more robust effects ($F[3,71]=5.14$, $p=.0028$), with significant increases in UNC5C transcripts after 2 ($t[25]=2.44$, $p<.05$) and 4 hours ($t[10]=3.50$, $p<.01$) (Figure 3.6C). The partial DRD1/DRD2 agonist apomorphine had an amplified effect ($F[3,56]=9.37$, $p=.0001$) and large increases in UNC5C transcripts were measured at every timepoint (1 hour: $t[18]=3.46$, $p<.01$; 2 hours: $t[12]=4.60$, $p<.01$; 4 hours: $t[12]=4.15$, $p<.01$) (Figure 3.6D). While an ANOVA indicated a significant effect of apomorphine on DCC expression ($F[3,52]=3.04$, $p=.0373$), no differences were seen with post hoc tests.

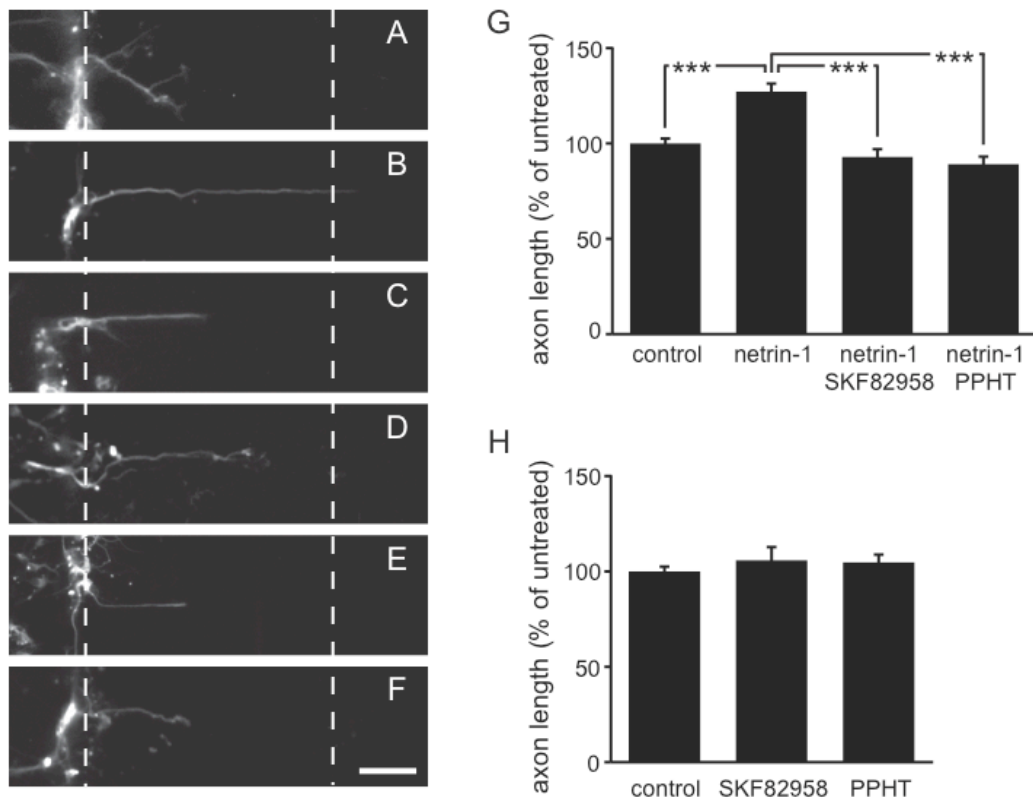


FIGURE 3.5- DR agonists impair Ntn-1-mediated outgrowth.

Neurons were grown in microfluidic chambers next to Ntn-1 containing medium. Two chambers were separated by 100 μ m microwells that allow for axon growth toward Ntn-1 containing medium. Individual axon outgrowth was examined in the absence (A,C,E) or presence of recombinant Ntn-1 protein (B,D,F). The addition of 10ng/ml recombinant Ntn-1 in the adjacent chamber (B) increased axon length over that of the untreated control (A) but co-application of Ntn-1 with 20 μ M SKF82958 (D) or 20 μ M PPHT (F) disrupted this effect, while either agonist alone (C,E) had no effect. Shown are representative photomicrographs for each condition with dotted lines denoting the borders of the microwells. Scale bar = 20 μ M. (G,H) Quantification of the average axon length in each treatment condition, presented as the % length of axons in untreated slides. N= 15 axons per slide X 6 slides per treatment. Mean +/- S.E.M. ***p<.001.

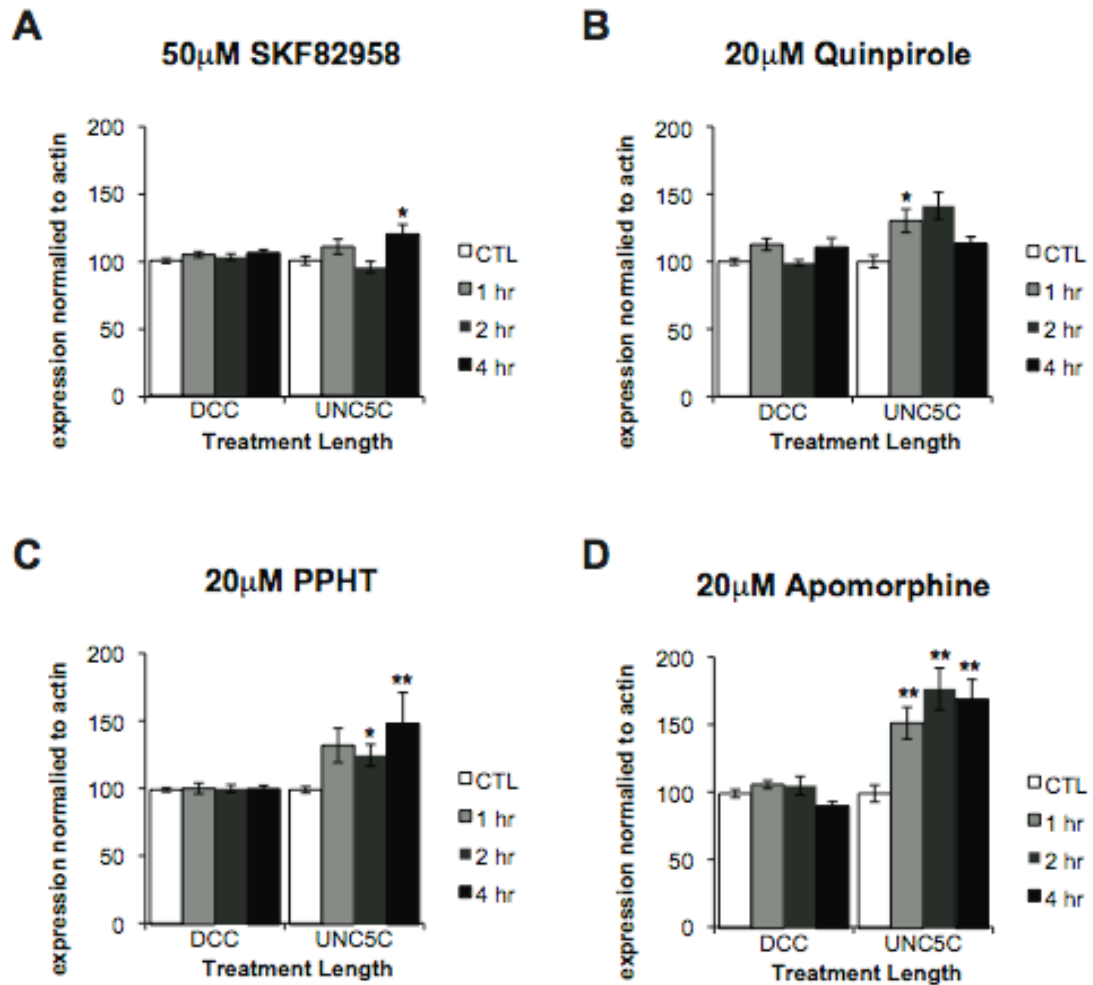


FIGURE 3.6: DR agonists regulate mRNA levels of Ntn-1 receptors.

E15 mFC neurons were grown 3 DIV and treated with the DRD1 agonist SKF82958 (A), the DRD2 agonists quinpirole (B) and PPHT (C), or the partial DRD1/DRD2 agonist apomorphine (D) for 1, 2, or 4 hours. N= 10-30 per group. Mean +/- S.E.M. *p<.05; **p<.01.

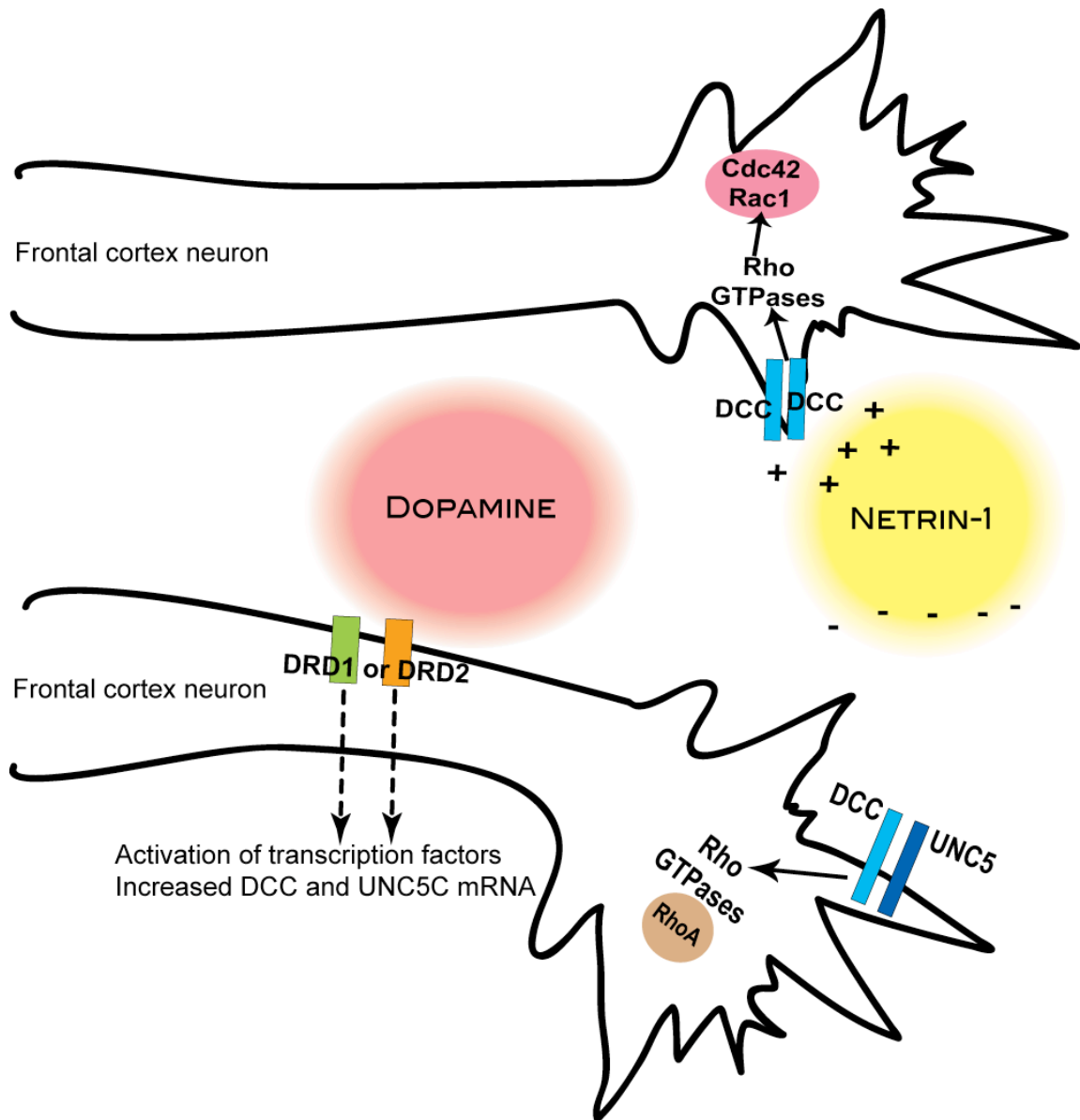


FIGURE 3.7: Model depicting DR modulation of Ntn-1 mediated axon guidance mechanisms.

Cortical neurons are attracted to Ntn-1 when homodimers of DCC are present on the surface of the growth cone. The interaction of DCC with Ntn-1 activates the Rho GTPase molecules Cdc42 and Rac1, signaling for an increase in actin polymerization and the formation of filopodia and lamellipodia in the direction of the Ntn-1 gradient. The activation of either DRD1 or DRD2 will increase mRNA levels of UNC5C, resulting in heterodimers of DCC and UNC5C on the surface of the cell. Interaction of Ntn-1 with UNC5C activates the Rho GTPase RhoA, resulting in growth cone repulsion and retraction, signaling for the movement of the growth cone away from Ntn-1 gradients.

Discussion:

SZ is characterized by decreased connectivity and hypofunction of glutamate neurons in the mFC (Murray et al., 2008, Seeman, 2009, Marek et al., 2010, Volk and Lewis, 2010). Aberrant dopaminergic signaling in the medial frontal cortex (mFC) and subcortical regions contributes to the psychotic and negative symptoms, as well as the cognitive deficits that characterize the disease (Rapoport et al., 2005, Howes and Kapur, 2009). The early onset of SZ suggests that abnormal axon pathfinding could occur early in the disease and thus contribute to altered circuit formation in the mFC. We therefore examined the hypothesis that an overactive DA system might influence axonal outgrowth of glutamatergic neurons in the mFC during early brain development thus causing a reduction in neuritic processes and a miswiring of glutamate neurons (McGlashan and Hoffman, 2000). As we show here, DA agonists disrupt neuronal attraction of glutamatergic axons to the guidance factor Ntn-1. This observation indicates that abnormally high DR activity or exposure to high levels of DR agonists during critical developmental periods may derail the proper formation of neuronal circuits and axon pathfinding events, with potential long-term effects on brain function.

Ntn-1 is a chemoattractant for cortical growth cones in the developing rat brain (Metin et al., 1997). Attraction to Ntn-1 is mediated by homodimers of DCC receptors while growth cone collapse and repulsion of Ntn-1 is mediated by heterodimers of UNC5C/DCC receptors (Hong et al., 1999, Lai Wing Sun et al., 2011). Changes in the ratio of DCC to UNC5C during development alter the response to Ntn-1 cues; increasing levels of UNC5C expressed and translocated at the growth cone change its response from attraction to repulsion (Hong et al., 1999). This is a proposed mechanism by which

axons, initially attracted, can keep growing through regions of high Ntn-1 expression and reach their final targets (Kaprielian et al., 2001). Therefore, the timing and titration of expression and translocation of both receptors is important, and interference from outside sources, such as observed here with DR agonists, can have detrimental consequences on normal pathfinding.

At E15, the time we collected the neurons for culture, the cortex consists of a thin layer of cells slated for the deep layers of the mature cortex (Kriegstein et al., 2006). During this developmental period, Ntn-1 serves as an intermediate cue for subcortical projections of mFC neurons, while soon after it guides callosal projections interhemispherically (Richards et al., 1997, Donahoo and Richards, 2009). Disturbed neuronal communication in SZ is observed between the hemispheres as well as in cortico-limbic circuits, supporting an involvement of Ntn-1 in the pathology of SZ (Ford et al., 2007).

DA afferents synapse with neurons in the mFC at E20 (Sesack et al., 1995, Carr et al., 1999, Carr and Sesack, 2000, Van den Heuvel and Pasterkamp, 2008). Cortical growth cones express functional DRs in E15 mFC cultures (Sullivan and Konradi, 2011) and DR signaling alters their response to Ntn-1 (this study); this suggests that in vivo, if DA afferents release abnormal levels of the amine into this region, Ntn-1-dependent mFC axon pathfinding could be disrupted. Alternatively, hypersensitive DA receptor pathways or environmental exposure to DR agonists could disrupt the axon pathfinding of cortical neurons.

Given that DR subtypes are differently coupled to cAMP pathways (Bronson and Konradi, 2010), the lack of specificity of DR agonists on modulating axons response to

Ntn-1 was surprising. Although in the adult rat brain both DR subtypes are found on glutamatergic principal neurons and gamma-aminobutyric acid (GABA) interneurons, there are many more glutamatergic DR positive cells in the cortex (Santana et al., 2009). In the neuronal outgrowth assays, it is unlikely that a trans-synaptic action via GABA neurons of one receptor subtype, and a direct action on glutamate neurons of the other receptor subtype occurs.

Axonal response to Ntn-1 is modulated by intracellular Ca^{2+} levels; modest levels of calcium promote attraction while excessive or insufficient calcium levels lead to repulsion (Gomez and Zheng, 2006). DRD1 activation increases protein kinase A activity, allowing calcium to flow into the cell through L-type calcium channels (Konradi et al., 1996b, Dudman et al., 2003). DRD2 receptors inhibit the flow of extracellular calcium, but mobilize intracellular calcium and activate phospholipase C pathways (Hernandez-Lopez et al., 2000). Thus activation of both DR subtypes can stimulate intracellular calcium signaling and provide a common pathway by which both DRD1 and DRD2 agonists change an axon's response to Ntn-1 (figure 3.7).

It has previously been shown that activation of serotonin receptors modulates the response of thalamocortical axons to Ntn-1 (Bonnin et al., 2007). These and our observations suggest that a general developmental role of modulatory neurotransmitters like DA and serotonin is to regulate axon guidance events in the fetal brain. Aberrant activity of these systems during crucial developmental periods could lead to miswiring of brain circuitries and later impair cognitive function. Thus, the hyperactivity of the DA system observed in SZ in adulthood might exert its most dramatic influence during early brain development.

CHAPTER IV.

POSTNATAL COCAINE ADMINISTRATION REGULATES AXON GUIDANCE MOLECULES IN THE PFC AND STRIATUM

Abstract

Psychostimulants regulate the abundance of axon guidance molecules and their receptors in adult animals but it not known if these effects occur in younger animals during periods of axonal pathfinding and synaptogenesis. Sprague Dawley rats received daily injections of cocaine or saline vehicle during two early postnatal (PN) periods: PN10-14 or PN17-21. mRNA expression of axon guidance-related genes was measured with QPCR in prefrontal cortex (PFC) and striatal (STR) tissue. PN cocaine exposure regulated the expression of *Dcc*, *Sema3c*, *Nrp1*, and *Nrp2*. Early exposure to drugs of abuse may therefore disrupt the natural trajectory of neuronal circuit formation by regulating the abundance of axon guidance molecules and/or their receptors.

Introduction

Axon guidance molecules (AGM) are expressed in the developing nervous system and influence the trajectory of outgrowth and path specification of axonal growth cones (Plachez and Richards, 2005). Directional steering by AGMs guides growth cones to their target location where synapse formation occurs (Shen and Cowan, 2010). AGMs can be attractive or repulsive, secreted or membrane-bound, and are divided into four major groups: ephrins (Eph receptors), netrins (*Dcc/Unc* receptors), semaphorins (Neuropilin/Plexin receptors), and slits (Robo receptors) (Bashaw and Klein, 2010).

Many components of AGM signaling are sensitive to neuronal activities that can be modulated by the neurotransmitter dopamine (DA), including membrane depolarization, kinase activity, and regulation of levels of calcium and cyclic nucleotides (Ming et al., 1999, Nishiyama et al., 2003, Bouchard et al., 2004, Neve et al., 2004, Gomez and Zheng, 2006). In adult animals, the administration of stimulants such as cocaine and amphetamine increases dopaminergic tone and regulates the expression of axon guidance-related genes (Bahi and Dreyer, 2005, Yetnikoff et al., 2007). Because adult animals are not undergoing axon pathfinding, these drug-induced changes may be related to the pathology of addiction.

It is not known how DA signaling effects axon guidance events in the developing brain and very little research has examined the consequences of early life stimulant exposure on AGM expression. Both prenatal and postnatal (PN) cocaine exposure increased expression of the eph receptor *Ephb1* in the cortex and striatum (STR) (Halladay et al., 2000). However, no studies have been carried out to examine the effects of stimulant exposure or aberrant DA signaling on other classes of AGMs during the time period in which axon guidance is occurring. In this study, we address this question by measuring mRNA levels of guidance-related genes from three different AGM families after PN cocaine exposure.

Material and Methods

Animals

All animals were housed and maintained in accordance with the policies of Vanderbilt University, which is accredited by the Association for the Assessment of

Accreditation of Laboratory Animal Care. Four timed-pregnant female Sprague-Dawley rats (Charles River, Wilmington, MA) were received at 18 days post conception and individually housed until pups were born. Weights for each animal were recorded daily throughout the duration of the study. Animals remained with the nursing mother at all times, except during drug administration.

Drug administration

Cocaine hydrochloride (Sigma; St. Louis, MO) was dissolved in 0.9 % saline and administered subcutaneously at 5mg/kg, in a volume of 1 μ l/g body weight, as shown in figure 4.1. 0.9% saline was used for all vehicle injections. Each animal was injected once per day for 5 days during either postnatal week 2 or 3. Animals were divided into one of four groups: A) vehicle from PN10 to PN14; B) cocaine from PN10 to PN14; C) vehicle from PN17 to PN21; D) cocaine from PN17 to PN21. Animals were sacrificed by rapid decapitation 2 hours after their last injection.

QPCR

Brains were flash frozen in methyl butane immediately after removal and stored at -80°C. PFC and STR tissue were dissected from brains using a sliding microtome. RNA extraction, cDNA synthesis, and QPCR were performed as previously described (Sullivan et al., 2011), with modifications. QPCR reactions were performed in a Stratagene ThermoCycler (Agilent, Santa Clara, CA) with Bio-Rad SYBR green mastermix (Bio-Rad, Hercules, CA). PCR cycling conditions were as follows: an initial step of 95°C for 5 min, followed by 40 cycles of 94°C for 15s, 55°C for 15s, 72°C for 30s, and data were

collected between 78-83°C, depending on primer specificity. A list of primer sequences used can be found in table 4.1. Genes were chosen for analysis based on previously reported findings in the literature. Values were normalized to the internal controls beta (β)-actin and general transcription factor IIB. Student's unpaired t-tests were used to determine statistical significance.

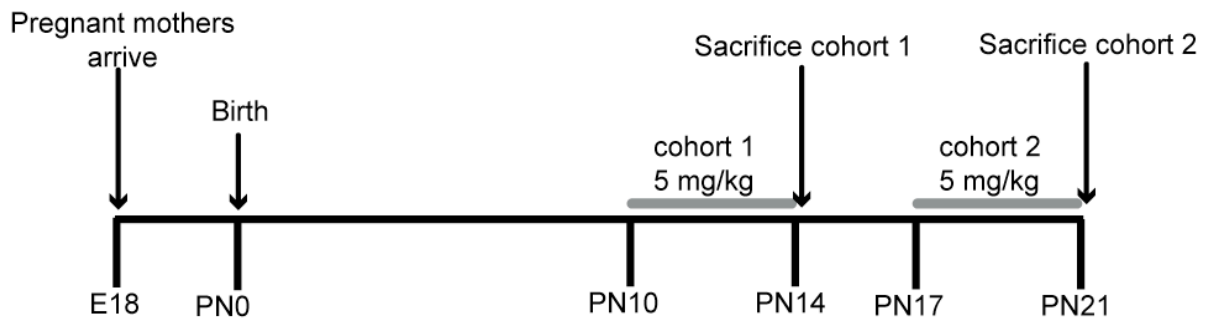


Figure 4.1: Overview of drug paradigm for postnatal cocaine administration.

Rats received one subcutaneous injection per day of 5mg/ml cocaine or saline vehicle during the second PN week (cohort 1), or the third PN week (cohort 2). Animals were sacrificed two hours after the last injection.

Table 4.1: List of primer sequences used in QPCR experiments.

Gene Name	Symbol	Direction	Sequence
Beta Actin	Actb	Forward	5' - CTATGAGCTGCCTGACGGT - 3'
		Reverse	5' - TGGCATAGAGGTCTTTACGGA - 3'
Deleted in colorectal cancer	Dcc	Forward	5' - CTATGCAAATGGTCCGGTTC - 3'
		Reverse	5' - GAGCACTTGGCACATCTGAA - 3'
Eph receptor B1	Ephb1	Forward	5'-AGGGTGTGTGTCACCAAGAGC-3'
		Reverse	5'-CACACCAGGTTGCTGTTTAC-3'
General transcription factor IIB	Gtf2b	Forward	5' - TGCATAGCTTCTGCTTGTC - 3'
		Reverse	5' - TCAGATCCACGCTCGTCTC - 3'
Neuropilin 1	Nrp1	Forward	5'-CCAATCAGAGTTCCCGACAT-3'
		Reverse	5'-AATAGACCACAGGGCTCACC-3'
Neuropilin 2	Nrp2	Forward	5'-ATGGCTTCAGGTGGATCTTG-3'
		Reverse	5'-AACAGCTTTGGCTGCTGAGT-3'
Semaphorin 3A	Sema3a	Forward	5'-TGGTTTCAGTCCCCAAGGAG-3'
		Reverse	5'-CATCCCAGGCACAATAAGG-3'
Semaphorin 3C	Sema3c	Forward	5'-GCAAAATGGCTGGCAAAG-3'
		Reverse	5'-GGGGTTGAAAGAGCATCGT-3'
Unc-5 homolog C	Unc5c	Forward	5' - TGTGTGGTTGTTGGAGAGG - 3'
		Reverse	5' - AGGGCATCCTGTGTGTCATC - 3'

Results

Cocaine administration regulates expression of axon guidance genes in the PFC and STR

Sprague Dawley rats were exposed to cocaine or vehicle during weeks 2 and 3 of postnatal development (figure 4.1). mRNA expression of 7 genes involved in axon guidance processes was measured with QPCR after cocaine exposure (figure 4.2 and table 4.2). Cocaine exposure from PN10-14 increased expression of Dcc and Sema3a in the PFC but decreased expression of Nrp1 in the STR (figure 4.2A-4.2B). Cocaine exposure from PN17-21 decreased expression of Nrp1 in both brain regions and expression of Nrp2 in the STR (figure 4.2C-4.2D). Dcc expression increased in the STR after cocaine exposure from PN17-21 (figure 4.2D). No changes were seen in Ephb1,

Sema3c, or Unc5c expression in after cocaine exposure in either brain region. A summary of gene changes can be found in table 4.3.

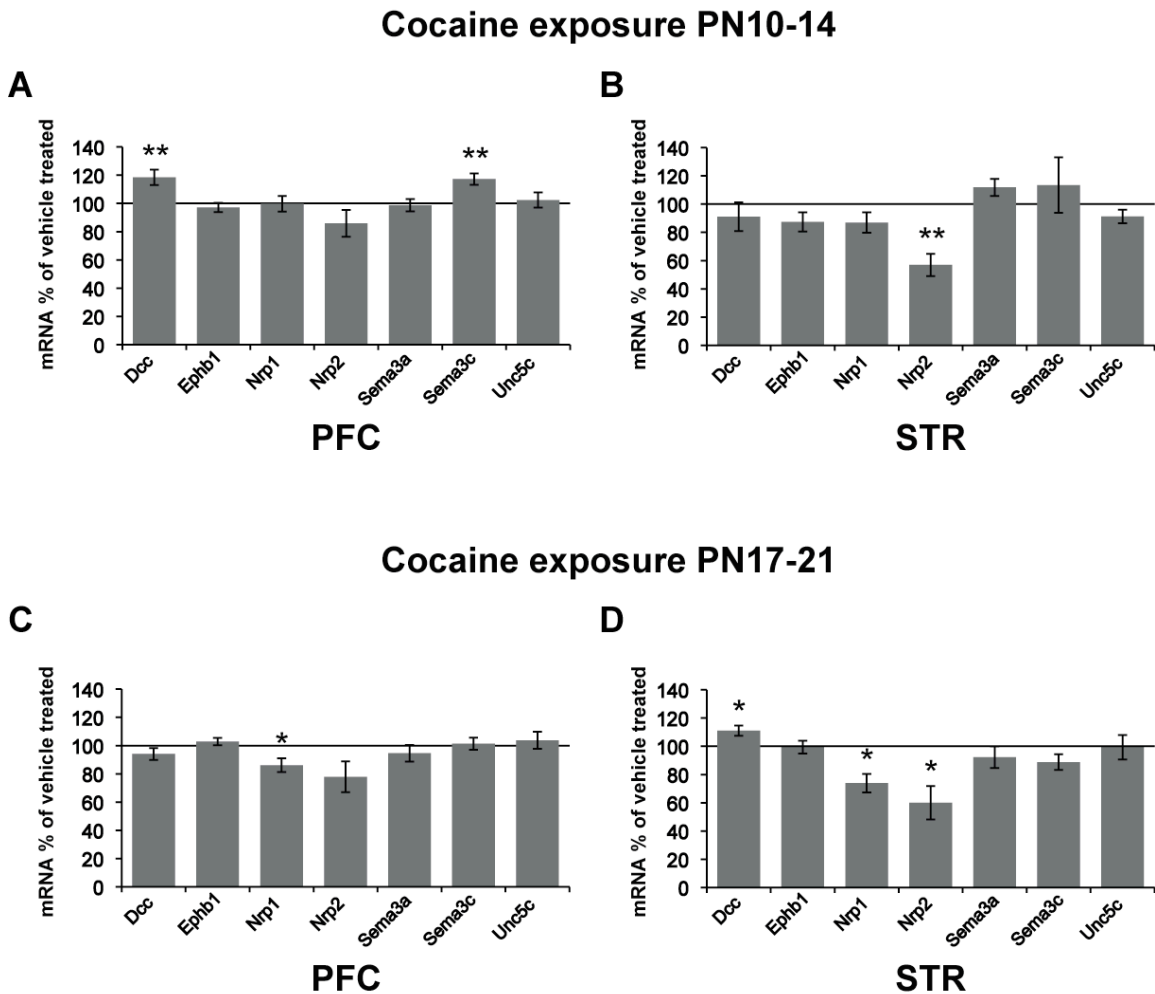


Figure 4.2: Postnatal cocaine exposure regulates expression of axon guidance genes in the PFC and STR.

Quantitative PCR measurement of mRNA levels of 7 genes involved in axon guidance events after cocaine exposure from PN10-14 (A,B) or from PN17-21 (C,D). Shown are expression levels of cocaine-exposed animals as a percent of the mRNA expression in vehicle treated animals. All values were normalized to the internal controls Actb and Gtf2b. Asterisks denote values significantly different between cocaine exposed and vehicle treated animals. PN10-14: vehicle N=12, cocaine N=12; PN17-21: vehicle N=11, cocaine N=14. Error \pm SEM. * $p < .05$; $p < .01$.

Table 4.2: mRNA analysis of axon guidance-related proteins.

Average mRNA copy numbers in PFC (A) and STR (B) tissue \pm SEM. Values were normalized to the internal controls Actb and Gtf2b. Asterisks denote values significantly different between cocaine exposed and vehicle exposed animals. * $p < .05$; $p < .01$.

A. PFC

Gene	Vehicle PN10-14	Cocaine PN10-14	Vehicle PN 17-21	Cocaine PN17-21
DCC	1.00 \pm .03	1.19 \pm .05 **	1.25 \pm .05	1.18 \pm .04
EphB1	1.05 \pm .02	1.02 \pm .03	1.07 \pm .03	1.10 \pm .03
NRP1	1.35 \pm .04	1.35 \pm .06	1.35 \pm .06	1.15 \pm .05*
NRP2	1.09 \pm .07	0.93 \pm .09	1.18 \pm .03	0.92 \pm .11
Sema3A	1.20 \pm .03	1.18 \pm .04	1.24 \pm .04	1.17 \pm .06
Sema3C	1.02 \pm .04	1.19 \pm .04**	1.16 \pm .04	1.18 \pm .04
UNC5C	1.08 \pm .05	1.10 \pm .05	1.33 \pm .08	1.38 \pm .06

B. STR

Gene	Vehicle PN10-14	Cocaine PN10-14	Vehicle PN 17-21	Cocaine PN17-21
DCC	1.28 \pm .09	1.16 \pm .10	1.12 \pm .03	1.24 \pm .04*
EphB1	1.31 \pm .07	1.15 \pm .07	1.13 \pm .03	1.13 \pm .05
NRP1	1.17 \pm .04	1.02 \pm .07	1.25 \pm .11	0.92 \pm .07*
NRP2	1.07 \pm .12	0.61 \pm .08**	1.23 \pm .12	0.74 \pm .12*
Sema3A	1.04 \pm .04	1.16 \pm .06	1.36 \pm .08	1.25 \pm .05
Sema3C	1.09 \pm .12	1.24 \pm .20	1.37 \pm .09	1.22 \pm .06
UNC5C	1.32 \pm .08	1.21 \pm .05	1.63 \pm .05	1.62 \pm .09

Table 4.3: Summary of gene changes in the PFC and STR after postnatal cocaine exposure.

Gene	PFC: PN10-14	PFC: PN17-21	STR: PN10-14	STR: PN17-21
Dcc	increased	no change	no change	increased
Ephb1	no change	no change	no change	no change
Nrp1	no change	decreased	no change	decreased
Nrp2	no change	no change	decreased	decreased
Sema3a	no change	no change	no change	no change
Sema3c	increased	no change	no change	no change
Unc5c	no change	no change	no change	no change

Discussion

Early life exposure to the stimulant cocaine alters the expression profile of genes involved in axon guidance and neuronal circuit formation. We examined the expression levels of 7 genes from three different AGM families in two brain regions after two different periods of cocaine exposure and report that cocaine-induced regulation of AGM-related genes is not restricted to a particular family, brain region, or time period. Rather, it appears that regulation of AGMs may occur through a generalized mechanism and it is likely that other AGMs are regulated by cocaine as well. Cocaine may induce widespread synaptic changes by regulating the abundance various families of AGMs simultaneously.

PN cocaine exposure increased expression of the netrin-1 receptor *Dcc* in the PFC after cocaine exposure during PN week 2 but expression of the *Unc5c* receptor was unchanged. Opposite results were seen in adult animals exposed to amphetamine where only *Unc5* levels were increased in the PFC (Yetnikoff et al., 2007). The observed differences could be due to the fact that *Dcc* levels in the PFC are highest in the embryonic brain and decrease with age but *Unc5* expression is highest in the adult brain. *Dcc* may be crucial for the formation of synapses and target selection, whereas *Unc5* may play more of a role in the maintenance of synapses.

While a previous study reported elevated *Ephb1* after prenatal and PN cocaine exposure in the STR (Halladay et al., 2000), we found no changes in *Ephb1* expression in either brain region at the two timepoints measured. This could be due to the differences in dosing paradigms and mRNA detection method used in the two studies. Halladay and

colleagues administered 30mg/ml cocaine twice per day from PN3-16, a significantly longer time period of exposure.

The semaphorin molecule Sema3c is a guiding repellent for mesencephalic DA neurons that express its receptors Nrp1 and Nrp2 (Hernandez-Montiel et al., 2008). Cocaine-induced changes in these molecules may modify mesolimbic DA connections in the PFC/STR and nigrostriatal terminals in the STR. Regulation of Nrp1 may also disrupt inter-hemispheric circuits as this receptor has been shown to mediate callosal connectivity in upper layer cortical neurons (Piper et al., 2009).

The rodent brain experiences a growth trajectory that is not directly comparable to humans. It is estimated that PN10-14 in the rodent brain corresponds to the third trimester in humans and PN17-21 in the rodent brain corresponds to early childhood in humans (Clancy et al., 2007). Based on our findings in rodents, prenatal exposure to cocaine during the third trimester of human gestation may disrupt the natural trajectory of axon outgrowth by regulating the abundance of AGMs. In addition, exposure to therapeutic stimulants for the treatment of conditions such as Attention Deficit Hyperactivity Disorder may also regulate AGM expression in young children.

CHAPTER V

BINGE COCAINE ADMINISTRATION IN ADOLESCENT RATS AFFECTS AMYGDALAR GENE EXPRESSION PATTERNS AND ALTERS ANXIETY-RELATED BEHAVIOR IN ADULTHOOD

Abstract

Administration of cocaine during adolescence alters neurotransmission and behavioral sensitization in adulthood, but its effect on the acquisition of fear memories and the development of emotion-based neuronal circuits is unknown. We examined fear learning and anxiety-related behaviors in adult male rats that were subjected to binge cocaine treatment during adolescence. We furthermore conducted gene expression analyses of the amygdala 22 hours after the last cocaine injection to identify molecular patterns that might lead to altered emotional processing. Rats injected with cocaine during adolescence displayed less anxiety in adulthood than their vehicle-injected counterparts. In addition, cocaine-exposed animals were deficient in their ability to develop contextual fear responses. Cocaine administration caused transient gene expression changes in the Wnt signaling pathway, of axon guidance molecules, and of synaptic proteins, suggesting that cocaine perturbs dendritic structures and synapses in the amygdala. Phosphorylation of glycogen synthase kinase 3 beta, a kinase in the Wnt signaling pathway, was altered immediately following the binge cocaine paradigm and returned to normal levels 22 hours after the last cocaine injection. Cocaine exposure during adolescence leads to

molecular changes in the amygdala and decreases fear learning and fear responses in adulthood.

Introduction

Cocaine is a psychostimulant drug that has long lasting behavioral and neurobiological consequences (Lidow, 2003, Nestler, 2005, Kauer and Malenka, 2007, Marin et al., 2008). While cocaine usage in teenagers has shown a downward trend in the last decade, many young Americans still experiment with drugs and/or alcohol during their formative adolescent years (NIDA InfoFacts, 2010). All drugs of abuse target subcortical dopaminergic reward pathways and it is important to fully understand how stimulation of these pathways can affect a developing brain with immature circuitry (Koob and Volkow, 2010).

Chronic drug use impairs cortical inhibition of impulsive actions and subcortical dopamine release in reward pathways, and promotes risk-taking and drug-seeking behaviors (Jentsch and Taylor, 1999). Administration of cocaine during adolescence and subsequent activation of dopaminergic pathways may restructure brain anatomy, physiology and function, and lead to various behavioral deficits in adulthood. We administered cocaine in a binge administration paradigm during adolescence (Black et al., 2006) and studied the behavioral response of cocaine-exposed rats to anxiety-evoking situations and fear learning.

The amygdalar nuclei form a circuit with the prefrontal cortex (PFC) and hippocampus that is responsible for detecting contextual and spatial information during fear conditioning, and for discriminating dangerous from innocuous stimuli (Fuchs et al.,

2009). We demonstrated previously that binge-cocaine exposure during adolescence alters normal PFC function in adult rats (Black et al., 2006). The PFC processes information from external stimuli that encode cues for drug-seeking behaviors, anxiety and fear learning (Davidson, 2002). Prelimbic FC afferent connections to the amygdala are required for the consolidation and expression of learned fear behaviors, whereas infralimbic FC-amygdala connections modulate extinction behaviors (Corcoran and Quirk, 2007). Corticoafferent projections of the basolateral amygdala to the PFC modify glutamatergic tone after chronic cocaine exposure (Orozco-Cabal et al., 2008). Efferents from the hippocampus to the amygdala are critical for the extinction of fear (Corcoran et al., 2005).

Recent evidence suggests that drugs of abuse modulate axon guidance molecules in adult rodents and cause synaptic remodeling that may reinforce the cycle of addiction (Halladay et al., 2000, Bahi and Dreyer, 2005, Yetnikoff et al., 2007). Here we provide evidence that cocaine exposure during adolescence results in gene expression changes in axon guidance and Wnt signaling pathways in the amygdala, and disrupts performance in amygdala-mediated fear learning and anxiety tasks.

Material and Methods

Animals

All animals were housed and maintained in accordance with the policies of the Vanderbilt Animal Care and Use Committee. Male Sprague-Dawley rats (n=111; Charles River, Wilmington, MA) weighing approximately 50g (postnatal day (P) 28 – P28) on arrival were housed in pairs in clear plastic cages. Food and water was available *ad*

libitum except where noted. The colony room was maintained on a 12h:12h light-dark cycle (lights on at 6:00 am). Animals were handled daily for at least a week before initiation of experiments. All behavioral testing took place during the light cycle and in independent groups of rats.

Drug Administration Protocol

Cocaine hydrochloride (Sigma; St. Louis, MO) was dissolved in 0.9 % saline and administered intraperitoneally (i.p) at 5, 10, and 15 mg/kg, in a volume of 1µl/g body weight. 0.9% saline was used for all vehicle injections. Three injections were given per day, 1 hour apart, in accordance with the binge cocaine protocol previously developed by our group (Black et al., 2006). Escalating doses of cocaine were administered within a 12-day period from P35 to P46, equivalent to the period from early adolescence to young adulthood in humans. From P35 to P36 rats received 5 mg/kg t.i.d. cocaine or vehicle. From P37 to P39, rats received 10 mg/kg t.i.d. cocaine or vehicle, and from P42-46, rats received 15 mg/kg t.i.d. cocaine or vehicle (figure 5.1).

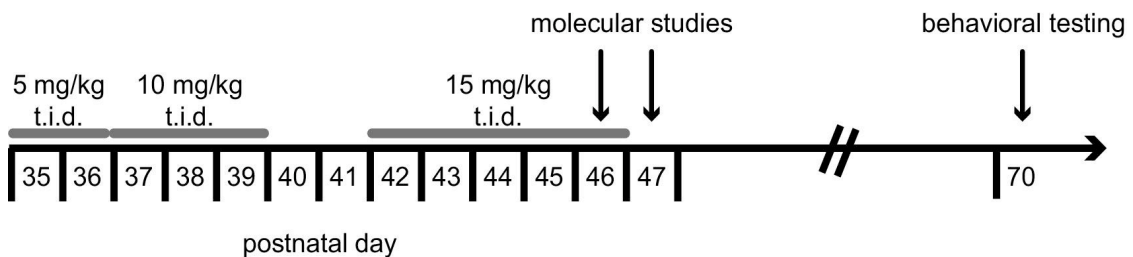


FIGURE 5.1: Overview of experimental time courses.

Ascending doses of cocaine were administered to adolescent rats from P35 to P46. Rats received I.P. injections three times per day (t.i.d.), 1 hour apart, of 5 mg/kg (P35-P36), 10mg/kg (P37-P39), or 15 mg/kg (P42-P46) cocaine or saline vehicle. Subsets of rats were sacrificed at various timepoints after the last injection for molecular studies, or tested as adults in behavioral tasks that evaluated amygdalar and hippocampal functions.

Elevated Plus Maze

All animals were habituated to the testing room for one hour. Adult male rats (P70) were placed on the elevated plus maze (Hamilton Kinder, Poway, CA) for 5 minutes and their movement was tracked using a ceiling-mounted video recording device and ANY-maze software (Stoelting, Wood Dale, IL). The maze was made of black plexiglass with 4-arms, 85 inches above the ground. The two closed arms had 40cm high walls while the open arms were without enclosing walls. All tests were carried out in red light. An animal was considered to be occupying a zone if 100% of its body was in that zone. Statistical significance was determined using the student's t-test.

Contextual Fear Conditioning

Video freeze software and operant chamber equipment (Med Associates, St. Albans, VT) were provided by the Vanderbilt Rat Neurobehavioral Core. On training day, adult male rats (P75) were habituated to the testing room for one hour prior to testing. Rats were placed in an operant chamber with natural scented oil as an odorant cue (The Body Shop; Littlehampton, UK) for a total of 7 minutes. After a two-minute acclimation period, animals were exposed to a 30 second, 5 kHz, 70 dB tone, the conditioned stimulus (CS), which coterminated with a 1 second, 0.5 mA foot-shock, the unconditioned stimulus (US). The tone and shock pairings were repeated three times and rats were removed 45 seconds after the last shock. 24 hours later, the animals were placed in the same chamber with scent, but without shock or auditory stimuli for 4 minutes. The animals' fear response was recorded as the percentage of time the animal spent freezing. A freezing episode was defined as the absence of movement for at least three seconds.

Repeated measures ANOVA for 1-minute bins, and post-hoc Tukey-Kramer HSD tests were used to determine statistical significance with JMP software (Cary, NC).

Open field

Animals were placed for 60 minutes in automated locomotor activity chambers (Med Associates, St.Albans, VT) measuring 43.2 X 43.2 X 30.5 cm (length X width X height). Movement and activity was monitored by photocell beam breaks and analyzed with the Activity Monitor Software (Med Associates). The perimeter along the walls of the chamber was designated as the “exterior” zone, while the space in the center of the arena 7.5 cm from the wall was designated as the “interior” zone. Resting time refers to episodes in which the animal did not ambulate for at least 2 seconds. Statistical analysis was carried out with repeated measures ANOVA for 5-minute bins.

Hole Board Food Search and Exploration Tasks

Experiments were carried out in sound-attenuated activity chambers (Med Associates) with pictures of easily identifiable geometrical shapes on each side (figure 5.3E,F). The chambers were fitted with floor inserts containing sixteen holes 1.25" in diameter placed on 3" centers (four rows of four equidistant holes) with an underlying food tray. The task was automated using infrared beams and software that logs hole entries. To increase the valence of food, rats were food restricted to 90% of their daily food intake measured over the previous five days, with their weights closely matched and monitored (figure 5.3A). Food restriction was initiated on P64 and maintained throughout the experiment. On P65, rats were placed in the chambers for 15 minutes with holes

unbaited. Exploratory behavior was calculated by measuring the number of holes the animal entered (novel entries), the number of times the animal returned to the same hole (repeat entries), and the total number of entries into any hole during the first 5 minutes. On P66, P69 and P70 rats spent 15 minutes in the chambers and four holes were baited with sucrose pellets. Acquisition began on P71, with the same four holes baited. Acquisition consisted of blocks of 10 one-minute sessions per day. Rats were removed after one minute or when all four baited holes had been visited and all food was retrieved, whichever came first. Acquisition trials were carried out on P71, P72, P73, P76, P77, P78 and P79. A reversal trial was carried out on P80. For the reversal trial, four new holes were baited (figure 5.3F). The pertinent calculations of the software were working memory ratio (novel entries into baited holes / all entries into baited holes) and reference memory ratio (all entries into baited holes/total entries into all holes). Statistical significance was determined using a student's t-test.

Morris Water Maze

A circular Morris water maze tank (175 cm diameter X 63.5 cm high) was filled 35.5 cm high with water (22°C) and made opaque using powdered milk. The perimeter of the tank was divided into 4 equally sized quadrants, each containing a drop spot, distinguished by the letters N, S, E, or W written above the water line. Distinct high-contrast visual cues were placed on the walls above each quadrant. A 10 cm square clear Plexiglas platform placed 2.5 cm below the water surface and at least 36 cm from the wall of the tank was used for escape. Ten rats were tested starting at 24 days post-cocaine treatment (P70). No drug was administered during this task.

Training. On days 1-3, rats completed 2 training sessions per day, each composed of 4 trials in the morning (~10:00 am) and 4 trials in the afternoon (~3:00 pm). The inter-trial interval was approximately 15 minutes. The escape platform was in the same quadrant for all training sessions (e.g. in N). For each trial, rats were removed from their homecage, placed into the water facing the tank wall, and allowed to swim freely for a maximum of 60 sec. Once a rat located the escape platform (e.g. located in the N quadrant), it was removed from the water and latency to escape was recorded. If a rat failed to locate the platform in the allotted time, it was guided to the platform and left there for 10 sec, before being removed and returned to its homecage. In this case, latency was recorded as 90 sec. Drop spots were pseudo-randomized so that each rat started a trial at each drop spot only once per session, and drop spots were matched between cocaine and vehicle treatment groups.

Reversal 1. On day 4 in the afternoon session, the platform was moved to a new quadrant (e.g. S) and latency to escape was recorded for 60 sec. The reversal consisted of 6 trials. The morning session on day 5 consisted of 4 trials with the platform located in the new quadrant (e.g. S).

Reversal 2. The second reversal was carried out during the afternoon session on day 5. The platform was moved to a new quadrant not previously used (e.g. E).

Microarrays

Rats were sacrificed 22 hours after the last cocaine injection on P47 by rapid decapitation. Brains were quickly removed and stored at -80°C until dissection on a freezing microtome. Amygdala was dissected in 2 mm round tissue punches at -1.7 mm

bregma and – 2.5 mm bregma (Paxinos and Watson, 1986), yielding two slices for the left and right side of brain. Each punch was 0.8 mm thick. The punches contained the central amygdaloid nucleus, basolateral amygdaloid nucleus, and basomedial amygdaloid nucleus with all their subdivisions. RNA was extracted with the RNagents kit (Promega, Madison, WI) according to company protocol. Double-stranded cDNA was synthesized with the help of an oligo-dT-T7 RNA polymerase primer and a cDNA synthesis kit (Invitrogen, Carlsbad, CA). Biotinylation was carried out with the Gene Chip Expression 3' Amplification kit for IVT (Affymetrix,). Hybridization to the array and washing and staining were performed according to company protocol. Samples from individual subjects were hybridized to individual arrays. Only samples that reached commonly accepted quality control criteria defined by Affymetrix, dChip (Li and Wong, 2001) and RMAExpress (Bolstad et al., 2003) were used in the analysis.

Programs used for data collection included GeneChip Operating Software (GCOS, Expression Console; Affymetrix) for scanning and to obtain quality control data, and RMAExpress (Bolstad et al., 2003) for quantile normalization and background correction to compute expression values for all probe sets. The Database for Annotation, Visualization and Integrated Discovery (DAVID, v6.7) (Dennis et al., 2003, Huang da et al., 2009), was used to group regulated genes into functional annotations provided by a number of databases.

QPCR

Microarray findings were verified with quantitative PCR (QPCR) in technical as well as biological replicates. RNA was extracted using the PureLink Micro to Midi RNA

extraction kit (Invitrogen). cDNA was synthesized from 0.3-1 μ g of total RNA with the iScript cDNA Synthesis kit (Bio-Rad, Hercules, CA). A primer set for each gene was designed with the help of Primerblast (<http://www.ncbi.nlm.nih.gov/tools/primer-blast>) for amplicons between 150 and 250 base pairs. Melt curve analysis and polyacrylamide gel electrophoresis were used to confirm the specificity of each primer pair. QPCR reactions were carried out using a Stratagene ThermoCycler and iQ SYBR Green Supermix (Bio-Rad) or Brilliant II SYBR Green Supermix (Agilent Technologies, Santa Clara, CA). PCR cycling conditions were as follows: an initial step of 95°C for 10 min, followed by 40 cycles of 94°C for 15s, 55°C for 15s, 78°C for 15s. Data were collected at 78°C. Dilution curves were generated for each primer in every experiment and on every plate by diluting cDNA from a control sample 1:4 three times, yielding a dilution series of 1.00, 0.25, and 0.0625, and .015. All samples were examined in duplicate. Values were normalized to the internal controls β -actin, alpha tubulin, 18s RNA, and general transcription factor IIB, which were not regulated by the drug paradigm. The list of primer pairs is shown in table 5.1.

Western Blotting

Groups of animals were sacrificed on P46 20 minutes after the first injection and 20 minutes after the final (third) injection, and on P47 22 hours after the final injection. Brains were removed and dissected as described above. Tissue was sonicated in Laemmli buffer, heated to 80°C for 10 minutes and proteins were electrophoresed on 10-20% gradient Tris-Glycine gels (Invitrogen). Proteins were transferred to PVDF membranes and blocked with animal-free blocking solution (Vector Laboratories, Burlingame, CA).

Primary antibodies were diluted in blocking solution and incubated with membranes overnight at 4°C. The following antibodies were used: anti-actin (Sigma, St.Louis, MO), anti-phospho GSK3 beta (Serine 9), and anti-total GSK3 beta, (Cell Signaling, Danvers, MA). Membranes were washed in TBS-T and incubated for an hour at room temperature with HRP-conjugated secondary antibodies (Vector Laboratories) prepared in blocking solution. Blots were immersed in chemiluminescent reagents (Pierce, Rockford, IL) and exposed and analyzed on the KODAK Imaging Station IS440. Statistical significance was determined using a student's t-test.

TABLE 5.1: Primer sequences for QPCR reactions

Name	Direction	Sequence
Adra1d	Forward	5' - TGGCCATCGTCGTGGGTGTC - 3'
	Reverse	5' - GCGCTTGAACCTCGCGACTGG - 3'
Alpha Tubulin	Forward	5' - GCTTCTTGGTTTTCCACAGC - 3'
	Reverse	5' - CCATGAAGGCACAATCAGAG - 3'
Beta Actin	Forward	5' - CTATGAGCTGCCTGACGGT - 3'
	Reverse	5' - TGGCATAGAGGTCTTTACGGA - 3'
Bmpr2	Forward	5' - CCCGTCCTAGGCGAATGAAGCC - 3'
	Reverse	5' - CGGGTGAGAAATCCGGCCAGGA - 3'
Ccnd2	Forward	5' - TTCTTGGCTGGAGTCCCGACT - 3'
	Reverse	5' - TTCCCACTCCAGCAGCTCCTG - 3'
Cdh13	Forward	5' - TTGACAGGCACGGCCACAGC - 3'
	Reverse	5' - GTGTATGCCGCCCTCCATGC - 3'
Chrm3	Forward	5' - TGGGAATTTCTCCTCAAACG - 3'
	Reverse	5' - AGGCCAGGCTTAAGAGGAAG - 3'
Csnk1a1	Forward	5' -GCCAGGCATCCCCAGTTGCT - 3'
	Reverse	5' - GTCTTCGAGGCTGGGTCCCA - 3'
Ctbp2	Forward	5' - CAGGTCCTGCGCAGCTTGTTGT - 3'
	Reverse	5' - CGCGGAGATGTCTACACCAGCA - 3'
Daam1	Forward	5' - ATGCCCCCTGTGGAGGAGCT - 3'
	Reverse	5' -CGGGCCAACTTGTTGCTCCCT - 3'
Gsk3B	Forward	5' - ATCAAGGCACATCCTTGGAC - 3'
	Reverse	5' - AGTTGAAGAGGGCAGGTGTG - 3'
Gtfl1B	Forward	5' - TCGGATAGCTTCTGCTTGTC - 3'
	Reverse	5' - TCAGATCCACGCTCGTCTC - 3'
Itgb6	Forward	5' - CCCAACGATGGGCTCTGTCCAC - 3'
	Reverse	5' - CGCTCCAGGGATGAGTTTCGC - 3'
Nfatc4	Forward	5' - CCAGAGCTCACCACCGAGCT - 3'
	Reverse	5' - AGTGATCCGGTGCACCTGGT - 3'
Nrp1	Forward	5' - CCAATCAGAGTTCCCGACAT - 3'
	Reverse	5' - AATAGACCACAGGGCTCACC - 3'
Pcdh17	Forward	5' - GTTCGGGCA ACTTGAGCGGAAT - 3'
	Reverse	5' - GGGGCCACAAAAGAAAGCAGC - 3'
Slit2	Forward	5' - TGCCTGGCTGTGAACCATGCC - 3'
	Reverse	5' - AGGCGTTGATGGGCAAGCAG - 3'
Stxbp1	Forward	5' - CCCGCTCTCCGCATCCTTC - 3'
	Reverse	5' - CGTTGGCCTGCGTCACTTCG - 3'
Syn3	Forward	5' - ACCCCAAAAGACAGCATCAC - 3'
	Reverse	5' - AGGCTAGTCGGAGAAGAGGC - 3'
Syt7	Forward	5' - AGGTGGACCTGACCCAGATGC - 3'
	Reverse	5' - GTCTGATGTGCCCCCGATGTC - 3'
Tak1	Forward	5' - AGATGATCGAAGCGCCATCGCA - 3'
	Reverse	5' - GCCGGAGCTCCACGATGAAAGC - 3'
Tgfb3	Forward	5' - TGCCCAACCCAGCTCCAAG - 3'
	Reverse	5' - CAACAGCCACTCGCGCACAG - 3'
Wnt11	Forward	5' -GCAGGTCTGCGAGGCTCTTC - 3'
	Reverse	5' - ACACCAGGCCCTCCAGCTGT - 3'
18s RNA	Forward	5' - TGGCTCAGCGTGTGCCTACC - 3'
	Reverse	5' - TAGTAGCGACGGGCGGTGTG - 3'

Results

Adolescent cocaine exposure decreases anxiety and conditioned fear behaviors in adult rats

In the elevated plus maze, cocaine-exposed rats spent significantly more time in the open arm than vehicle-treated rats (figure 5.2A). Rats that received cocaine during adolescence had fewer entries into the closed arms and less distance traveled inside the closed arms than the vehicle-treated group (figure 5.2B,C). No difference was observed in the center and open arms in either distance traveled or number of entries.

To examine learned fear we used the conditioned freezing paradigm. The amygdala, the brain area most closely associated with fear and anxiety, evolved with the olfactory system, and in the rat receives dense projections from the olfactory bulb to alert the animal to scents associated with danger (Davis, 1992, Moreno and Gonzalez, 2007). Therefore, we used scented oils in the operant chambers during fear conditioning and on the testing day. While no difference in freezing was observed on the day of training, the cocaine-exposed group froze less on the testing day than the vehicle group (figure 5.2D). A time by group interaction was found ($F(3,14)=4.89$; $p=0.016$), and post-hoc analysis confirmed significant decreases in freezing behavior at minute 1 (vehicle= $29.4 \pm 8.4\%$; cocaine= $11.3 \pm 5.6\%$) and minute 2 (vehicle= $62.9 \pm 8.2\%$; cocaine= $19.0 \pm 7.5\%$) (figure 5.2E). Thus, cocaine exposed animals did not develop the same contextual fear response as the vehicle - exposed rats.

Movement and behavior of rats in the open field area were monitored for a total of 60 minutes. The cocaine-exposed rats spent a greater proportion of time in the interior zone than vehicle - exposed rats (main effect of treatment, $F(1,11)=8.8$, $p=0.01$; figure 5.2F). This was not just restricted to a quick crossing of the interior, but was also observ-

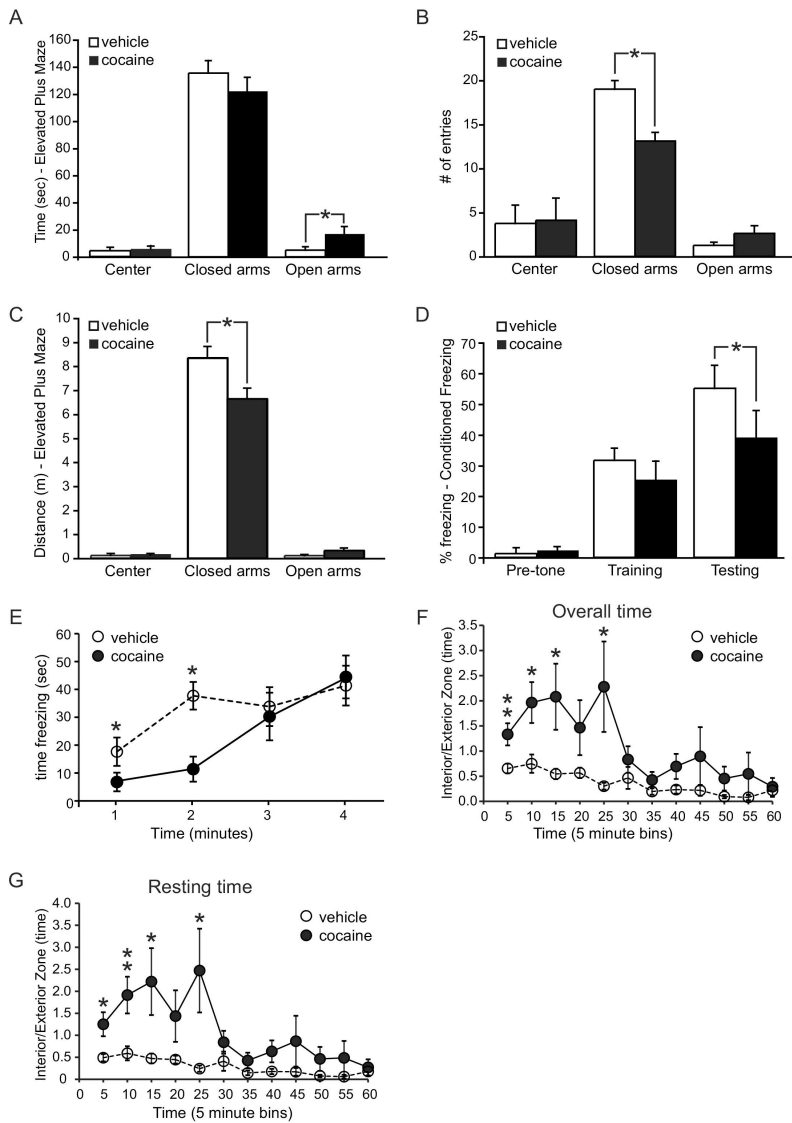


FIGURE 5.2: Adolescent binge cocaine exposure disrupts fear learning and anxiety behaviors in adult rats. A,B,C: Behavior in the elevated plus maze. A: Total time spent in center, closed, and open arms shows cocaine-exposed rats spent more time in the open arms than vehicle treated animals. B: Total number of entries into each zone of the maze showed cocaine-exposed rats entered the closed arms less frequently. C: Distance traveled in each zone showed cocaine-exposed animals traveled less in the closed arms. D,E: Results of the conditioned freezing paradigm. D: Percent freezing before and during training, and on testing day. ‘Pre-tone’ measures the first 190 seconds the animal was placed in the chamber prior to shock or tone. ‘Training’ refers to the pre- and post-tone, as well as the conditioning phase where animals received the conditioned (tone) and unconditioned (shock) stimuli. ‘Testing’ is the average measure of freezing over 4 minutes, 24 hours after conditioning. E: Freezing time during the testing period of the contextual fear conditioning paradigm. Post-hoc analysis revealed significant decreases in freezing behavior at 1 and 2 minutes. F,G: Behavior in the open field. Zone time was recorded for 60 minutes and separated into 5-minute bins. White circle, vehicle; black circle, cocaine. Shown is the ratio of time spent in the interior part of the chamber over time spent in the exterior part of the chamber (I/E) for all observed movements (F), and time spent resting, in which the animal did not ambulate for at least 2 seconds (G). All data average \pm SEM; Elevated Plus Maze vehicle n= 8; cocaine n= 9; contextual fear conditioning vehicle n= 10; cocaine n= 9; open field vehicle n=6; cocaine n=8.

ed in the resting time measures ($F(1,11)=10.9$, $p=0.01$; figure 5.2G). Overall distance traveled was not different between the groups (cocaine: 5901 ± 521 ; vehicle 6724 ± 659 ; cm average \pm SEM).

Adolescent cocaine exposure increases novelty seeking and exploratory behaviors in adult rats

In the hole board exploration task, exploration and anxiety were measured by the number of novel entries, repeat entries, and total entries with the snout into a hole during a 5-minute novel exposure to the 16-hole chamber. Cocaine-exposed rats entered the chamber's holes at a higher frequency than the saline-exposed rats, although holes were not baited (figure 5.3B). Distance traveled and time spent ambulating or resting in the interior part of the chamber that included the holes, and the residual perimeter next to the walls of the chamber, were comparable for both groups (figure 5.3C, D). However, cocaine-exposed rats had a higher ratio of time spent resting in the interior part of the chamber/residual part of the chamber (figure 5.3D).

Adolescent cocaine exposure does not impair spatial learning and memory in adult rats

The hole board food search task and the Morris water maze task were used to assess spatial learning and memory function. The hole board food search task measures working memory and reference memory. The working memory ratios and reference memory ratios were between 30-50% on the first day of acquisition (figure 5.3G,H), after three days of habituation. Both groups of rats improved in their performance over time and no significant differences were seen in any aspect of the task, indicating that the

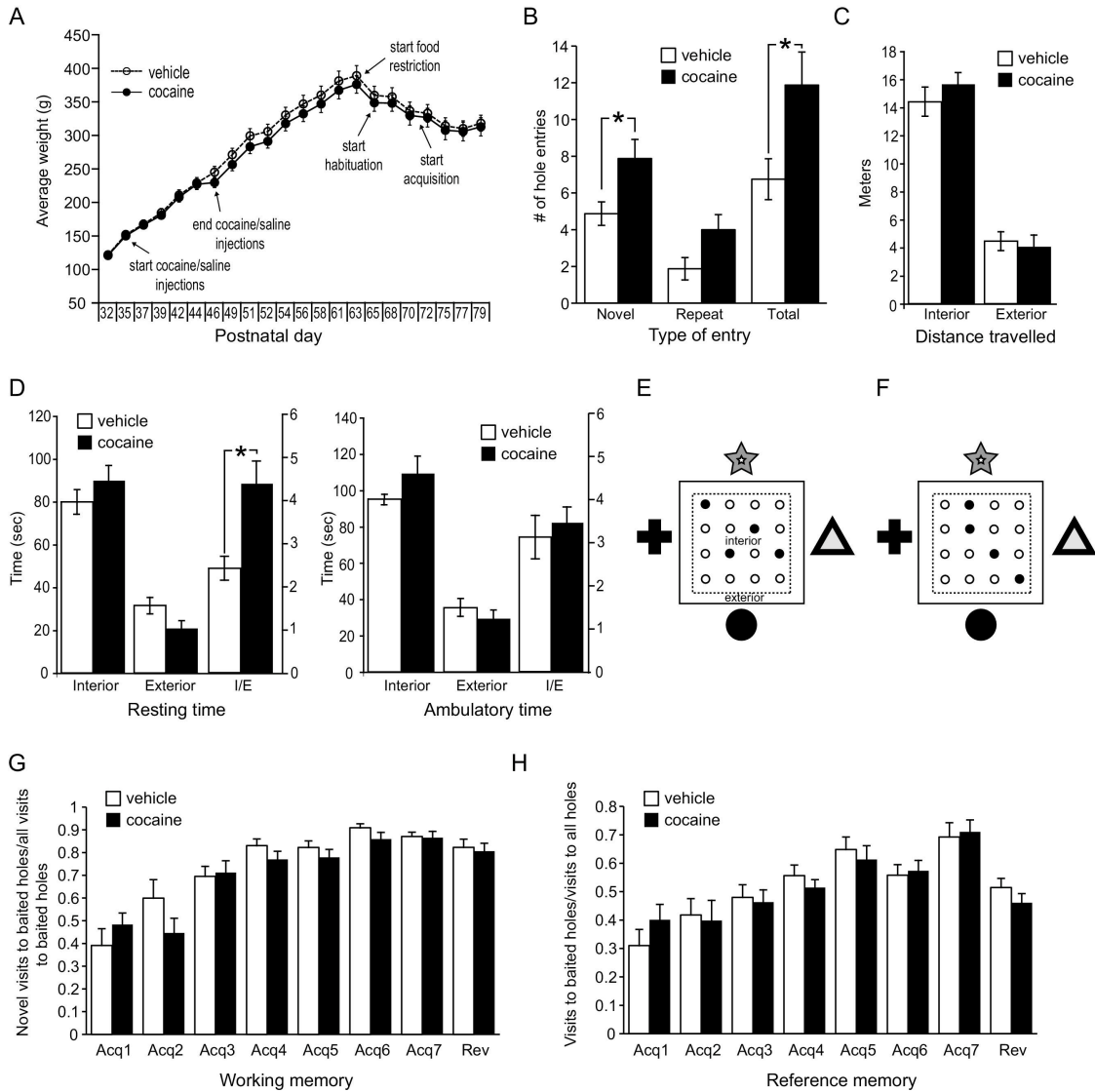


FIGURE 5.3: Exploration and novelty seeking is increased in adult rodents after binge cocaine administration in adolescence. A: Weight curves and treatment schedules for animals undergoing the hole board tasks. B-D: Hole board exploration. E-H: Hole board food search task. B: Novel, repeat, and total entries into unbaited holes during a 5-minute novel exposure to the hole board chamber. C: Distance traveled in the interior and exterior part of the chamber during novel exposure. D: Resting (not ambulating for at least 2 seconds) and ambulatory time spent in the interior part of the chamber or the exterior part of the chamber during novel exposure. I/E is the ratio of interior time over exterior time. E, F: Hole board food search design with baited holes in black. High-contrast shapes were placed on the four walls of the chamber as reference points. Areas of internal and external measurements are shown. E: Holes baited during habituation and acquisition; F: Holes baited during the reversal trial. G: Working memory ratio (novel entries into baited holes / all entries into baited holes) in the hole board food search task. F: Reference memory ratio (all entries into baited holes/total entries into all holes) in the hole board food search task. All data average \pm SEM; vehicle n=8; cocaine n=8.

cocaine-exposed rats learned the task as well as the vehicle-treated rats. Although upon novel exposure to the operant chamber (hole board exploration) differences in hole entries were observed between the groups, no differences were seen on the subsequent three days of habituation when holes were baited with sucrose pellets. Working and reference memory trials were therefore not influenced by different levels of anxiety to enter the holes. In a reversal test on the 8th day, no significant differences were observed between the groups. The reversal showed that rats had learned to not re-visit the baited holes, as their working memory ratio was similar to the last acquisition day (figure 5.3G). The decrease in reference memory ratio upon reversal shows that the rats first visited the previously baited, now unbaited holes, before checking the other holes (figure 5.3H). The decrease in reference memory ratio verified that the rats were using their memory to find the sucrose pellets.

The Morris water maze task was carried out in morning and afternoon sessions on five consecutive days (figure 5.4). On the afternoon sessions of days 4 and 5, different reversals of the platform location were introduced. No difference in performance was observed between the groups.

Binge cocaine exposure regulates amygdalar gene expression in adolescent rats

To determine if a molecular pattern was associated with impaired fear learning and anxiety, we conducted gene expression microarray assays on the amygdala from a subset of rats killed 22 hours after the last injection. Genes that were changed by less than 10% were excluded as well as those that were considered below detection level in 40% or more of all samples. Significance was determined with a student's t-test and only genes

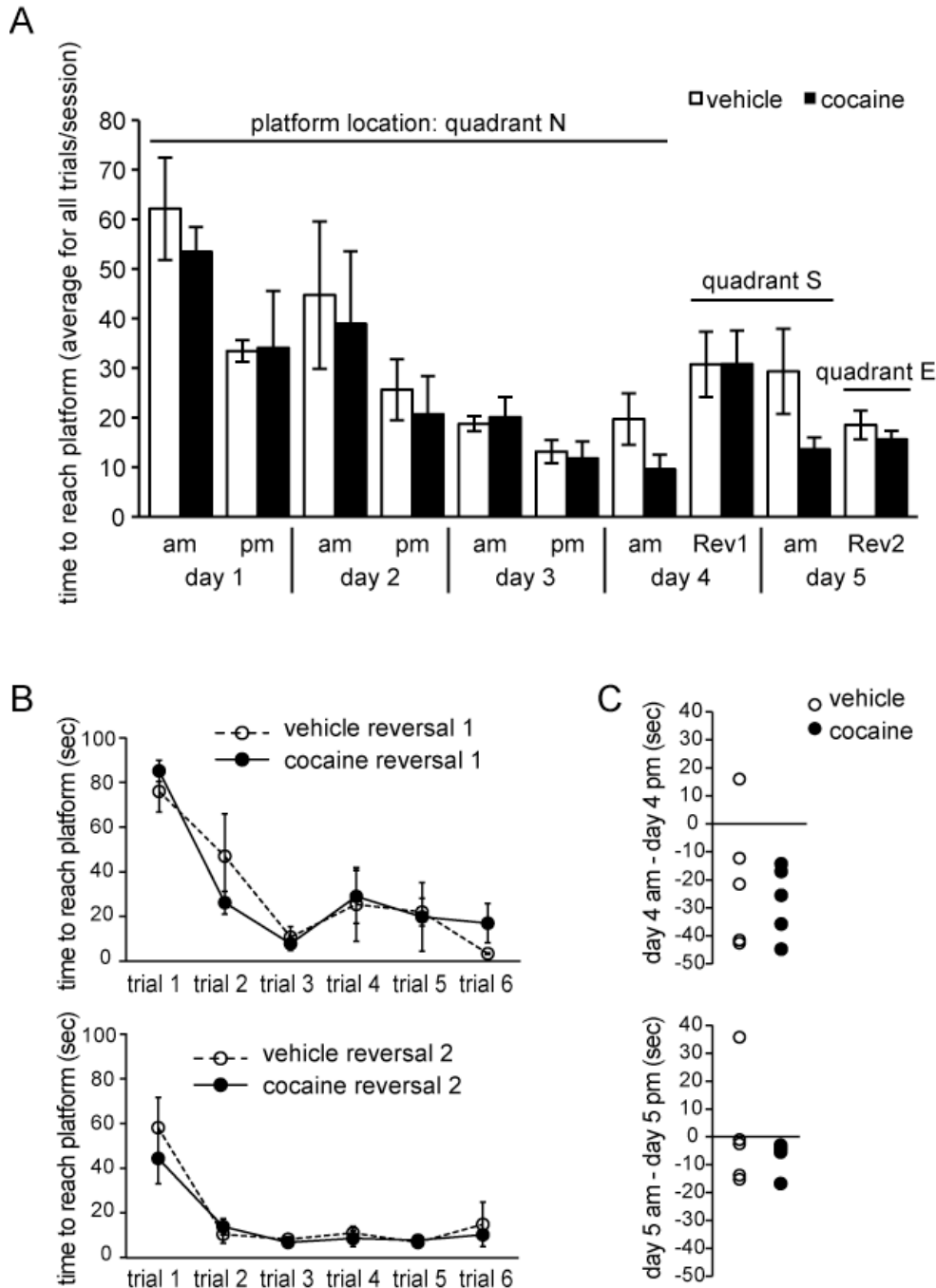


FIGURE 5.4: Spatial learning and memory were not altered in adult rats after adolescent cocaine exposure. The Morris water maze task was carried out in morning and afternoon sessions on five consecutive days, with 4 trials per session. In the afternoon sessions of days 4 and 5, different reversals of the platform location were introduced. No difference in performance was observed between the groups. A: Morris Water Maze data with all trials per session averaged. Quadrant with platform location is shown above the bar graphs. Time to reach platform is averaged for all trials per session per day. B: Individual trials for reversal sessions 1 and 2. C: Difference in time to reach the platform between day 4 am and day 4 pm (first reversal; $F(1,8)=0.37$, $p=0.560$), and between day 5 am and day 5 pm (second reversal; $F(1,8)=0.6$, $p=0.463$). White circle, vehicle; black circle, cocaine. Abbreviations: Rev, reversal; N = north, S = south, E = east; data average \pm SEM, vehicle $n=5$; cocaine $n=5$.

that had a p value of less than 0.05 were considered for further analysis. We used the DAVID database to examine annotation clusters that identify common pathways in a list of regulated genes (Dennis et al., 2003, Huang da et al., 2009). Because of redundancy in annotation records, we used annotation clustering to identify enriched gene groups in multiple categorical classifications.

A group of downregulated genes was identified with an enrichment score of 3.37, which contained genes in pathways termed “synapse”, “synapse part”, “plasma membrane”, and “cell junction”. Members of this group are shown in table 5.2. No particular pathway was identified in the group of upregulated genes. However, in the entire group of regulated genes several pathways were significantly affected by cocaine exposure. These pathways were related to development of synapse structure and growth and included “axon guidance” (table 5.3) and “Wnt signaling” (table 5.4). Quantitative PCR (QPCR) on a subset of genes confirmed the gene array data (figure 5.5). The list of primer sequences is provided in table 5.1. A technical replicate was performed for several genes in each pathway (figure 5.5A).

Wnt signaling is dysregulated following adolescent cocaine exposure

Additional analysis in another cohort was performed to verify regulation of the Wnt signaling pathway (figure 5.5B). The altered expression of Wnt5a and Wnt7a could not be verified in the QPCR analysis and only showed trends for regulation (data not shown). However, Wnt11, a gene that had a low present call in the microarray analysis, was found to be significantly elevated in cocaine exposed animals (figure 5.5B). The microarray analyses revealed an increase in glycogen synthase kinase 3 beta (GSK3B)

TABLE 5.2: Adolescent cocaine exposure leads to downregulation of plasma membrane and synaptic genes in the amygdala. Microarray analysis revealed a group of 37 genes classified as “synaptic” or “plasma membrane part” that were downregulated in animals that received cocaine during adolescence. Shown are the probe set IDs, gene name, accession number, fold changes, and p-value (based on log₂-transformed data). Vehicle n=6; cocaine n=7.

Probe ID	Gene Name	Accession	Fold Change	p Value
1370121_at	Add1: adducin 1 (alpha)	NM_016990	-1.19	4.27E-02
1370621_at	CD3z: CD3 antigen, zeta polypeptide	D13555	-1.13	3.10E-02
1369559_a_at	CD47: CD47 antigen (Rh-related antigen, integrin-associated signal transducer)	NM_019195	-1.18	2.50E-02
1369025_at	CD5: CD5 antigen	NM_019295	-1.11	3.28E-02
1373102_at	Cdh13: cadherin 13	BI282750	-1.19	6.45E-03
1369112_at	Chrm3: cholinergic receptor, muscarinic 3	M18088	-1.17	4.30E-02
1373067_at	Ctnnb1: catenin (cadherin associated protein), beta 1	AI102738	-1.18	4.84E-02
1370625_at	Faim2: Fas apoptotic inhibitory molecule 2	AF044201	-1.21	3.06E-02
1398246_s_at	Fcgr3: Fc receptor, IgG, low affinity III	NM_053843	-1.15	4.41E-02
1369267_at	Gabrg3: gamma-aminobutyric acid A receptor, gamma 3	NM_024370	-1.25	1.85E-02
1370590_at	Gpsm1: G-protein signaling modulator 1 (AGS3-like)	AF107723	-1.17	4.08E-02
1377546_at	Gria4: glutamate receptor, ionotropic, 4	BF397279	-1.31	1.48E-02
1371180_a_at	Grm1: glutamate receptor, metabotropic 1	Y18810	-1.16	4.15E-02
1378625_at	Grm8: glutamate receptor, metabotropic 8	BF392502	-1.19	2.01E-03
1368783_at	Icos: inducible T-cell costimulator	NM_022610	-1.13	4.78E-02
1368979_at	Kalrn: kalirin, RhoGEF kinase	NM_032062	-1.11	3.53E-02
1370078_at	Lin7b: lin-7 homologue b (C. elegans)	NM_021758	-1.13	3.10E-03
1384190_at	Mapk8ip3: mitogen-activated protein kinase 8 interacting protein 3	BF553848	-1.17	2.53E-02
1395927_at	Pdzk1: PDZ domain containing 1	BE116199	-1.12	3.12E-02
1388966_at	P2ry1: purinergic receptor P2Y, G-protein coupled 2	BM388250	-1.13	4.61E-02
1393207_at	Rab35: RAB35, member RAS oncogene family	BF566116	-1.12	4.31E-02
1369338_at	Robo1: roundabout homologue 1 (Drosophila)	NM_022188	-1.17	4.98E-02
1369054_at	Rph3a: rabphilin 3A homologue (mouse)	NM_133518	-1.27	2.29E-02
1368907_at	Scamp5: secretory carrier membrane protein 5	NM_031726	-1.14	4.45E-03
1368445_at	Shank1: SH3 and multiple ankyrin repeat domains 1	BE105448	-1.17	1.32E-02
1369715_at	Slc6a11: solute carrier family 6, member 11; gamma-aminobutyric acid transporter	M95763	-1.30	5.00E-02
1387693_a_at	Slc6a9: solute carrier family 6, member 9; glycine transporter	M95413	-1.30	2.49E-02
1368896_at	Smad7: MAD homologue 7 (Drosophila)	NM_030858	-1.14	1.47E-02
1381263_at	Slc27a4: solute carrier family 27 (fatty acid transporter), member 4	H33747	-1.15	4.24E-02
1370840_at	Stxbp1: syntaxin binding protein 1	NM_013038	-1.11	7.16E-03
1369423_at	Syn3: synapsin III	NM_017109	-1.26	1.45E-02
1387527_at	Syng1: synaptogyrin 1	NM_019166	-1.17	4.07E-02
1370514_a_at	Syt7: synaptotagmin VII	AI713274	-1.13	1.48E-02
1378407_at	Trim9: tripartite motif-containing 9	BF401415	-1.23	2.07E-02
1369330_at	Unc13a: unc-13 homologue A (C. elegans)	NM_022861	-1.12	1.74E-02
1384158_at	Unc13c: unc-13 homologue C (C. elegans)	AW522416	-1.20	4.86E-02
1387716_at	Utrn: utrophin	NM_013070	-1.32	2.47E-02

TABLE 5.3: Adolescent cocaine exposure alters the expression of axon guidance genes in the amygdala. Regulated axon pathway genes are listed with their respective probe set IDs, gene name, and accession number. Vehicle n=6; cocaine n=7.

Probe ID	Gene Name	Accession	Fold Change	p Value
1380330_at	Ablim2: actin binding LIM protein family, member 2	BI288159	-1.15	4.52E-02
1382389_at	Arhgef5: Rho guanine nucleotide exchange factor 5	AI179755	1.21	2.93E-02
1389244_x_at	Cxcr4: chemokine (C-X-C motif) receptor 4	AA945737	1.23	7.72E-03
1369476_at	Efnb1: ephrin B1	NM_017089	-1.13	3.11E-02
1378997_at	Ephb6: Eph receptor B6	BM391684	1.19	3.31E-02
1370267_at	Gsk3b: glycogen synthase kinase 3 beta	BF287444	1.44	2.64E-02
1392582_at	Lrrc4c_predicted: leucine rich repeat containing 4 C	AA819053	4.3	2.45E-03
1372032_at	neuroblastoma ras oncogene	AA851914	1.14	7.86E-03
1390573_a_at	Nfatc4: nuclear factor of activated T-cells, calcineurin-dependent 4	BG377358	-1.11	1.91E-02
1370570_at	Nrp1: neuropilin 1	AF016296	1.29	2.59E-02
1396426_at	p21 protein (Cdc42/Rac)-activated kinase 4	BF404920	-1.14	3.02E-03
1369338_at	Robo: roundabout homologue 1 (Drosophila)	NM_022188	-1.17	4.98E-02
1378389_at	similar to nuclear factor of activated T-cells, calcineurin-dependent 4	BM385157	1.18	2.33E-02
1395986_at	Slit2: slit homologue 2 (Drosophila)	BF391439	1.33	5.19E-03
1377651_at	Trio: triple functional domain (PTPRF interacting)	AI577848	-1.37	1.70E-02

TABLE 5.4: Adolescent cocaine exposure alters the expression of Wnt signaling pathway genes in the amygdala. Regulated Wnt signaling pathway genes are listed with their respective probe set IDs, gene name, and accession number. Vehicle n=6; cocaine n=7.

Probe ID	Gene Name	Accession	Fold Change	p Value
1368534_at	Adra1d: adrenergic receptor, alpha-1d	NM_024483	1.71	4.62E-02
1376843_at	Bmpr2: bone morphogenic protein receptor, type II	BE118651	1.68	5.03E-03
1368534_at	Adra1d: adrenergic receptor, alpha-1d	NM_024483	1.71	4.62E-02
1375353_at	Cables1: Cdk5 and Abl enzyme substrate 1	BI296696	1.22	4.78E-02
1373089_at	Cdh3: cadherin 3, type 1, P-cadherin	AI010270	1.4	2.13E-02
1375619_at	Cdh8: cadherin 8	BF417982	-1.18	3.60E-02
1375719_s_at	Cdh13: cadherin 13	BI282750	-1.32	1.68E-02
1372299_at	Cdkn1c: cyclin-dependent kinase inhibitor 1 C (P57)	AI013919	1.53	7.78E-03
1372685_at	Cdkn3: cyclin-dependent kinase inhibitor 3	BE113362	1.19	3.30E-03
1389759_at	Celsr1: cadherin EGF LAG seven-pass G-type receptor 1	AW433901	1.25	3.47E-02
1383946_at	Cldn1: claudin 1	AI137640	1.53	4.93E-02
1385852_at	Crebbp: CREB binding protein	BF566908	1.3	4.53E-02
1394689_at	Csnk1a1: casein kinase 1, alpha 1	BE117217	1.23	7.57E-03
1387113_at	Ctbp2: C-terminal binding protein 2	NM_053335	1.25	3.88E-02
1373067_at	Ctnnb1: catenin (cadherin associated protein), beta 1	AI02738	-1.18	4.84E-02
1375266_at	Ccnd2: cyclin D2	BG380633	1.21	3.52E-02
1374480_at	Daam1: dishevelled associated activator of morphogenesis 1	BE107255	1.12	2.74E-02
1374530_at	Fzd7: frizzled homologue 7 (Drosophila)	AI010048	1.35	3.95E-02
1368337_at	Glycam1: glycosylation dependent cell adhesion molecule 1	NM_012794	1.72	1.74E-02
1370267_at	Gsk3b: glycogen synthase kinase 3 beta	BF287444	1.44	2.64E-02
1367571_a_at	IGF-2: insulin-like growth factor 2	NM_031511	1.47	4.38E-02
1367648_at	Igfbp2: insulin-like growth factor binding protein 2	NM_013122	1.68	4.48E-02
1382439_at	Itgb6: integrin, beta 6	AI070686	2.09	1.74E-02
1393138_at	Jund: Jun D proto-oncogene	BE329377	-1.11	4.77E-02
1388155_at	Krt1-18: keratin complex 1, acidic, gene 18	BI286012	1.49	4.43E-02
1371530_at	Krt2-8: keratin complex 2, basic, gene 8	BF281337	1.81	2.16E-02
1399075_at	map 3k7: mitogen activated protein kinase kinase 7; Tak1: Tgf beta activated kinase 1	AI146037	1.12	8.56E-03
1390573_a_at	Nfatc4: nuclear factor of activated T-cells, cytoplasmic, calcineurin-dependent 4	BG377358	-1.11	1.91E-02
1393144_at	Nmi: N-myc (and STAT) interactor	BM388202	1.14	2.44E-02
1395408_at	Nostrin: nitric oxide synthase trafficker	AI058709	1.13	3.63E-02
1377676_at	Nucks: nuclear ubiquitous casein kinase and cyclin-dependent kinase substrate	AI599187	1.13	3.37E-02
1384509_s_at	Pcdh17: protocadherin 17	BF558981	1.49	4.84E-02
1370490_at	Pcdh3: protocadherin 3	L43592	-1.35	7.82E-03
1370950_at	Ppap2b: phosphatidic acid phosphatase type 2B subunit B delta	AW253995	1.29	2.70E-02
1395502_at	Ppp2r5d: protein phosphatase 2, regulatory	BF557865	-1.11	3.60E-02
1382274_at	Rarres1: retinoic acid receptor responder 1	AA819288	-1.26	1.08E-02
1378389_at	similar to nuclear factor of activated T-cells, calcineurin-dependent 1	BM385157	1.18	2.33E-02
1391557_at	Sox15: SRY (sex-determining region Y)-Box 15	AI009685	-1.14	2.96E-02
1367859_at	Tgfb3: transforming growth factor, beta 3	NM_013174	1.33	4.50E-02
1368359_a_at	Vgf: VGF nerve growth factor inducible	NM_030997	-1.21	3.29E-02
1382375_at	Wnt5a: wingless-type MMTV integration site 5 A	AI639128	-1.27	4.87E-02
1380958_at	Wnt7a: wingless-related MMTV integration site 7 A	BG671935	-1.18	2.61E-03

mRNA levels in the amygdala 22 hours after the last injection (table 5.4). To determine if cocaine regulates GSK3B activity, we measured total GSK3B protein as well as levels of GSK3B phosphorylated at serine residue 9, in the amygdala of rats that were sacrificed 20 minutes after the first or third injection on the last day of the dosing paradigm, or 22 hours after the last injection. Phosphorylation of GSK3B at serine residue 9 was increased after the first injection but decreased after the third injection. No changes were seen in the total amount of GSK3B protein (Figure 5.6). No changes in phosphorylated or

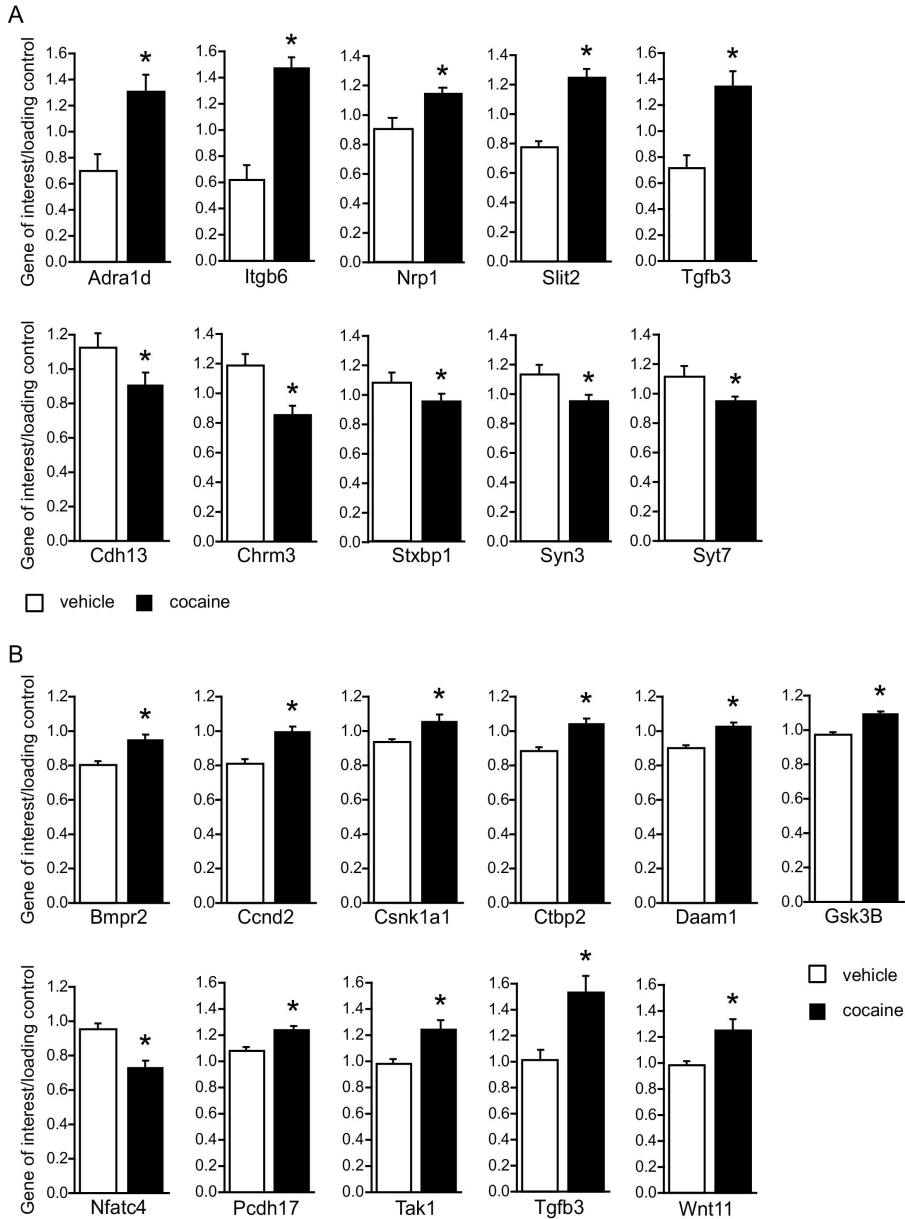


FIGURE 5.5: Adolescent cocaine exposure affects the expression of synaptic and developmental genes in the amygdala. Quantitative PCR verification of gene expression changes observed in the microarray analyses. A: Technical replicate performed on the original cohort of animals from microarray studies confirms the microarray results. B: Biological replicate performed on an additional cohort of animals confirms regulation of genes of the Wnt signaling pathway. Slit2 ($p \leq 0.01$; not shown) and Tgfb3 were also examined to verify findings in the original cohort. Values were normalized to the control genes beta actin, alpha tubulin, 18s RNA, and GtfIIB. For a complete list of gene names, please refer to tables 5.2-5.4. Statistical significance was determined with a student's t-test, * $p \leq 0.05$. Average + SEM; technical replicate vehicle $n=6$; cocaine $n=6$; biological replicate vehicle $n=10$; cocaine $n=8$. were sacrificed 20 minutes after the first or third injection on the last day of the dosing paradigm, or 22 hours after the last injection. Phosphorylation of GSK3B at serine residue 9 was increased after the first injection but decreased after the third injection. No changes were seen in the total amount of GSK3B protein (figure 5.6). No changes in phosphorylated or total GSK3B were seen 22 hours after the last injection, indicating that GSK3B phosphorylation had returned to normal levels.

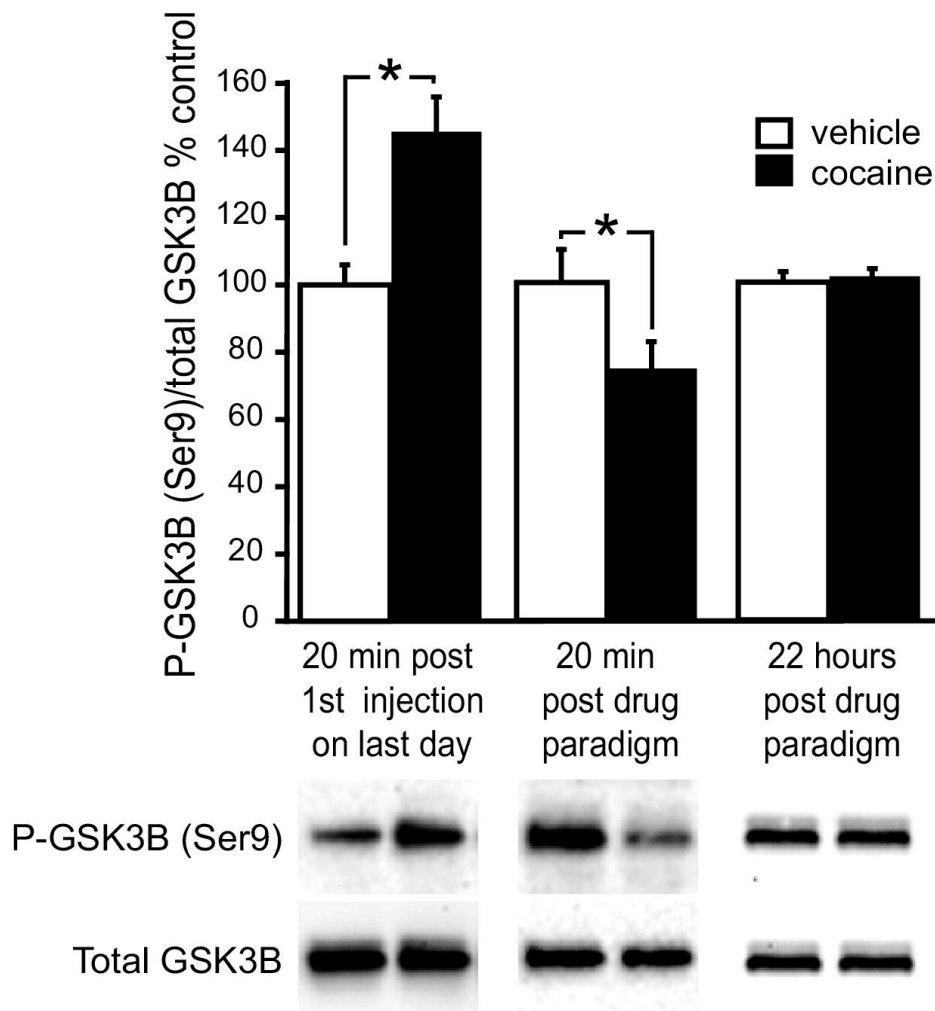


FIGURE 5.6: Cocaine administration during adolescence regulates GSK3B phosphorylation patterns in the amygdala. Representative western blots of total GSK3B protein and phosphorylated GSK3B in amygdala tissue punches from animals sacrificed 20 minutes after the first injection on the last day of the paradigm (left bar graphs), 20 minutes after the last injection (center bar graphs), or 22 hours after the last injection (right bar graphs). Phosphorylated GSK3B protein was normalized to total GSK3B protein. Percent change in intensity relative to vehicle samples is graphed. Average + SEM; for blots of rats sacrificed 20 minutes after the first or last injection, vehicle n=7; cocaine n=7; for blots of rats sacrificed 22 hours after the injection paradigm, vehicle n=6; cocaine n=6. * $p \leq 0.05$.

total GSK3B were seen 22 hours after the last injection, indicating that GSK3B phosphorylation had returned to normal levels.

Discussion:

Exposure to drugs of abuse during adolescence could affect the developmental trajectory of the brain with lasting consequences for structure, function and behavior. Here we provide evidence that adolescent cocaine abuse has deleterious behavioral effects in adulthood, well after cessation of drug use. During cocaine exposure, protein phosphorylation and gene expression patterns were altered, as measured on the last day of cocaine treatment. This interference with normal molecular processes led to altered behavior in adulthood. A previous study in the PFC showed that the changes in gene expression patterns are mostly transient, while the behavioral consequences are long-lasting (Black et al., 2006). Since we used the same experimental paradigm, it is reasonable to assume that the molecular patterns in the amygdala normalize as well, an assumption supported by the fact that in the present study GSK3B phosphorylation was normalized 22 hours after the last cocaine injection. However, transient changes in gene and protein expression can interfere with the normal program of brain development and have permanent consequences beyond that age period.

Cocaine exposure during adolescence decreased guarded behaviors and fear learning in adult rats. Although fear learning was abnormal, learning and memory paradigms not related to fear were normal. Rats exposed to cocaine during adolescence were more likely to enter into the open arm of an elevated plus maze, or the less protected areas of the open field, and to inspect the holes in the hole board without hesitation.

These behavioral changes indicated that cocaine exposure in adolescence reduces cautious behavior in adulthood.

Increased impulsivity and risk-taking in human cocaine users are well known (Marzuk et al., 1992, Bornovalova et al., 2005), though it is not known if this is a pre-existing trait leading to drug use, or a consequence of drug use. Here we used a rat model with no pre-existing traits and show that drug exposure during adolescence decreases cautious behavior in adulthood. Thus, drug use during adolescence can lead to long-term adverse behaviors. Although it is presently not known if similar adaptations can occur during adult cocaine use, it should not detract from the importance of the long-lasting effects of adolescent cocaine use. Onset of drug use during adolescence is a significant predictor of the subsequent development of addiction (Grant and Dawson, 1998), and as we show here, as well as in our previous study (Black et al., 2006), alters behavior in adulthood.

The behavioral changes observed indicate that cocaine affects amygdalar physiology. Therefore we conducted gene expression analyses to identify groups of genes or pathways in the amygdala that are altered immediately after cocaine exposure. Groups of genes involved in synaptic function, axon guidance and Wnt signaling, were significantly changed in the amygdala of cocaine-exposed rats. Changes of axon guidance molecules by psychostimulants have also been reported in other brain areas but this study is the first to report cocaine-induced alterations in axon guidance molecules in the amygdala (Halladay et al., 2000, Bahi and Dreyer, 2005, Jassen et al., 2006, Xiao et al., 2006, Grant et al., 2007, Yetnikoff et al., 2007). These systems are dynamically regulated by cocaine and a given gene or protein may be initially increased and subsequently

repressed, or vice versa. Thus, although the direction of regulation might be dependent on the timing of tissue harvest after the final cocaine injection, the fact that cocaine affects these transcripts is a crucial observation.

Axon guidance and Wnt signaling are important developmental processes that modulate the correct target selection of synapses and dendritic structures, as well as the patterning of neurotransmission and overall neuronal circuit formation (Chen and Cheng, 2009, Bashaw and Klein, 2010). In the adult striatum, GSK3B regulates the heightened locomotor activity and sensitivity after cocaine administration (Miller et al., 2009). Decreased phosphorylation of GSK3B at serine residue 9 in the amygdala was seen previously in the adult rodent after cocaine exposure (Perrine et al., 2008). After the first injection on the last day of our paradigm, GSK3B was hyperphosphorylated but after the third injection phosphorylation was decreased, presumably through the activation of a feed-back mechanism. The molecular data indicate that cocaine dysregulates the signaling pathways associated with GSK3B in the amygdala. GSK3B regulates the activity of beta catenin, a transcription factor that promotes the expression of many target genes, including receptors, cell adhesion molecules, cell cycle regulators, growth factors, and cytoskeletal proteins (figure 5.7). The downregulation of synaptic proteins, together with the alterations in axon guidance and Wnt pathway genes, points to a reorganization of synapses and dendritic structures in the amygdala by cocaine, which might be the reason for the long-term behavioral changes we observed.

Psychostimulants like amphetamine and cocaine prevent the clearance of dopamine and other biogenic amines from the synapse and potentiate their signaling (Kahlig et al., 2005). Dopamine as well as serotonin modulate developmental processes

such as proliferation, cell migration, and differentiation (Jones et al., 2000, Ohtani et al., 2003, Popolo et al., 2004, Bonnin et al., 2007, Crandall et al., 2007). From the present study we conclude that during adolescence aberrant monoamine signaling can affect developmental processes that pattern connectivity in the amygdala, with lasting effects on fear, anxiety, and emotion. The transient exposure to cocaine during adolescence could result in “mis-wiring” of emotional circuitry and fear recognition systems, leading to detrimental behaviors later in life.

Decreased anxiety could be perceived as a favorable characteristic, but recognition of danger and judicious behavior is imperative for the survival of a species (Griskevicius et al., 2009). Since healthy levels of anxiety mediate cautious behavior in novel or dangerous situations, we conclude that the decreased caution after adolescent cocaine exposure could lead to increased “risk-taking” in adulthood.

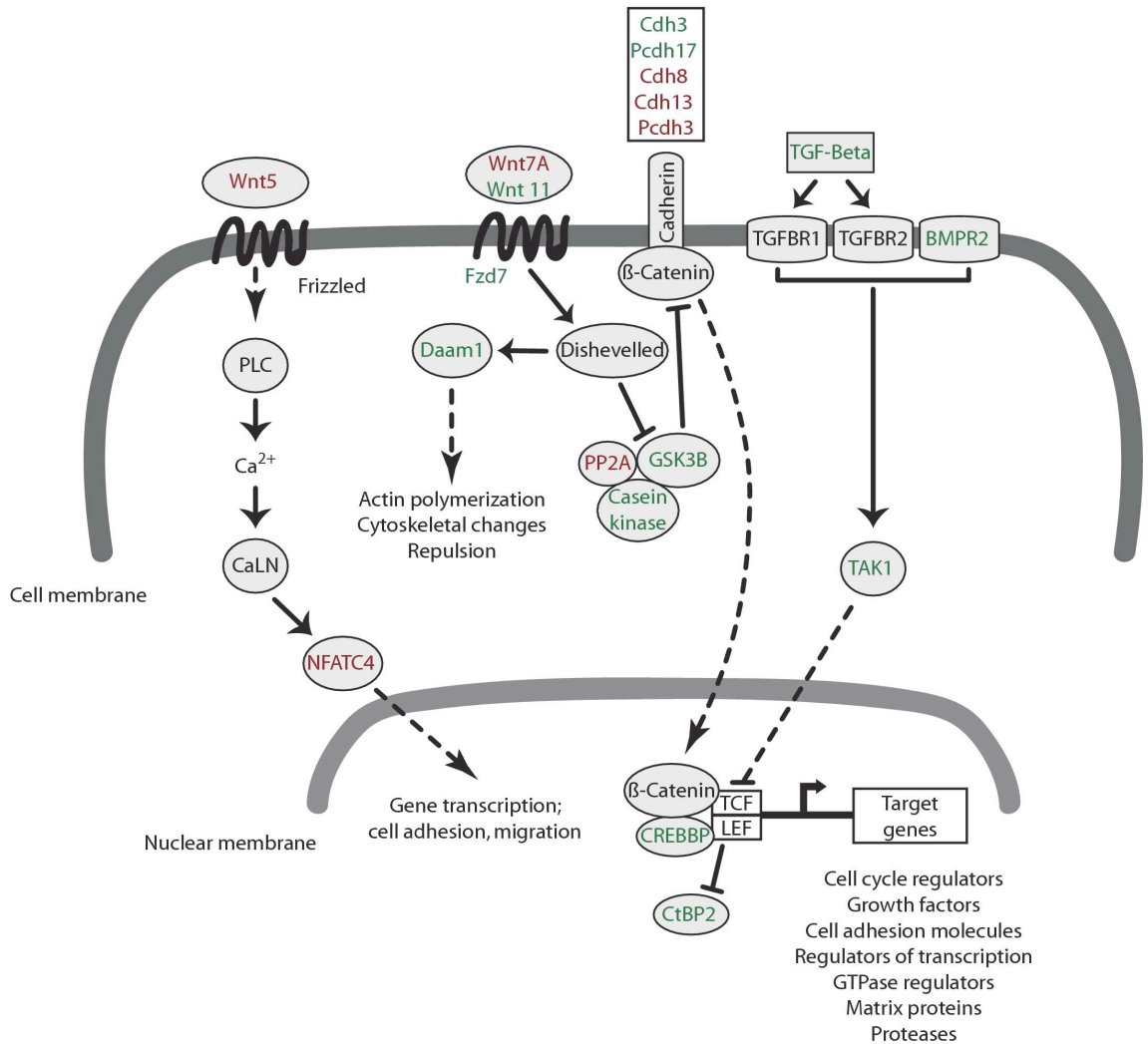


FIGURE 5.7: Schematic representation of cocaine-induced amygdalar gene changes in the Wnt pathway. Adolescent cocaine exposure regulated the mRNA expression of many genes involved in Wnt signaling pathways. These signaling pathways can alter the morphology of the actin cytoskeleton and participate in the remodeling of synaptic and dendritic structures following exposure to drugs of abuse. Signaling by Wnt molecules leads to the activation of transcription factors and target genes. In the canonical Wnt pathway, dishevelled inhibits a kinase-associated scaffolding complex (GSK3B, casein kinase, PP2A) that normally facilitates the degradation of beta catenin. Free beta catenin translocates to the nucleus where it activates the transcription of Wnt target genes. Dishevelled, as well as axon guidance molecules, also induce changes in actin polymerization and cytoskeletal proteins via the activation of Rho GTPases. The calcium-mediated Wnt signaling pathway is controlled by the Wnt5 molecules and activates transcription of cell surface proteins and cell adhesion molecules. Shown in green are upregulated genes and shown in red are downregulated genes. Solid arrows show direct interactions and dashed arrows denote signaling processes with intermediates not shown. Abbreviations: CaLN, calmodulin; LEF, lymphoid enhanced binding factor; PLC, phospholipase C; TAK1, Tgf beta activated kinase 1; TCF, t-cell transcription factor; TGFBR1/2, transforming growth factor beta receptor 1/2. For a detailed list of all other genes names see table 5.4.

CHAPTER VI

SUMMARY AND FUTURE DIRECTIONS

The purpose of this study was to evaluate the molecular and behavioral consequences of DA system stimulation during brain development. The combination of *in vitro* studies of embryonic neurons with early PN drug exposure provides insight into DA-mediated effects over a range of developmental time-periods.

DRD1 and DRD2 have unique expression patterns in the developing brain

Expression of the two main DRs, DRD1 and DRD2, was measured in the developing rat brain from E15 to E21. During this period of embryogenesis, which roughly corresponds to the second trimester of human fetal development (Clancy et al., 2007), the initial patterns of connectivity and DA innervation are established in the mFC and STR, laying a foundation for the neural circuitry that plays an integral role in the modulation of neurotransmission. Two different methodologies were used to measure mRNA levels of the receptors and similar patterns of DR expression were observed with each. *In situ* hybridization was used to provide a broad overview of the major areas containing DRs, but was combined with QPCR for more accurate and sensitive quantification of DR levels.

DR expression in the cortex was not confined to the mFC and was observed throughout the cortex, including the orbital, lateral, and motor cortices as well as the septum. However, DRD2, and to a lesser extent DRD1, appeared to be more

concentrated in the deeper cortical layers at later developmental timepoints (Figures 2.2-2.3), which is in agreement with a previous study that reported that layer 5 contains the highest levels of DRs (Lidow et al., 1998). Deep cortical layers are largely composed of principal neurons and relay information to subcortical brain areas (Caviness et al., 2008).

At the earliest time-point measured, E15, low levels of DRs were detected in both brain regions (Figure 2.4). The trajectories of both DRs changed significantly over time in the two brain regions but at different rates. Significant differences were seen in the trajectories of the two receptors when compared to one another, indicating that the induction of DR-subtypes is not uniform. Very steep increases in DR mRNA were observed at E17 in the STR and at E19 in the mFC, which is in concordance with the arrival of DA fibers in those brain regions. While levels of both DRs were significantly higher in the STR compared to the mFC, the ratio of DRD1:DRD2 differed between the mFC and the STR: DRD1 levels were higher than DRD2 in the mFC but DRD2 was higher than DRD1 in the STR (Tables 2.2 and 2.3). The STR most likely contains more DRs because it receives DA innervation from both the VTA and the SN. This study did not compare levels of DRs in multiple regions of the STR as it is likely prone to error due to the size of rat brains at early embryonic time-points.

To determine the expression patterns of DRs *in vitro*, mRNA levels of DRD1 and DRD2 were measured in primary neuronal cultures after 1-6 DIV, isolated from rat brains at E15 (Figure 2.5). The trajectory of DR expression was similar to that seen in tissue samples, with large inductions of receptor mRNA overtime, and levels of DRD1 higher than DRD2 in the mFC. In the STR, DRD2 was higher than DRD1 at only one time-point but overall the trajectories of the two receptors were different. This lack of DRD2

mRNA induction was not observed in cultured neurons obtained from E18 embryos. Because neurogenesis is ongoing from E15 to E21, the neuronal population obtained at E15 will not be the same as that obtained from later time-points. Cells born after E15 may contribute to the induction of DRD2 mRNA by providing environmental cues, transcription factors, and more DRD2 positive neurons. Therefore, the levels of DRs in primary neuronal cultures were not directly comparable to the levels of DRs in tissue samples. However, DA innervation at later time-points may also promote induction of receptor mRNAs.

DR signaling cascades are functional in the absence of DR innervation

Since DA could be a contributing factor in the organization of neuronal networks in DR-expressing neurons of the developing brain, the functionality of DRs was assessed in primary neuronal cultures, obtained from E15 or E18 embryos. These time-points were chosen to compare the signaling properties of DRs before and after DA fibers have reached the mFC and STR (Figure 1.1). Little DA innervation occurs in the STR at E15, while the mFC receives no innervation. At E18, dopaminergic fibers are present throughout the STR but remain in the intermediate zone of the cortex, waiting to enter the cortical plate until E20 (Van den Heuvel and Pasterkamp, 2008).

At E15 both DRs were functionally coupled to phosphorylation cascades, indicating that DR-mediated signaling can occur in the developing brain prior to DA innervation (Figure 2.6 and 2.7). In the mFC, DRD1 stimulation increased ERK1/2 phosphorylation at both time-points but CREB phosphorylation was only increased at E18. Likewise, DRD2 stimulation decreased CREB only at E18 in the mFC but

decreased ERK1/2 at both time-points in the STR. In the STR DRD1 stimulation increased CREB and ERK1/2 phosphorylation at E15 and E18, as well as GSK3 β phosphorylation at E15. DRD2 stimulation decreased GSK3 β at both time-points in the mFC and STR. The robustness of phosphorylation responses seen in the STR may be due to the fact that DA fibers innervate the STR before the mFC, suggesting that exposure to DA aids in the functional maturation of DRs. Region-specific disparities in DRD2-mediated CREB and ERK1/2 phosphorylation may contribute to specific developmental events that occur in the two functionally distinct brain regions. Pretreatment of E18 mFC cells with the DRD1 antagonist SCH23390 did not disrupt DRD2-mediated activation of GSK3 β (Figure 2.8), indicating that the DR agonists used in this study do not cross-react with multiple DR-subtypes.

Because DA positive fibers do not invade the cortical plate until E20, DRs in the fetal brain may be activated by other monoamines such as serotonin, which is released by the placenta (Bonnin 2010), or another ligand that is expressed developmentally. Alternatively, other sources may deliver DA into the mFC during embryogenesis. At early stages of gestation the blood brain barrier has not been completely sealed, exposing the embryo to the maternal blood supply for nutrition. Platelets and lymphocytes express both the dopamine transporter DAT and the vesicular monoamine transporter (VMAT) and can uptake and release DA (Amenta et al., 2001, Zucker et al., 2001, Frankhauser et al., 2006). The placenta is a source of serotonin for the embryonic brain and may contain other monoamines, like DA (Bonnin et al., 2011). Additionally, cells in the mFC may transiently express monoamines for a short period of development and release them

locally to modulate developmental processes such as axon guidance (Bonnin and Levitt, 2011).

Drugs were applied exogenously in cell culture treatment and high amounts are needed to achieve concentrations that will actually reach DRs in the synapse. Although *in vivo* baseline levels of DA are in the nanomolar range (Goto et al., 2007), burst spike-firing increases DA levels from hundreds of μM to mM levels (Grace and Bunney, 1984, Garris et al., 1994, Goto et al., 2007). It has also been demonstrated that the majority of DRD1-like receptors in the striatum require μM DA levels for activation (Richfield et al., 1989, Rice and Cragg, 2008).

Finally, the activation of DRs at E15 when mRNA levels are extremely low indicates that DRs may be supersensitive in the developing brain. Given the low expression levels of DRs, the concentration of DR agonists Activation of DRs at these early time-points may influence developmental processes via molecules such as CREB, ERK1/2, and GSK3 β , all of which may signal to the nucleus to transcribe genes important for growth and development.

Ntn-1 receptors are expressed in the developing mFC

The Ntn-1 receptors DCC and UNC5C were expressed in the developing mFC and co-localized with DRs (Figures 3.1 and 3.2). While expression of UNC5C followed a trajectory similar to that of DRs and appeared to be concentrated in deep cortical layers, the pattern of DCC expression differed greatly (Figure 3.1D and 3.1E). DCC levels were high at E15, peaked at E18, then decreased with age (Figure 3.1). DCC was expressed in

a medial to lateral gradient, presumably to guide crossing fibers as the corpus callosum forms (Figure 3.1A and 3.1B).

DA projections from the VTA synapse onto the pioneer neurons in the mFC that send the first axons across from one hemisphere to the other (Carr and Sesack, 2000). In addition, many intracellular signaling molecules affected by DR activity have the capability to modulate axon guidance events, including PKA, calcium in growth cones, and cyclic nucleotides (Ming et al., 1997, Ming et al., 1999, Halladay et al., 2000, Nishiyama et al., 2003, Bouchard et al., 2004, Bonnin et al., 2007). Since DRs are functionally active at this time, release of DA and activation of DR-mediated signaling pathways may contribute to the normal development of inter-cortical connectivity.

DR stimulation disrupts Ntn-1 mediated attraction of mFC axons

Two types of *in vitro* assays were used to assess the guidance properties of Ntn-1 in the presence of DR activation. First, explant assays were used to measure directional outgrowth of mFC neurites in response to Ntn-1 expressing HEK293T cell aggregates (Figure 3.3). Under basal conditions, Ntn-1 attracted mFC tissue explants by promoting neurite outgrowth in regions of the explant proximal to the Ntn-1 gradient (Figure 3.3B, 3.4B, and 3.4E). Treatment with the DRD1 agonist SKF82958 or the DRD2 agonist quinpirole disrupted this effect, causing explants to have more symmetrical outgrowth, resembling the effects seen with non-Ntn-1 cells (Figure 3.3 and 3.4). However, results from this experiment indicated that the presence of Ntn-1 or the addition of DR agonists did not alter the total outgrowth of mFC explants (Figure 3.4F), indicating that Ntn-1 functions as a guidance cue for the directional steering of axons.

This finding was supported by data obtained through the use of microfluidic nanochambers, which allow dissociated neuronal cultures to be grown in a channel connected to a channel containing recombinant Ntn-1 protein (Figure 3.5). The two channels are separated by microwells that are permissible for individual axon growth. The length of axons in the microwells was not affected by the treatment of DR agonists but was significantly increased when mFC cells were cultured next to a gradient of Ntn-1 (Figure 3.5E). As with explant assays, this effect was disrupted when cultures were treated with DR agonists in the presence of Ntn-1. Co-treatment with Ntn-1 and the DRD1 agonist SKF82958 or the DRD2 agonist PPHT resulted in an ~30% reduction in axon length compared to cultures treated with Ntn-1 alone (Figure 3.5E). In both types of outgrowth assays, treatment with DR agonists resulted in outgrowth properties similar to that seen in untreated controls, suggesting that DR stimulation decreases an axon's responsiveness to Ntn-1 cues and inhibits directional steering of growth cones.

DR stimulation regulates the abundance of Ntn-1 receptor transcripts

To identify a molecular basis for the observed outgrowth responses, levels of the Ntn-1 receptors DCC and UNC5C were measured with QPCR in E15 mFC cultures after treatment with DR agonists (Figure 3.6). Both DRD1 and DRD2 agonists increased expression of UNC5C, the receptor that mediates repulsive guidance responses. SKF82958 and quinpirole induced moderate increases in UNC5C expression, while more robust responses were seen after treatment with the potent DRD2 agonist PPHT. Co-stimulation of both receptor subtypes with the partial DRD1/DRD2 agonist apomorphine resulted in the most dramatic changes in UNC5C expression, with ~50-75% increases

that were maintained after 4 hours. No changes in DCC expression were observed after DR stimulation.

By regulating the abundance of UNC5C transcripts, DR stimulation could change the ratio of DCC:UNC5C in mFC neurons. Since homodimers of DCC promote attraction, increased expression of UNC5C may result in more DCC:UNC5C heterodimers and promote repulsion or decreased attraction to Ntn-1 cues. This effect could be important for axon fibers crossing the midline, as they will need to be attracted to the midline initially but repelled away from the midline once they have crossed. The dynamic ratio of DCC to UNC5C during mFC development implies a functional switch in growth cone responses to Ntn-1 cues that may be augmented by DR-induced increases in UNC5C expression. Additionally, Ntn-1 is expressed in high levels in the subventricular zone of the STR and the ratio of Ntn-1 receptor expression could be important for corticofugal mFC axons as they project subcortically (Serafini et al., 1996, Metin et al., 1997, Donahoo and Richards, 2009).

Further investigation is needed to fully understand the effects of DR signaling on Ntn-1 mediated guidance in the mFC. While the specificity of DR agonists was demonstrated in figure 2.8 by co-application of the DR agonist PPHT with the DRD1 antagonist SCH23390, it is possible that DR agonists may interact with other non-DA receptors to regulate axon guidance. It will be important to further decipher the components of DR signaling that directly affect the Ntn-1 system to establish a link between the two pathways. This study could be strengthened through the use of additional pharmacological agents that target DRs and their second messenger pathways.

However, DR antagonists do not simply block DRs but instead induce signaling cascades of their own which could confound data interpretation (Konradi and Heckers, 1995, Jassen et al., 2006, Sutton et al., 2007). Manipulation of DR expression *in vivo* through the use of in utero electroporation would provide information about the trajectory of mFC axon outgrowth when DR levels are altered. Transfection of DR siRNA into tissues *in vivo* or neuronal cultures *in vitro* could be combined with DR agonist treatment to show that lack of DRs prevents inhibition of ntn-1-mediated attraction. Importantly, the trajectory of mFC projections could be tracked in whole embryonic brains after removal of DRs to determine if DR stimulation is required for the normal development of mFC projections.

Likewise, knockdown of UNC5C receptor mRNA in combination with DR agonist treatment would establish a relationship between DA signaling and ntn-1-mediated repulsive events. It is not clear if increased UNC5C levels translate to more UNC5C receptor in the growth cone membrane. Cell-surface biotinylation of ntn-1 receptors would determine if alterations in translocation rate result from DR stimulation.

Because both DRD1 and DRD2 produced similar effects on axon guidance and ntn-1 receptor expression, it is necessary to determine how the seemingly different pathways of both receptors cause the same response. Both DRs mobilize calcium intracellularly and affect transcription of genes involved in growth and development. Axon guidance is very sensitive to calcium transients but too much or too little calcium can switch an axon cue from attraction to repulsion. Measuring calcium levels in the growth cone after DR stimulation may provide information about DR-subtype-specific calcium transients associated with guidance. For example, DRD2 may decrease calcium

transients while DRD1 increases them. Under these conditions, both receptors could cause suboptimal calcium homeostasis and prevent attraction to ntn-1 cues. If calcium homeostasis is the underlying cause of DR-mediated inhibition of ntn-1 attraction, then it is very likely that DRs accomplish this by activating the $G_{\alpha s}$ (DRD1), $G_{\alpha i}$ (DRD2), or $G_{\alpha q}$ (DRD2) pathways. Each of these g-proteins can affect intracellular calcium levels. Selective stimulation of DRs in combination with inhibitors of their respective signaling molecules, such as PKA, GSK3 β , and PLC, is necessary to elucidate DR signaling pathways involved in ntn-1 mediated guidance. Further insight into the mechanism of DR action could be obtained by identifying UNC5C transcription factors that are regulated by DR agonists.

The early expression and functionality of DRs and their capability to activate signaling cascades provides the DA system with a powerful position to influence the progression of brain development and neural network connectivity. Based on the data shown here, any source of prenatal DA, including maternally supplied DA, and abnormalities in fetal DR function could thus lead to a miswiring of the brain with detrimental consequences for brain function later in life.

DR-mediated disruption of axon guidance may not be specific for the Ntn-1 pathway, as increased prenatal dopaminergic signaling has been shown to regulate expression of ephrin family genes in the STR (Halladay et al., 2000). Other families of axon guidance genes may be regulated by DR stimulation as well, but further research employing functional outgrowth assays in dopaminergic regions will be needed to address these questions.

Postnatal cocaine administration regulates expression of axon guidance-related genes in the mFC and STR

Many axon guidance molecules (AGMs) are present in the adolescent and adult brain, well after synapse formation has occurred. AGMs may have additional roles in developed brains such as maintaining synaptic connections and dendritic architecture. The psychostimulant drugs cocaine and amphetamine regulate expression of AGMs in adult animals. Lack of the Ntn-1 receptor DCC disrupts sensitization, suggesting that it contributes to the symptoms and neuropathology of addiction (Bahi and Dreyer, 2005, Yetnikoff et al., 2007, Yetnikoff et al., 2010, Sullivan et al., 2011). Because these drugs increase dopaminergic tone, they can be used to examine the effects of DR stimulation on axon guidance pathways *in vivo*. The molecular and behavioral consequences of PN cocaine exposure were examined at three different developmental time periods in the rat.

mRNA levels of 7 axon-guidance related genes were measured after cocaine administration during weeks 2 and 3 of PN rat development (Figure 4.1). Cocaine regulated expression of 3 different families of AGMs in the PFC and STR, indicating that stimulant-induced gene expression changes are not limited to one axon guidance family but instead may be a generalized effect (Figure 4.2 and Table 4.2-4.3). Because the time periods examined here correspond to the third trimester of human fetal development, these data indicate that cocaine usage during pregnancy may regulate expression of AGMs in utero (Clancy et al., 2007).

Adolescent binge cocaine administration regulates expression of developmental and synaptic genes

In an adolescent binge cocaine paradigm, cocaine was administered in ascending doses to male rats from PN35-46. Immediately after the last injection, a subset of animals were sacrificed and examined in gene expression and protein phosphorylation studies. A previous study using the same paradigm described gene changes in the PFC after adolescent cocaine exposure but few were related to developmental processes (Black et al., 2006). Cocaine exposure altered performance in an attentional task that is mediated by the PFC, suggesting that other aspects of PFC function may be impaired as well. Since the PFC participates in amygdala-based responses to anxiety and learned fear (Davidson, 2002, Corcoran and Quirk, 2007, Sotres-Bayon and Quirk, 2010), molecular and behavioral components of amygdalar activity were assessed after adolescent cocaine exposure.

Gene expression studies were conducted in amygdala tissue using microarray technology. Adolescent cocaine exposure regulated the expression of groups of genes important for growth and development in the amygdala, including axon guidance events, Wnt signaling, and synaptic connectivity (Tables 5.2-5.4). These changes were confirmed with QPCR in biological and technical replicates (Figure 5.4). Cocaine administration produced irregular phosphorylation patterns of GSK3 β , a kinase that regulates Wnt pathway signaling, that normalized after 21 days (Figure 5.5). Additional research is needed to determine if these changes occur after adult cocaine administration as well, or if they are specific for adolescent cocaine exposure, and whether cocaine exposure causes neuroanatomical alterations in amygdalar synaptic structure. Transient

changes in genes responsible for establishing connectivity, such as AGMs, may cause abnormal circuit formation, resulting in long term behavioral changes.

Adolescent binge cocaine administration decreases fear and anxiety in adult rats

To address this question, another subset of animals were maintained into adulthood with no additional cocaine exposure and subjected to tests that measure behaviors regulated by the PFC and amygdala (Figure 5.1). Cocaine-exposed animals spent more time in the center area of an open field arena and more time in the open arm of an elevated plus maze as compared to vehicle treated animals, indicating a decrease in levels of innate anxiety (Figure 3.2). During the hole board exploration task, cocaine exposed animals were more exploratory and novelty seeking, exploring more holes at a higher frequency than vehicle treated animals (Figure 3.3).

In a contextual fear conditioning paradigm, no differences in freezing behavior were observed upon presentation of a shock paired with a conditioned stimulus. However, 24 hours later, vehicle treated animals froze significantly more than cocaine exposed animals when presented with the same context but no stimulus, suggesting that cocaine exposure impairs the development of normal learned fear responses and the retrieval of fear memories (Figure 3.2). Cocaine exposure did not cause a generalized learning deficit because both groups of animals developed equal fear responses on day 1 of the paradigm. Likewise, spatial learning and memory behaviors were intact as the two groups performed equally well in the Morris Water Maze and the hole board search food task (Figure 3.3).

The immediate gene changes in the amygdala after cocaine exposure may establish circuitry that promotes risk-taking behaviors and decreased anxiety later in life. While this may be considered advantageous to some, it is necessary for the survival of a species to be able to discern an innocuous stimuli from a harmful one, and to exercise caution when danger is present.

Research presented here demonstrates that DA system stimulation in the developing brain disrupts axon guidance events and may alter neuronal circuit formation in multiple brain areas by regulating the expression of genes and proteins involved in growth and development. Since the amygdala, FC, and STR are important for cognition, attention, movement, emotion, and learning, aberrant connectivity of these regions could impair behavior later in life, as seems to be the case in schizophrenia (Zalesky et al., 2011).

FULL AUTHOR LIST:

Chapter II: EXPRESSION AND FUNCTIONALITY OF DOPAMINE RECEPTORS IN THE EMBRYONIC RAT BRAIN: IMPLICATIONS FOR MODULATION OF DEVELOPMENTAL PROCESSES

Sullivan, S.E., and Konradi, C.

Chapter III: DOPAMINE RECEPTOR STIMULATION DISRUPTS NETRIN-1 AXON GUIDANCE IN CORTICAL NEURONS

Sullivan, S.E., Brewer, B., Bonnin, A., Li, D., and Konradi, C.

Chapter IV: POSTNATAL COCAINE ADMINISTRATION REGULATES AXON GUIDANCE MOLECULES IN THE PFC AND STRIATUM

Sullivan, S.E., Hanlin, R.H., and Konradi, C.

Chapter V: BINGE COCAINE ADMINISTRATION IN ADOLESCENT RATS AFFECTS AMYGDALAR GENE EXPRESSION PATTERNS AND ALTERS ANXIETY-RELATED BEHAVIOR IN ADULTHOOD

Sullivan, S.E., Black, Y.D., Naydenov, A.V., Vassolar, F.R., Hanlin, R.H., and Konradi, C.

REFERENCES

Abramoff MD, Magalhaes, P.J., Ram, S.J. (Image Processing with ImageJ. *Biophotonics International* 11:36-42.2004).

Akil M, Pierri JN, Whitehead RE, Edgar CL, Mohila C, Sampson AR, Lewis DA (Lamina-specific alterations in the dopamine innervation of the prefrontal cortex in schizophrenic subjects. *Am J Psychiatry* 156:1580-1589.1999).

Akiyama H, Kamiguchi H (Phosphatidylinositol 3-kinase facilitates microtubule-dependent membrane transport for neuronal growth cone guidance. *J Biol Chem* 285:41740-41748).

Alberch J, Brito B, Notario V, Castro R (Prenatal haloperidol treatment decreases nerve growth factor receptor and mRNA in neonate rat forebrain. *Neurosci Lett* 131:228-232.1991).

- Aldridge GM, Podrebarac DM, Greenough WT, Weiler IJ (The use of total protein stains as loading controls: an alternative to high-abundance single-protein controls in semi-quantitative immunoblotting. *J Neurosci Methods* 172:250-254.2008).
- Amenta F, Bronzetti E, Cantalamessa F, El-Assouad D, Felici L, Ricci A, Tayebati SK (Identification of dopamine plasma membrane and vesicular transporters in human peripheral blood lymphocytes. *J Neuroimmunol* 117:133-142.2001).
- Andreasen NC, Carpenter WT, Jr. (Diagnosis and classification of schizophrenia. *Schizophr Bull* 19:199-214.1993).
- Araki KY, Sims JR, Bhide PG (Dopamine receptor mRNA and protein expression in the mouse corpus striatum and cerebral cortex during pre- and postnatal development. *Brain Res* 1156:31-45.2007).
- Arnsten AF, Li BM (Neurobiology of executive functions: catecholamine influences on prefrontal cortical functions. *Biol Psychiatry* 57:1377-1384.2005).
- Bahi A, Dreyer JL (Cocaine-induced expression changes of axon guidance molecules in the adult rat brain. *Mol Cell Neurosci* 28:275-291.2005).
- Barzilai A, Melamed E (Molecular mechanisms of selective dopaminergic neuronal death in Parkinson's disease. *Trends Mol Med* 9:126-132.2003).
- Bashaw GJ, Klein R (Signaling from axon guidance receptors. *Cold Spring Harb Perspect Biol* 2:a001941.2010).
- Beaulieu JM, Gainetdinov RR (The physiology, signaling, and pharmacology of dopamine receptors. *Pharmacol Rev* 63:182-217.2011).
- Beaulieu JM, Gainetdinov RR, Caron MG (Akt/GSK3 signaling in the action of psychotropic drugs. *Annu Rev Pharmacol Toxicol* 49:327-347.2009).
- Beaulieu JM, Sotnikova TD, Marion S, Lefkowitz RJ, Gainetdinov RR, Caron MG (An Akt/beta-arrestin 2/PP2A signaling complex mediates dopaminergic neurotransmission and behavior. *Cell* 122:261-273.2005).
- Beaulieu JM, Tirotta E, Sotnikova TD, Masri B, Salahpour A, Gainetdinov RR, Borrelli E, Caron MG (Regulation of Akt signaling by D2 and D3 dopamine receptors in vivo. *J Neurosci* 27:881-885.2007).
- Benes FM (Amygdalocortical circuitry in schizophrenia: from circuits to molecules. *Neuropsychopharmacology* 35:239-257.2010).
- Benjamini Y, Hochberg Y (Controlling the false discovery rate: a practical and powerful approach to multiple testing. *J R Statist Soc B* 57:289-300.1995).

- Berger B, Verney C, Gay M, Vigny A (Immunocytochemical characterization of the dopaminergic and noradrenergic innervation of the rat neocortex during early ontogeny. *Prog Brain Res* 58:263-267.1983).
- Bertran-Gonzalez J, Bosch C, Maroteaux M, Matamales M, Herve D, Valjent E, Girault JA (Opposing patterns of signaling activation in dopamine D1 and D2 receptor-expressing striatal neurons in response to cocaine and haloperidol. *J Neurosci* 28:5671-5685.2008).
- Black YD, Maclaren FR, Naydenov AV, Carlezon WA, Jr., Baxter MG, Konradi C (Altered attention and prefrontal cortex gene expression in rats after binge-like exposure to cocaine during adolescence. *J Neurosci* 26:9656-9665.2006).
- Blackwood DH, Pickard BJ, Thomson PA, Evans KL, Porteous DJ, Muir WJ (Are some genetic risk factors common to schizophrenia, bipolar disorder and depression? Evidence from DISC1, GRIK4 and NRG1. *Neurotox Res* 11:73-83.2007).
- Blum K, Liu Y, Shriner R, Gold MS (Reward circuitry dopaminergic activation regulates food and drug craving behavior. *Curr Pharm Des* 17:1158-1167.2011).
- Bolstad BM, Irizarry RA, Astrand M, Speed TP (A comparison of normalization methods for high density oligonucleotide array data based on variance and bias. *Bioinformatics* 19:185-193.2003).
- Bonnin A (2010) Guidance and Outgrowth Assays for Embryonic Thalamic Axons. In: *Protocols for Neural Cell Culture, Fourth Edition*(Doering, L. C., ed), pp 329-341.
- Bonnin A, Goeden N, Chen K, Wilson ML, King J, Shih JC, Blakely RD, Deneris ES, Levitt P (A transient placental source of serotonin for the fetal forebrain. *Nature* 472:347-350.2011).
- Bonnin A, Levitt P (Fetal, maternal, and placental sources of serotonin and new implications for developmental programming of the brain. *Neuroscience* 197:1-7.2011).
- Bonnin A, Torii M, Wang L, Rakic P, Levitt P (Serotonin modulates the response of embryonic thalamocortical axons to netrin-1. *Nat Neurosci* 10:588-597.2007).
- Bornovalova MA, Daughters SB, Hernandez GD, Richards JB, Lejuez CW (Differences in impulsivity and risk-taking propensity between primary users of crack cocaine and primary users of heroin in a residential substance-use program. *Exp Clin Psychopharmacol* 13:311-318.2005).
- Bouchard JF, Horn KE, Stroh T, Kennedy TE (Depolarization recruits DCC to the plasma membrane of embryonic cortical neurons and enhances axon extension in response to netrin-1. *J Neurochem* 107:398-417.2008).

- Bouchard JF, Moore SW, Tritsch NX, Roux PP, Shekarabi M, Barker PA, Kennedy TE (Protein kinase A activation promotes plasma membrane insertion of DCC from an intracellular pool: A novel mechanism regulating commissural axon extension. *J Neurosci* 24:3040-3050.2004).
- Brami-Cherrier K, Valjent E, Garcia M, Pages C, Hipskind RA, Caboche J (Dopamine induces a PI3-kinase-independent activation of Akt in striatal neurons: a new route to cAMP response element-binding protein phosphorylation. *J Neurosci* 22:8911-8921.2002).
- Brasser SM, Spear NE (Contextual conditioning in infants, but not older animals, is facilitated by CS conditioning. *Neurobiol Learn Mem* 81:46-59.2004).
- Bronson SE, Konradi C (2010) Second Messenger Cascades. In: Handbook of basal ganglia structure and function, vol. 20 (Steiner, H. and Tseng, K. Y., eds), pp 447-460 Amsterdam: Elsevier.
- Brose N, Betz A, Wegmeyer H (Divergent and convergent signaling by the diacylglycerol second messenger pathway in mammals. *Current Opinion in Neurobiology* 14:328-340.2004).
- Buckholtz JW, Treadway MT, Cowan RL, Woodward ND, Benning SD, Li R, Ansari MS, Baldwin RM, Schwartzman AN, Shelby ES, Smith CE, Cole D, Kessler RM, Zald DH (Mesolimbic dopamine reward system hypersensitivity in individuals with psychopathic traits. *Nat Neurosci* 13:419-421.2011).
- Bunzow JR, Van Tol HH, Grandy DK, Albert P, Salon J, Christie M, Machida CA, Neve KA, Civelli O (Cloning and expression of a rat D2 dopamine receptor cDNA. *Nature* 336:783-787.1988).
- Cantrell AR, Smith RD, Goldin AL, Scheuer T, Catterall WA (Dopaminergic modulation of sodium current in hippocampal neurons via cAMP-dependent phosphorylation of specific sites in the sodium channel alpha subunit. *J Neurosci* 17:7330-7338.1997).
- Carr DB, O'Donnell P, Card JP, Sesack SR (Dopamine terminals in the rat prefrontal cortex synapse on pyramidal cells that project to the nucleus accumbens. *J Neurosci* 19:11049-11060.1999).
- Carr DB, Sesack SR (Dopamine terminals synapse on callosal projection neurons in the rat prefrontal cortex. *J Comp Neurol* 425:275-283.2000).
- Cavara NA, Orth A, Hicking G, Seebohm G, Hollmann M (Residues at the tip of the pore loop of NR3B-containing NMDA receptors determine Ca²⁺ permeability and Mg²⁺ block. *BMC Neurosci* 11:133.2010).

- Caviness VS, Bhide PG, Nowakowski RS (Histogenetic processes leading to the laminated neocortex: migration is only a part of the story. *Dev Neurosci* 30:82-95.2008).
- Cepeda C, Levine MS (Dopamine and N-methyl-D-aspartate receptor interactions in the neostriatum. *Dev Neurosci* 20:1-18.1998).
- Charron F, Tessier-Lavigne M (Novel brain wiring functions for classical morphogens: a role as graded positional cues in axon guidance. *Development* 132:2251-2262.2005).
- Chen SY, Cheng HJ (Functions of axon guidance molecules in synapse formation. *Curr Opin Neurobiol* 19:471-478.2009).
- Clancy B, Kersh B, Hyde J, Darlington RB, Anand KJ, Finlay BL (Web-based method for translating neurodevelopment from laboratory species to humans. *Neuroinformatics* 5:79-94.2007).
- Collo G, Zanetti S, Missale C, Spano P (Dopamine D3 receptor-preferring agonists increase dendrite arborization of mesencephalic dopaminergic neurons via extracellular signal-regulated kinase phosphorylation. *Eur J Neurosci* 28:1231-1240.2008).
- Corcoran KA, Desmond TJ, Frey KA, Maren S (Hippocampal inactivation disrupts the acquisition and contextual encoding of fear extinction. *J Neurosci* 25:8978-8987.2005).
- Corcoran KA, Quirk GJ (Activity in prelimbic cortex is necessary for the expression of learned, but not innate, fears. *J Neurosci* 27:840-844.2007).
- Coyle JT (Substance use disorders and Schizophrenia: a question of shared glutamatergic mechanisms. *Neurotox Res* 10:221-233.2006).
- Crandall JE, McCarthy DM, Araki KY, Sims JR, Ren JQ, Bhide PG (Dopamine receptor activation modulates GABA neuron migration from the basal forebrain to the cerebral cortex. *J Neurosci* 27:3813-3822.2007).
- Cross DA, Alessi DR, Cohen P, Andjelkovich M, Hemmings BA (Inhibition of glycogen synthase kinase-3 by insulin mediated by protein kinase B. *Nature* 378:785-789.1995).
- Davidson RJ (Anxiety and affective style: role of prefrontal cortex and amygdala. *Biological Psychiatry* 51:68-80.2002).
- Davis M (The role of the amygdala in fear and anxiety. *Annual Review of Neuroscience* 15:353-375.1992).

- Dawson NM, Hamid EH, Egan MF, Meredith GE (Changes in the pattern of brain-derived neurotrophic factor immunoreactivity in the rat brain after acute and subchronic haloperidol treatment. *Synapse* 39:70-81.2001).
- De Vries TJ, Mulder AH, Schoffelmeer AN (Differential ontogeny of functional dopamine and muscarinic receptors mediating presynaptic inhibition of neurotransmitter release and postsynaptic regulation of adenylate cyclase activity in rat striatum. *Brain Res Dev Brain Res* 66:91-96.1992).
- Dell'Acqua ML, Smith KE, Gorski JA, Horne EA, Gibson ES, Gomez LL (Regulation of neuronal PKA signaling through AKAP targeting dynamics. *Eur J Cell Biol* 85:627-633.2006).
- Dennis G, Jr., Sherman BT, Hosack DA, Yang J, Gao W, Lane HC, Lempicki RA (DAVID: Database for Annotation, Visualization, and Integrated Discovery. *Genome Biol* 4:P3.2003).
- Dickson BJ (Rho GTPases in growth cone guidance. *Curr Opin Neurobiol* 11:103-110.2001).
- Donahoo AL, Richards LJ (Understanding the mechanisms of callosal development through the use of transgenic mouse models. *Semin Pediatr Neurol* 16:127-142.2009).
- Donohoe DR, Weeks K, Aamodt EJ, Dwyer DS (Antipsychotic drugs alter neuronal development including ALM neuroblast migration and PLM axonal outgrowth in *Caenorhabditis elegans*. *Int J Dev Neurosci* 26:371-380.2008).
- Dudman JT, Eaton ME, Rajadhyaksha A, Macias W, Taher M, Barczak A, Kameyama K, Haganir R, Konradi C (Dopamine D1 receptors mediate CREB phosphorylation via phosphorylation of the NMDA receptor at Ser897-NR1. *Journal of Neurochemistry* 87:922-934.2003).
- Eastwood SL, Harrison PJ (Decreased mRNA expression of netrin-G1 and netrin-G2 in the temporal lobe in schizophrenia and bipolar disorder. *Neuropsychopharmacology* 33:933-945.2008).
- Eastwood SL, Law AJ, Everall IP, Harrison PJ (The axonal chemorepellant semaphorin 3A is increased in the cerebellum in schizophrenia and may contribute to its synaptic pathology. *Mol Psychiatry* 8:148-155.2003).
- Enjalbert A, Bockaert J (Pharmacological characterization of the D2 dopamine receptor negatively coupled with adenylate cyclase in rat anterior pituitary. *Mol Pharmacol* 23:576-584.1983).
- Finger JH, Bronson RT, Harris B, Johnson K, Przyborski SA, Ackerman SL (The netrin 1 receptors *Unc5h3* and *Dcc* are necessary at multiple choice points for the guidance of corticospinal tract axons. *J Neurosci* 22:10346-10356.2002).

- Fisone G, Hakansson K, Borgkvist A, Santini E (Signaling in the basal ganglia: postsynaptic and presynaptic mechanisms. *Physiol Behav* 92:8-14.2007).
- Flaum M, Schultz SK (When does amphetamine-induced psychosis become schizophrenia? *Am J Psychiatry* 153:812-815.1996).
- Ford JM, Krystal JH, Mathalon DH (Neural synchrony in schizophrenia: from networks to new treatments. *Schizophr Bull* 33:848-852.2007).
- Frankhauser P, Grimmer Y, Bugert P, Deuschle M, Schmidt M, Schloss P (Characterization of the neuronal dopamine transporter DAT in human blood platelets. *Neurosci Lett* 399:197-201.2006).
- Fuchs RA, Bell GH, Ramirez DR, Eaddy JL, Su ZI (Basolateral amygdala involvement in memory reconsolidation processes that facilitate drug context-induced cocaine seeking. *Eur J Neurosci* 30:889-900.2009).
- Fuchs RA, Eaddy JL, Su ZI, Bell GH (Interactions of the basolateral amygdala with the dorsal hippocampus and dorsomedial prefrontal cortex regulate drug context-induced reinstatement of cocaine-seeking in rats. *Eur J Neurosci* 26:487-498.2007).
- Fujii T, Uchiyama H, Yamamoto N, Hori H, Tatsumi M, Ishikawa M, Arima K, Higuchi T, Kunugi H (Possible association of the semaphorin 3D gene (SEMA3D) with schizophrenia. *J Psychiatr Res* 45:47-53.2011).
- Gad JM, Keeling SL, Wilks AF, Tan SS, Cooper HM (The expression patterns of guidance receptors, DCC and Neogenin, are spatially and temporally distinct throughout mouse embryogenesis. *Dev Biol* 192:258-273.1997).
- Gallo G, Letourneau PC (Axon guidance: A balance of signals sets axons on the right track. *Curr Biol* 9:R490-492.1999).
- Gallo G, Letourneau PC (Regulation of growth cone actin filaments by guidance cues. *J Neurobiol* 58:92-102.2004).
- Garris PA, Ciolkowski EL, Pastore P, Wightman RM (Efflux of dopamine from the synaptic cleft in the nucleus accumbens of the rat brain. *Journal of Neuroscience* 14:6084-6093.1994).
- Genro JP, Kieling C, Rohde LA, Hutz MH (Attention-deficit/hyperactivity disorder and the dopaminergic hypotheses. *Expert Rev Neurother* 10:587-601.2010).
- George SR, O'Dowd BF (A novel dopamine receptor signaling unit in brain: heterooligomers of D1 and D2 dopamine receptors. *ScientificWorldJournal* 7:58-63.2007).

- Girault JA, Greengard P (The neurobiology of dopamine signaling. *Arch Neurol* 61:641-644.2004).
- Goldstein M, Harada K, Meller E, Schalling M, Hokfelt T (Dopamine autoreceptors. Biochemical, pharmacological, and morphological studies. *Annals of the New York Academy of Sciences* 604:169-175.1990).
- Gomez TM, Zheng JQ (The molecular basis for calcium-dependent axon pathfinding. *Nat Rev Neurosci* 7:115-125.2006).
- Gothelf D, Frisch A, Michaelovsky E, Weizman A, Shprintzen RJ (Velo-Cardio-Facial Syndrome. *J Ment Health Res Intellect Disabil* 2:149-167.2009).
- Goto Y, Grace AA (The dopamine system and the pathophysiology of schizophrenia: a basic science perspective. *Int Rev Neurobiol* 78:41-68.2007).
- Goto Y, Otani S, Grace AA (The Yin and Yang of dopamine release: a new perspective. *Neuropharmacology* 53:583-587.2007).
- Grace AA, Bunney BS (The control of firing pattern in nigral dopamine neurons: burst firing. *Journal of Neuroscience* 4:2877-2890.1984).
- Grant A, Hoops D, Labelle-Dumais C, Prevost M, Rajabi H, Kolb B, Stewart J, Arvanitogiannis A, Flores C (Netrin-1 receptor-deficient mice show enhanced mesocortical dopamine transmission and blunted behavioural responses to amphetamine. *Eur J Neurosci* 26:3215-3228.2007).
- Grant BF, Dawson DA (Age of onset of drug use and its association with DSM-IV drug abuse and dependence: results from the National Longitudinal Alcohol Epidemiologic Survey. *J Subst Abuse* 10:163-173.1998).
- Griskevicius V, Goldstein NJ, Mortensen CR, Sundie JM, Cialdini RB, Kenrick DT (Fear and Loving in Las Vegas: Evolution, Emotion, and Persuasion. *J Mark Res* 46:384-395.2009).
- Guo H, Tang Z, Yu Y, Xu L, Jin G, Zhou J (Apomorphine induces trophic factors that support fetal rat mesencephalic dopaminergic neurons in cultures. *Eur J Neurosci* 16:1861-1870.2002).
- Hall A, Lalli G (Rho and Ras GTPases in axon growth, guidance, and branching. *Cold Spring Harb Perspect Biol* 2:a001818.2010).
- Halladay AK, Yue Y, Michna L, Widmer DA, Wagner GC, Zhou R (Regulation of EphB1 expression by dopamine signaling. *Brain Res Mol Brain Res* 85:171-178.2000).
- Harvey JA, Romano AG, Gabriel M, Simansky KJ, Du W, Aloyo VJ, Friedman E (Effects of prenatal exposure to cocaine on the developing brain: anatomical,

- chemical, physiological and behavioral consequences. *Neurotox Res* 3:117-143.2001).
- Hernandez-Lopez S, Tkatch T, Perez-Garci E, Galarraga E, Bargas J, Hamm H, Surmeier DJ (D2 dopamine receptors in striatal medium spiny neurons reduce L-type Ca²⁺ currents and excitability via a novel PLC[β]₁-IP₃-calcineurin-signaling cascade. *J Neurosci* 20:8987-8995.2000).
- Hernandez-Montiel HL, Tamariz E, Sandoval-Minero MT, Varela-Echavarria A (Semaphorins 3A, 3C, and 3F in mesencephalic dopaminergic axon pathfinding. *Journal of Comparative Neurology* 506:387-397.2008).
- Herrero MT, Barcia C, Navarro JM (Functional anatomy of thalamus and basal ganglia. *Childs Nerv Syst* 18:386-404.2002).
- Hong K, Hinck L, Nishiyama M, Poo MM, Tessier-Lavigne M, Stein E (A ligand-gated association between cytoplasmic domains of UNC5 and DCC family receptors converts netrin-induced growth cone attraction to repulsion. *Cell* 97:927-941.1999).
- Hong K, Nishiyama M, Henley J, Tessier-Lavigne M, Poo M (Calcium signalling in the guidance of nerve growth by netrin-1. *Nature* 403:93-98.2000).
- Howes OD, Kapur S (The dopamine hypothesis of schizophrenia: version III--the final common pathway. *Schizophr Bull* 35:549-562.2009).
- Huang da W, Sherman BT, Lempicki RA (Systematic and integrative analysis of large gene lists using DAVID bioinformatics resources. *Nat Protoc* 4:44-57.2009).
- Iwakura Y, Nawa H, Sora I, Chao MV (Dopamine D1 receptor-induced signaling through TrkB receptors in striatal neurons. *J Biol Chem* 283:15799-15806.2008).
- Jassen AK, Yang H, Miller GM, Calder E, Madras BK (Receptor regulation of gene expression of axon guidance molecules: implications for adaptation. *Mol Pharmacol* 70:71-77.2006).
- Jentsch JD, Taylor JR (Impulsivity resulting from frontostriatal dysfunction in drug abuse: implications for the control of behavior by reward-related stimuli. *Psychopharmacology* 146:373-390.1999).
- Jones LB, Stanwood GD, Reinoso BS, Washington RA, Wang HY, Friedman E, Levitt P (In utero cocaine-induced dysfunction of dopamine D1 receptor signaling and abnormal differentiation of cerebral cortical neurons. *J Neurosci* 20:4606-4614.2000).
- Jope RS, Johnson GV (The glamour and gloom of glycogen synthase kinase-3. *Trends Biochem Sci* 29:95-102.2004).

- Jung AB, Bennett JP, Jr. (Development of striatal dopaminergic function. I. Pre- and postnatal development of mRNAs and binding sites for striatal D1 (D1a) and D2 (D2a) receptors. *Brain Res Dev Brain Res* 94:109-120.1996).
- Kahlig KM, Binda F, Khoshbouei H, Blakely RD, McMahon DG, Javitch JA, Galli A (Amphetamine induces dopamine efflux through a dopamine transporter channel. *Proc Natl Acad Sci U S A* 102:3495-3500.2005).
- Kalsbeek A, Voorn P, Buijs RM, Pool CW, Uylings HB (Development of the dopaminergic innervation in the prefrontal cortex of the rat. *Journal of Comparative Neurology* 269:58-72.1988).
- Kandel ER, Schwartz, J.H., and Jessel, T.M. (2000) *Principles of Neural Science*: McGraw-Hill Companies, Inc.
- Kaprielian Z, Runko E, Imondi R (Axon guidance at the midline choice point. *Dev Dyn* 221:154-181.2001).
- Karlsgodt KH, Sun D, Jimenez AM, Lutkenhoff ES, Willhite R, van Erp TG, Cannon TD (Developmental disruptions in neural connectivity in the pathophysiology of schizophrenia. *Dev Psychopathol* 20:1297-1327.2008).
- Kauer JA, Malenka RC (Synaptic plasticity and addiction. *Nat Rev Neurosci* 8:844-858.2007).
- Kaupp UB, Seifert R (Cyclic nucleotide-gated ion channels. *Physiol Rev* 82:769-824.2002).
- Keleman K, Dickson BJ (Short- and long-range repulsion by the *Drosophila* Unc5 netrin receptor. *Neuron* 32:605-617.2001).
- Komatsuzaki K, Dalvin S, Kinane TB (Modulation of G(α 2)) signaling by the axonal guidance molecule UNC5H2. *Biochem Biophys Res Commun* 297:898-905.2002).
- Konradi C, Heckers S (Haloperidol-induced Fos expression in striatum is dependent upon transcription factor cyclic AMP response element binding protein. *Neuroscience* 65:1051-1061.1995).
- Konradi C, Leveque J-C, Hyman S (Amphetamine and dopamine-induced immediate early gene expression in striatal neurons depends on postsynaptic NMDA receptors and calcium. *Journal of Neuroscience* 16:4231-4239.1996a).
- Konradi C, Leveque JC, Hyman SE (Amphetamine and dopamine-induced immediate early gene expression in striatal neurons depends on postsynaptic NMDA receptors and calcium. *J Neurosci* 16:4231-4239.1996b).

- Koob GF, Volkow ND (Neurocircuitry of addiction. *Neuropsychopharmacology* 35:217-238.2010).
- Kriegstein A, Noctor S, Martinez-Cerdeno V (Patterns of neural stem and progenitor cell division may underlie evolutionary cortical expansion. *Nat Rev Neurosci* 7:883-890.2006).
- Kuppenbender KD, Standaert DG, Feuerstein TJ, Penney JB, Jr., Young AB, Landwehrmeyer GB (Expression of NMDA receptor subunit mRNAs in neurochemically identified projection and interneurons in the human striatum. *J Comp Neurol* 419:407-421.2000).
- Lai Wing Sun K, Correia JP, Kennedy TE (Netrins: versatile extracellular cues with diverse functions. *Development* 138:2153-2169.2011).
- Lee SP, So CH, Rashid AJ, Varghese G, Cheng R, Lanca AJ, O'Dowd BF, George SR (Dopamine D1 and D2 receptor Co-activation generates a novel phospholipase C-mediated calcium signal. *J Biol Chem* 279:35671-35678.2004).
- Lefkowitz RJ, Shenoy SK (Transduction of receptor signals by beta-arrestins. *Science* 308:512-517.2005).
- Leung KM, van Horck FP, Lin AC, Allison R, Standart N, Holt CE (Asymmetrical beta-actin mRNA translation in growth cones mediates attractive turning to netrin-1. *Nat Neurosci* 9:1247-1256.2006).
- Lewis DA, Levitt P (Schizophrenia as a disorder of neurodevelopment. *Annu Rev Neurosci* 25:409-432.2002).
- Li C, Wong WH (Model-based analysis of oligonucleotide arrays: expression index computation and outlier detection. *Proceedings of the National Academy of Sciences of the United States of America* 98:31-36.2001).
- Li D, Collier DA, He L (Meta-analysis shows strong positive association of the neuregulin 1 (NRG1) gene with schizophrenia. *Hum Mol Genet* 15:1995-2002.2006a).
- Li W, Aurandt J, Jurgensen C, Rao Y, Guan KL (FAK and Src kinases are required for netrin-induced tyrosine phosphorylation of UNC5. *J Cell Sci* 119:47-55.2006b).
- Lidow MS (Consequences of prenatal cocaine exposure in nonhuman primates. *Brain Res Dev Brain Res* 147:23-36.2003).
- Lidow MS, Wang F, Cao Y, Goldman-Rakic PS (Layer V neurons bear the majority of mRNAs encoding the five distinct dopamine receptor subtypes in the primate prefrontal cortex. *Synapse* 28:10-20.1998).

- Lin AC, Holt CE (Local translation and directional steering in axons. *EMBO J* 26:3729-3736.2007).
- Lindgren N, Uziel A, Gojny M, Haycock J, Erbs E, Greengard P, Hokfelt T, Borrelli E, Fisone G (Distinct roles of dopamine D2L and D2S receptor isoforms in the regulation of protein phosphorylation at presynaptic and postsynaptic sites. *Proc Natl Acad Sci U S A* 100:4305-4309.2003).
- Liu G, Beggs H, Jurgensen C, Park HT, Tang H, Gorski J, Jones KR, Reichardt LF, Wu J, Rao Y (Netrin requires focal adhesion kinase and Src family kinases for axon outgrowth and attraction. *Nat Neurosci* 7:1222-1232.2004).
- Lu BS, Zee PC (Neurobiology of sleep. *Clin Chest Med* 31:309-318.2010).
- Mah S, Nelson MR, Delisi LE, Reneland RH, Markward N, James MR, Nyholt DR, Hayward N, Handoko H, Mowry B, Kammerer S, Braun A (Identification of the semaphorin receptor PLXNA2 as a candidate for susceptibility to schizophrenia. *Mol Psychiatry* 11:471-478.2006).
- Majumdar D, Gao Y, Li D, Webb DJ (Co-culture of neurons and glia in a novel microfluidic platform. *J Neurosci Methods* 196:38-44.2011).
- Marek GJ, Behl B, Beshpalov AY, Gross G, Lee Y, Schoemaker H (Glutamatergic (N-methyl-D-aspartate receptor) hypofrontality in schizophrenia: too little juice or a miswired brain? *Mol Pharmacol* 77:317-326.2010).
- Marin MT, Cruz FC, Planeta CS (Cocaine-induced behavioral sensitization in adolescent rats endures until adulthood: lack of association with GluR1 and NR1 glutamate receptor subunits and tyrosine hydroxylase. *Pharmacol Biochem Behav* 91:109-114.2008).
- Marin O, Rubenstein JL (A long, remarkable journey: tangential migration in the telencephalon. *Nat Rev Neurosci* 2:780-790.2001).
- Marzuk PM, Tardiff K, Smyth D, Stajic M, Leon AC (Cocaine use, risk taking, and fatal Russian roulette. *JAMA* 267:2635-2637.1992).
- McCarthy D, Lueras P, Bhide PG (Elevated dopamine levels during gestation produce region-specific decreases in neurogenesis and subtle deficits in neuronal numbers. *Brain Res* 1182:11-25.2007).
- McCurlley AT, Callard GV (Characterization of housekeeping genes in zebrafish: male-female differences and effects of tissue type, developmental stage and chemical treatment. *BMC Mol Biol* 9:102.2008).
- McGlashan TH, Hoffman RE (Schizophrenia as a disorder of developmentally reduced synaptic connectivity. *Arch Gen Psychiatry* 57:637-648.2000).

- Meijering E (Neuron tracing in perspective. *Cytometry A* 77:693-704.2010).
- Mena MA, Davila V, Bogaluvsky J, Sulzer D (A synergistic neurotrophic response to l-dihydroxyphenylalanine and nerve growth factor. *Mol Pharmacol* 54:678-686.1998).
- Merida I, Avila-Flores A, Merino E (Diacylglycerol kinases: at the hub of cell signalling. *Biochem J* 409:1-18.2008).
- Metin C, Deleglise D, Serafini T, Kennedy TE, Tessier-Lavigne M (A role for netrin-1 in the guidance of cortical efferents. *Development* 124:5063-5074.1997).
- Miller JS, Tallarida RJ, Unterwald EM (Cocaine-induced hyperactivity and sensitization are dependent on GSK3. *Neuropharmacology* 56:1116-1123.2009).
- Ming G, Song H, Berninger B, Inagaki N, Tessier-Lavigne M, Poo M (Phospholipase C-gamma and phosphoinositide 3-kinase mediate cytoplasmic signaling in nerve growth cone guidance. *Neuron* 23:139-148.1999).
- Ming GL, Song HJ, Berninger B, Holt CE, Tessier-Lavigne M, Poo MM (cAMP-dependent growth cone guidance by netrin-1. *Neuron* 19:1225-1235.1997).
- Montminy M (Transcriptional regulation by cyclic AMP. *Annu Rev Biochem* 66:807-822.1997).
- Moore SW, Kennedy TE (Protein kinase A regulates the sensitivity of spinal commissural axon turning to netrin-1 but does not switch between chemoattraction and chemorepulsion. *J Neurosci* 26:2419-2423.2006).
- Moore SW, Tessier-Lavigne M, Kennedy TE (Netrins and their receptors. *Adv Exp Med Biol* 621:17-31.2007).
- Moreno N, Gonzalez A (Evolution of the amygdaloid complex in vertebrates, with special reference to the anamnio-amniotic transition. *J Anat* 211:151-163.2007).
- Murray RM, Lappin J, Di Forti M (Schizophrenia: from developmental deviance to dopamine dysregulation. *Eur Neuropsychopharmacol* 18 Suppl 3:S129-134.2008).
- Nestler EJ (The neurobiology of cocaine addiction. *Sci Pract Perspect* 3:4-10.2005).
- Neve KA, Seamans JK, Trantham-Davidson H (Dopamine receptor signaling. *J Recept Signal Transduct Res* 24:165-205.2004).
- NIDA InfoFacts (2010) Monitoring the Future Study: Trends in Prevalence of Various Drugs for 8th-Graders, 10th-Graders, and 12th-Graders. In: NIDA InfoFacts: High School and Youth Trends, vol. 2010: National Institute of Drug Abuse.

- Nishiyama M, Hoshino A, Tsai L, Henley JR, Goshima Y, Tessier-Lavigne M, Poo MM, Hong K (Cyclic AMP/GMP-dependent modulation of Ca²⁺ channels sets the polarity of nerve growth-cone turning. *Nature* 423:990-995.2003).
- Nishiyama M, von Schimmelmann MJ, Togashi K, Findley WM, Hong K (Membrane potential shifts caused by diffusible guidance signals direct growth-cone turning. *Nature Neuroscience* 11:762-771.2008).
- O'Donnell M, Chance RK, Bashaw GJ (Axon growth and guidance: receptor regulation and signal transduction. *Annu Rev Neurosci* 32:383-412.2009).
- Ohtani N, Goto T, Waeber C, Bhide PG (Dopamine modulates cell cycle in the lateral ganglionic eminence. *J Neurosci* 23:2840-2850.2003).
- Orozco-Cabal L, Liu J, Pollandt S, Schmidt K, Shinnick-Gallagher P, Gallagher JP (Dopamine and corticotropin-releasing factor synergistically alter basolateral amygdala-to-medial prefrontal cortex synaptic transmission: functional switch after chronic cocaine administration. *J Neurosci* 28:529-542.2008).
- Patel TB, Du Z, Pierre S, Cartin L, Scholich K (Molecular biological approaches to unravel adenylyl cyclase signaling and function. *Gene* 269:13-25.2001).
- Paxinos G, Watson C (1986) *The rat brain, in stereotaxic coordinates*. San Diego: Academic Press.
- Perrine SA, Miller JS, Unterwald EM (Cocaine regulates protein kinase B and glycogen synthase kinase-3 activity in selective regions of rat brain. *J Neurochem* 107:570-577.2008).
- Picchioni MM, Murray RM (Schizophrenia. *BMJ* 335:91-95.2007).
- Piper M, Plachez C, Zalucki O, Fothergill T, Goudreau G, Erzurumlu R, Gu C, Richards LJ (Neuropilin 1-Sema signaling regulates crossing of cingulate pioneering axons during development of the corpus callosum. *Cerebral Cortex* 19 Suppl 1:i11-21.2009).
- Piper M, van Horck F, Holt C (The role of cyclic nucleotides in axon guidance. *Adv Exp Med Biol* 621:134-143.2007).
- Plachez C, Richards LJ (Mechanisms of axon guidance in the developing nervous system. *Curr Top Dev Biol* 69:267-346.2005).
- Popolo M, McCarthy DM, Bhide PG (Influence of dopamine on precursor cell proliferation and differentiation in the embryonic mouse telencephalon. *Dev Neurosci* 26:229-244.2004).
- Prasad AA, Pasterkamp RJ (Axon guidance in the dopamine system. *Adv Exp Med Biol* 651:91-100.2009).

- Prasad SE, Howley S, Murphy KC (Candidate genes and the behavioral phenotype in 22q11.2 deletion syndrome. *Dev Disabil Res Rev* 14:26-34.2008).
- Rajadhyaksha A, Barczak A, Macias W, Leveque JC, Lewis SE, Konradi C (L-Type Ca(2+) channels are essential for glutamate-mediated CREB phosphorylation and c-fos gene expression in striatal neurons. *J Neurosci* 19:6348-6359.1999).
- Rajadhyaksha A, Leveque J, Macias W, Barczak A, Konradi C (Molecular components of striatal plasticity: the various routes of cyclic AMP pathways. *Dev Neurosci* 20:204-215.1998).
- Rajadhyaksha AM, Kosofsky BE (Psychostimulants, L-type calcium channels, kinases, and phosphatases. *Neuroscientist* 11:494-502.2005).
- Rajasekharan S, Kennedy TE (The netrin protein family. *Genome Biol* 10:239.2009).
- Rapoport JL, Addington A, Frangou S (The neurodevelopmental model of schizophrenia: what can very early onset cases tell us? *Curr Psychiatry Rep* 7:81-82.2005).
- Rashid AJ, So CH, Kong MM, Furtak T, El-Ghundi M, Cheng R, O'Dowd BF, George SR (D1-D2 dopamine receptor heterooligomers with unique pharmacology are coupled to rapid activation of Gq/11 in the striatum. *Proceedings of the National Academy of Sciences of the United States of America* 104:654-659.2007).
- Rice ME, Cragg SJ (Dopamine spillover after quantal release: rethinking dopamine transmission in the nigrostriatal pathway. *Brain Res Rev* 58:303-313.2008).
- Richards LJ, Koester SE, Tuttle R, O'Leary DD (Directed growth of early cortical axons is influenced by a chemoattractant released from an intermediate target. *J Neurosci* 17:2445-2458.1997).
- Richfield EK, Penney JB, Young AB (Anatomical and affinity state comparisons between dopamine D1 and D2 receptors in the rat central nervous system. *Neuroscience* 30:767-777.1989).
- Round J, Stein E (Netrin signaling leading to directed growth cone steering. *Curr Opin Neurobiol* 17:15-21.2007).
- Rutecki PA (Neuronal excitability: voltage-dependent currents and synaptic transmission. *J Clin Neurophysiol* 9:195-211.1992).
- Sales N, Martres MP, Bouthenet ML, Schwartz JC (Ontogeny of dopaminergic D-2 receptors in the rat nervous system: characterization and detailed autoradiographic mapping with [¹²⁵I]iodosulpride. *Neuroscience* 28:673-700.1989).
- Santana N, Mengod G, Artigas F (Quantitative analysis of the expression of dopamine D1 and D2 receptors in pyramidal and GABAergic neurons of the rat prefrontal cortex. *Cereb Cortex* 19:849-860.2009).

- Schambra UB, Duncan GE, Breese GR, Fornaretto MG, Caron MG, Fremeau RT, Jr. (Ontogeny of D1A and D2 dopamine receptor subtypes in rat brain using in situ hybridization and receptor binding. *Neuroscience* 62:65-85.1994).
- Schmidt U, Beyer C, Oestreicher AB, Reisert I, Schilling K, Pilgrim C (Activation of dopaminergic D1 receptors promotes morphogenesis of developing striatal neurons. *Neuroscience* 74:453-460.1996).
- Seamans JK, Yang CR (The principal features and mechanisms of dopamine modulation in the prefrontal cortex. *Prog Neurobiol* 74:1-58.2004).
- Seeman P (Targeting the dopamine D2 receptor in schizophrenia. *Expert Opin Ther Targets* 10:515-531.2006).
- Seeman P (Glutamate and dopamine components in schizophrenia. *J Psychiatry Neurosci* 34:143-149.2009).
- Seeman P, Schwarz J, Chen JF, Szechtman H, Perreault M, McKnight GS, Roder JC, Quirion R, Boksa P, Srivastava LK, Yanai K, Weinshenker D, Sumiyoshi T (Psychosis pathways converge via D2high dopamine receptors. *Synapse* 60:319-346.2006).
- Selbie LA, Hill SJ (G protein-coupled-receptor cross-talk: the fine-tuning of multiple receptor-signalling pathways. *Trends Pharmacol Sci* 19:87-93.1998).
- Serafini T, Colamarino SA, Leonardo ED, Wang H, Beddington R, Skarnes WC, Tessier-Lavigne M (Netrin-1 is required for commissural axon guidance in the developing vertebrate nervous system. *Cell* 87:1001-1014.1996).
- Sesack SR, Snyder CL, Lewis DA (Axon terminals immunolabeled for dopamine or tyrosine hydroxylase synapse on GABA-immunoreactive dendrites in rat and monkey cortex. *J Comp Neurol* 363:264-280.1995).
- Shekarabi M, Moore SW, Tritsch NX, Morris SJ, Bouchard JF, Kennedy TE (Deleted in colorectal cancer binding netrin-1 mediates cell substrate adhesion and recruits Cdc42, Rac1, Pak1, and N-WASP into an intracellular signaling complex that promotes growth cone expansion. *J Neurosci* 25:3132-3141.2005).
- Shen K, Cowan CW (Guidance molecules in synapse formation and plasticity. *Cold Spring Harb Perspect Biol* 2:a001842.2010).
- Shi X, McGinty JF (D1 and D2 dopamine receptors differentially mediate the activation of phosphoproteins in the striatum of amphetamine-sensitized rats. *Psychopharmacology (Berl)* 214:653-663.2011).
- Shu T, Valentino KM, Seaman C, Cooper HM, Richards LJ (Expression of the netrin-1 receptor, deleted in colorectal cancer (DCC), is largely confined to projecting neurons in the developing forebrain. *J Comp Neurol* 416:201-212.2000).

- Sillitoe RV, Vogel MW (Desire, disease, and the origins of the dopaminergic system. *Schizophr Bull* 34:212-219.2008).
- Sullivan SE, Black YD, Naydenov AV, Vassoler FR, Hanlin RP, Konradi C (Binge cocaine administration in adolescent rats affects amygdalar gene expression patterns and alters anxiety-related behavior in adulthood. *Biol Psychiatry* 70:583-592.2011).
- Sullivan SE, Konradi C (Expression and function of dopamine receptors in the developing medial frontal cortex and striatum of the rat. *Neuroscience*.2011).
- Snitz BE, MacDonald A, 3rd, Cohen JD, Cho RY, Becker T, Carter CS (Lateral and medial hypofrontality in first-episode schizophrenia: functional activity in a medication-naive state and effects of short-term atypical antipsychotic treatment. *Am J Psychiatry* 162:2322-2329.2005).
- Song ZM, Undie AS, Koh PO, Fang YY, Zhang L, Dracheva S, Sealson SC, Lidow MS (D1 dopamine receptor regulation of microtubule-associated protein-2 phosphorylation in developing cerebral cortical neurons. *J Neurosci* 22:6092-6105.2002).
- Sotres-Bayon F, Quirk GJ (Prefrontal control of fear: more than just extinction. *Curr Opin Neurobiol* 20:231-235.2010).
- Souza BR, Romano-Silva MA, Tropepe V (Dopamine D2 receptor activity modulates Akt signaling and alters GABAergic neuron development and motor behavior in zebrafish larvae. *J Neurosci* 31:5512-5525.2011).
- Stanwood GD, Washington RA, Shumsky JS, Levitt P (Prenatal cocaine exposure produces consistent developmental alterations in dopamine-rich regions of the cerebral cortex. *Neuroscience* 106:5-14.2001).
- Suh PG, Park JI, Manzoli L, Cocco L, Peak JC, Katan M, Fukami K, Kataoka T, Yun S, Ryu SH (Multiple roles of phosphoinositide-specific phospholipase C isozymes. *BMB Rep* 41:415-434.2008).
- Sunahara RK, Dessauer CW, Whisnant RE, Kleuss C, Gilman AG (Interaction of G α with the cytosolic domains of mammalian adenylyl cyclase. *J Biol Chem* 272:22265-22271.1997).
- Surmeier DJ, Ding J, Day M, Wang Z, Shen W (D1 and D2 dopamine-receptor modulation of striatal glutamatergic signaling in striatal medium spiny neurons. *Trends Neurosci* 30:228-235.2007).
- Sutton LP, Honardoust D, Mouyal J, Rajakumar N, Rushlow WJ (Activation of the canonical Wnt pathway by the antipsychotics haloperidol and clozapine involves dishevelled-3. *J Neurochem* 102:153-169.2007).

- Svenningsson P, Nishi A, Fisone G, Girault JA, Nairn AC, Greengard P (DARPP-32: an integrator of neurotransmission. *Annu Rev Pharmacol Toxicol* 44:269-296.2004).
- Tamagnone L, Comoglio PM (Signalling by semaphorin receptors: cell guidance and beyond. *Trends Cell Biol* 10:377-383.2000).
- Taylor AM, Blurton-Jones M, Rhee SW, Cribbs DH, Cotman CW, Jeon NL (A microfluidic culture platform for CNS axonal injury, regeneration and transport. *Nat Methods* 2:599-605.2005).
- Todd RD (Neural development is regulated by classical neurotransmitters: dopamine D2 receptor stimulation enhances neurite outgrowth. *Biol Psychiatry* 31:794-807.1992).
- Tong J, Killeen M, Steven R, Binns KL, Culotti J, Pawson T (Netrin stimulates tyrosine phosphorylation of the UNC-5 family of netrin receptors and induces Shp2 binding to the RCM cytodomain. *J Biol Chem* 276:40917-40925.2001).
- Ubersax JA, Ferrell JE, Jr. (Mechanisms of specificity in protein phosphorylation. *Nat Rev Mol Cell Biol* 8:530-541.2007).
- Valjent E, Corvol JC, Pages C, Besson MJ, Maldonado R, Caboche J (Involvement of the extracellular signal-regulated kinase cascade for cocaine-rewarding properties. *J Neurosci* 20:8701-8709.2000).
- Van den Heuvel DM, Pasterkamp RJ (Getting connected in the dopamine system. *Prog Neurobiol* 85:75-93.2008).
- Vehof J, Al Hadithy AF, Burger H, Snieder H, Risselada AJ, Wilffert B, Cohen D, Arends J, Wiersma D, Mulder H, Bruggeman R (Association between the ROBO1 gene and body mass index in patients using antipsychotics. *Psychiatr Genet* 21:202-207.2011).
- Verney C, Berger B, Adrien J, Vigny A, Gay M (Development of the dopaminergic innervation of the rat cerebral cortex. A light microscopic immunocytochemical study using anti-tyrosine hydroxylase antibodies. *Brain Res* 281:41-52.1982).
- Volk DW, Lewis DA (Prefrontal cortical circuits in schizophrenia. *Curr Top Behav Neurosci* 4:485-508.2010).
- Wen Z, Guirland C, Ming GL, Zheng JQ (A CaMKII/calcineurin switch controls the direction of Ca(2+)-dependent growth cone guidance. *Neuron* 43:835-846.2004).
- Wong W, Scott JD (AKAP signalling complexes: focal points in space and time. *Nat Rev Mol Cell Biol* 5:959-970.2004).

- Xiang Y, Li Y, Zhang Z, Cui K, Wang S, Yuan XB, Wu CP, Poo MM, Duan S (Nerve growth cone guidance mediated by G protein-coupled receptors. *Nat Neurosci* 5:843-848.2002).
- Xiao D, Miller GM, Jassen A, Westmoreland SV, Pauley D, Madras BK (Ephrin/Eph receptor expression in brain of adult nonhuman primates: implications for neuroadaptation. *Brain Research* 1067:67-77.2006).
- Yang C, Kazanietz MG (Divergence and complexities in DAG signaling: looking beyond PKC. *Trends Pharmacol Sci* 24:602-608.2003).
- Yetnikoff L, Eng C, Benning S, Flores C (Netrin-1 receptor in the ventral tegmental area is required for sensitization to amphetamine. *Eur J Neurosci* 31:1292-1302.2010).
- Yetnikoff L, Labelle-Dumais C, Flores C (Regulation of netrin-1 receptors by amphetamine in the adult brain. *Neuroscience* 150:764-773.2007).
- Yu TW, Bargmann CI (Dynamic regulation of axon guidance. *Nat Neurosci* 4 Suppl:1169-1176.2001).
- Zalesky A, Fornito A, Seal ML, Cocchi L, Westin CF, Bullmore ET, Egan GF, Pantelis C (Disrupted axonal fiber connectivity in schizophrenia. *Biol Psychiatry* 69:80-89.2011).
- Zhang L, Bai J, Undie AS, Bergson C, Lidow MS (D1 dopamine receptor regulation of the levels of the cell-cycle-controlling proteins, cyclin D, P27 and Raf-1, in cerebral cortical precursor cells is mediated through cAMP-independent pathways. *Cereb Cortex* 15:74-84.2005).
- Zhang L, Lidow MS (D1 dopamine receptor regulation of cell cycle in FGF- and EGF-supported primary cultures of embryonic cerebral cortical precursor cells. *Int J Dev Neurosci* 20:593-606.2002).
- Zhang Y, Bertolino A, Fazio L, Blasi G, Rampino A, Romano R, Lee ML, Xiao T, Papp A, Wang D, Sadee W (Polymorphisms in human dopamine D2 receptor gene affect gene expression, splicing, and neuronal activity during working memory. *Proc Natl Acad Sci U S A* 104:20552-20557.2007).
- Zhou QY, Grandy DK, Thambi L, Kushner JA, Van Tol HH, Cone R, Pribnow D, Salon J, Bunzow JR, Civelli O (Cloning and expression of human and rat D1 dopamine receptors. *Nature* 347:76-80.1990).
- Zucker M, Weizman A, Rehavi M (Characterization of high-affinity [3H]TBZOH binding to the human platelet vesicular monoamine transporter. *Life Sci* 69:2311-2317.2001).